

Nonlinear structure formation

Contents

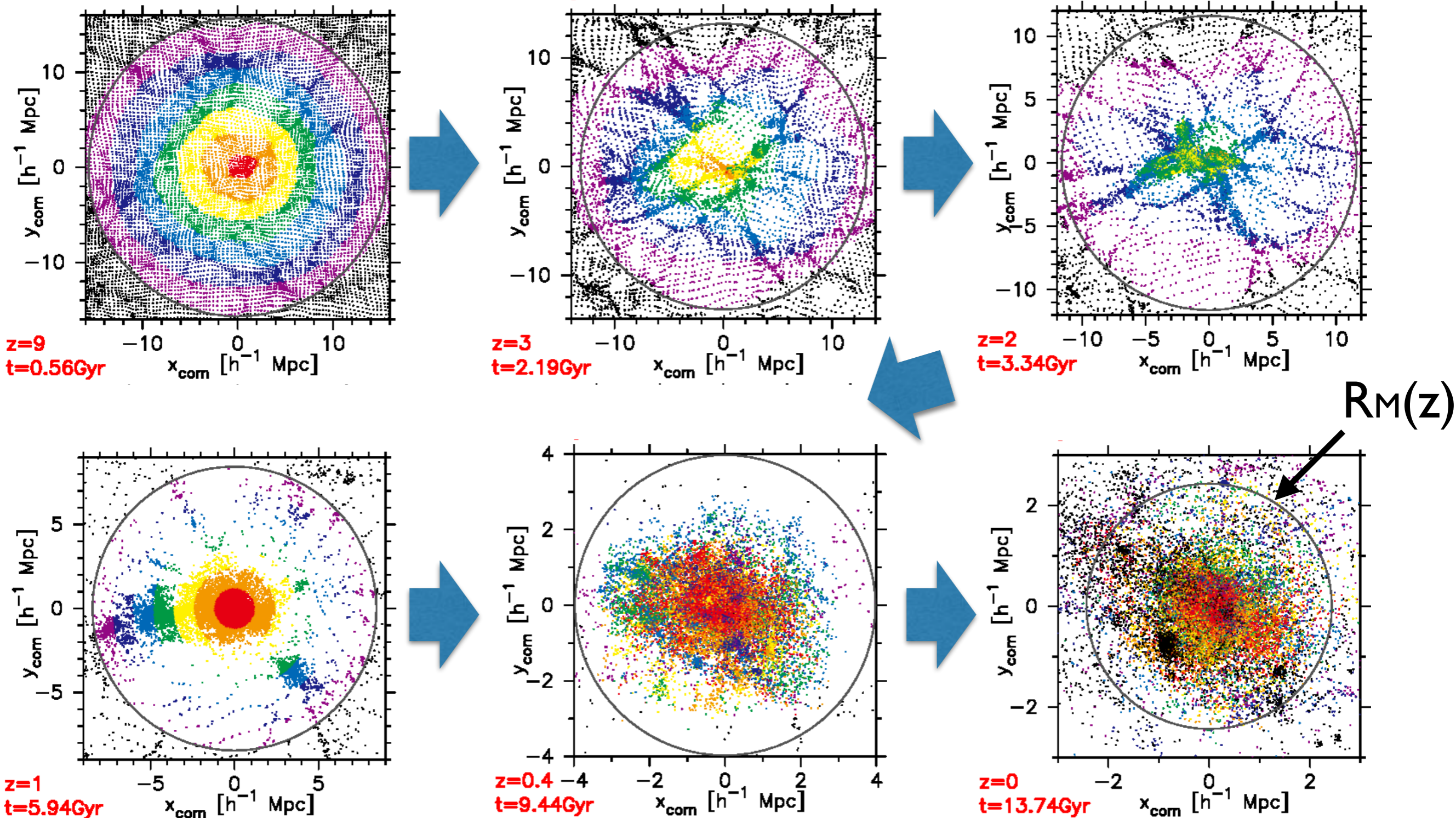
- Spherical collapse model
- Zel'dovich approximation
- Eulerian Perturbation theory

Spherical collapse model (SCM)

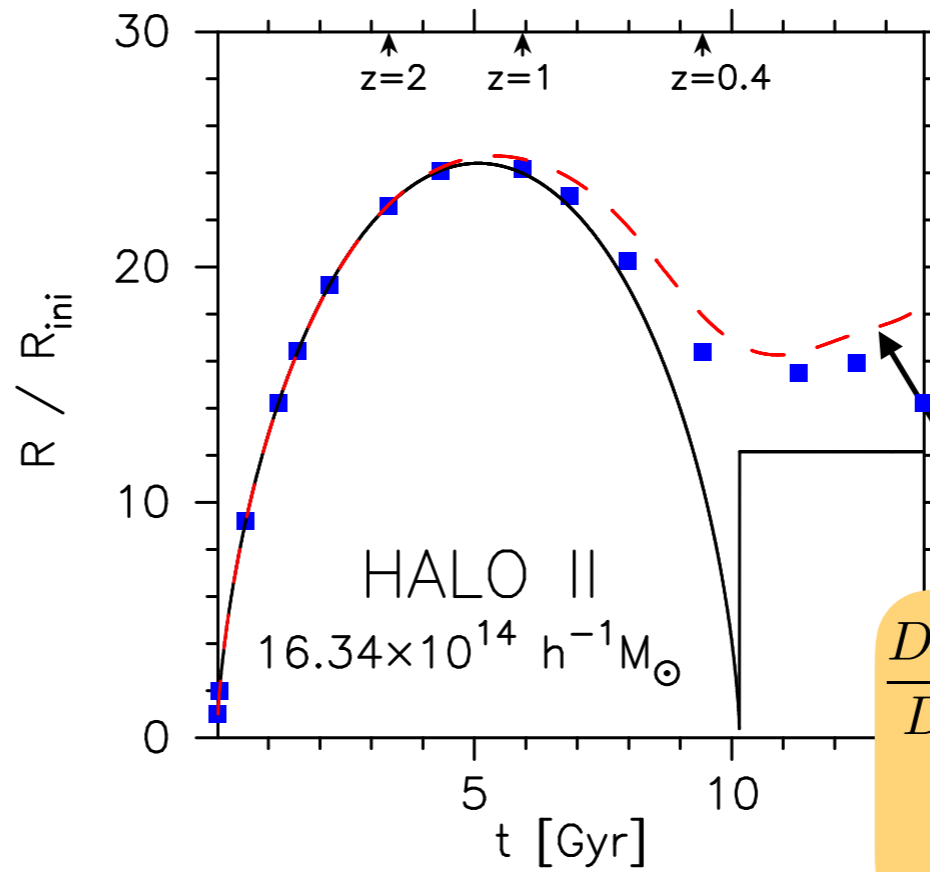
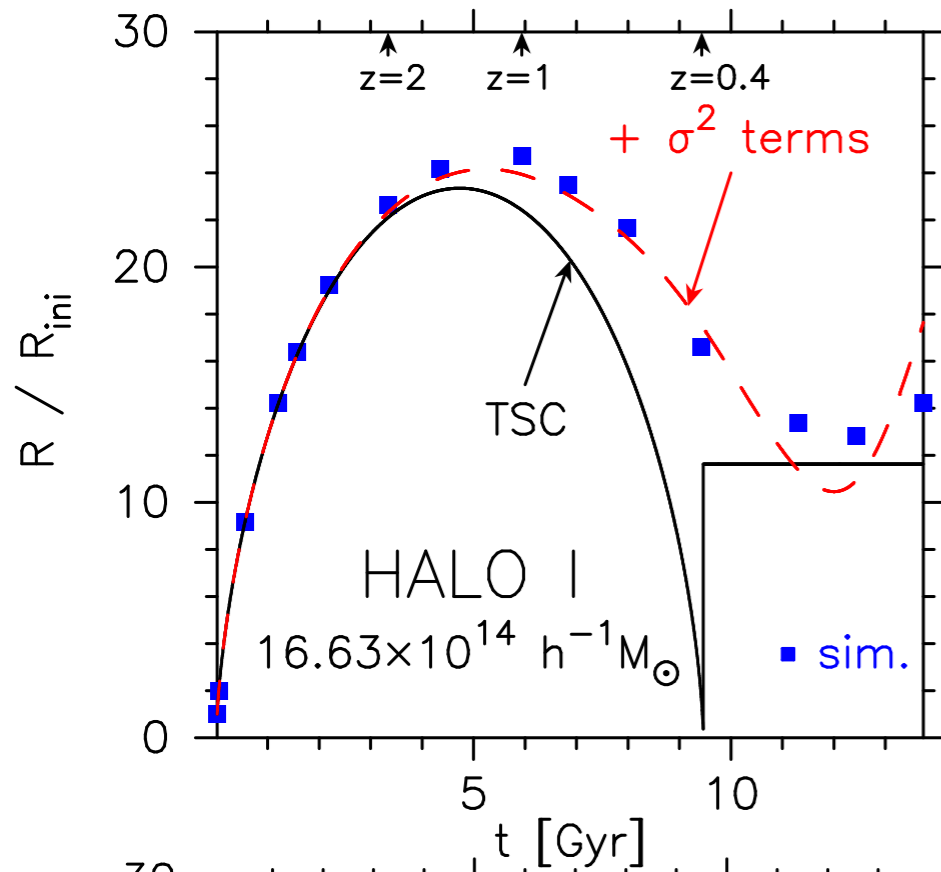
Halo formation

Halo I ($M \sim 10^{15} M_{\text{sun}}/h$)

Suto, Kitayama, Osato, Sasaki & Suto (16)

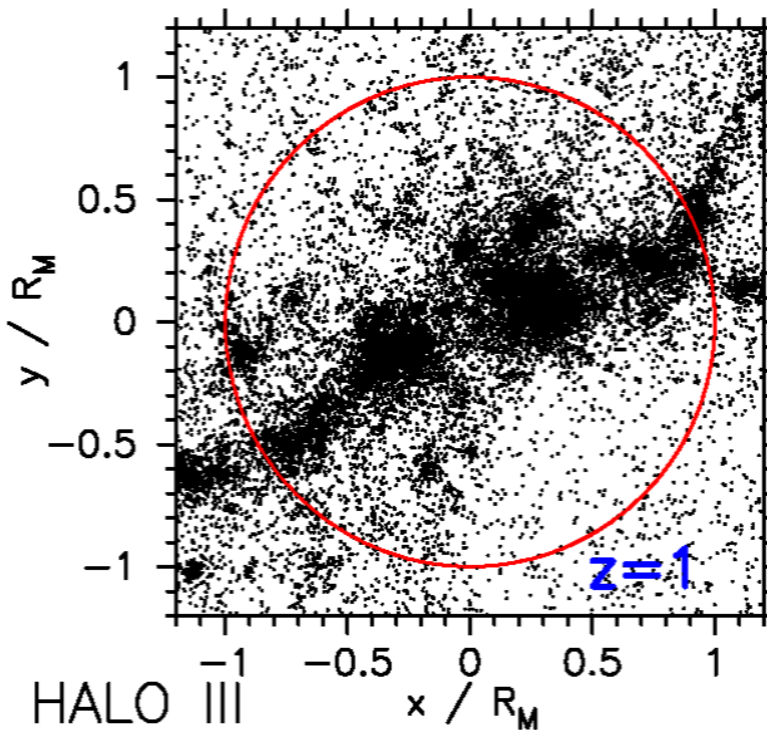
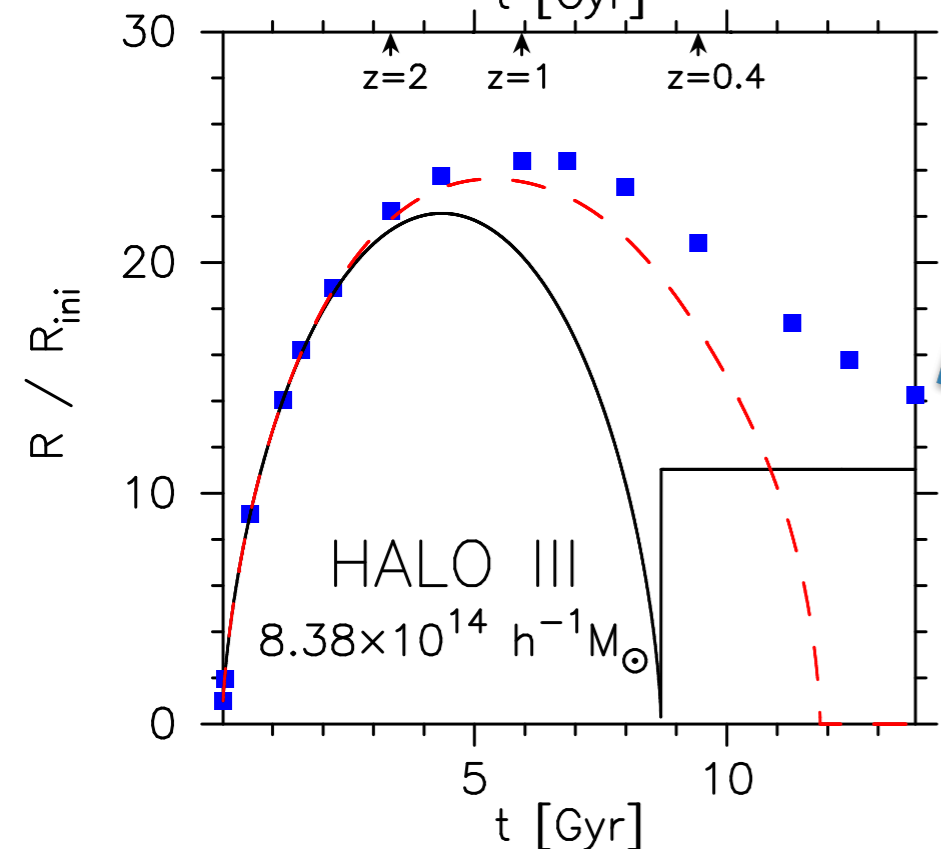


Comparison with SCM



Evolution of $R_M(z)$

$$\frac{Dv_r}{Dt} = -\frac{1}{\rho} \frac{\partial(\rho\sigma_r^2)}{\partial r} - \frac{2\sigma_r^2 - \sigma_{\tan}^2}{r} - \frac{GM}{r^2} \quad (\text{Jeans eq.})$$

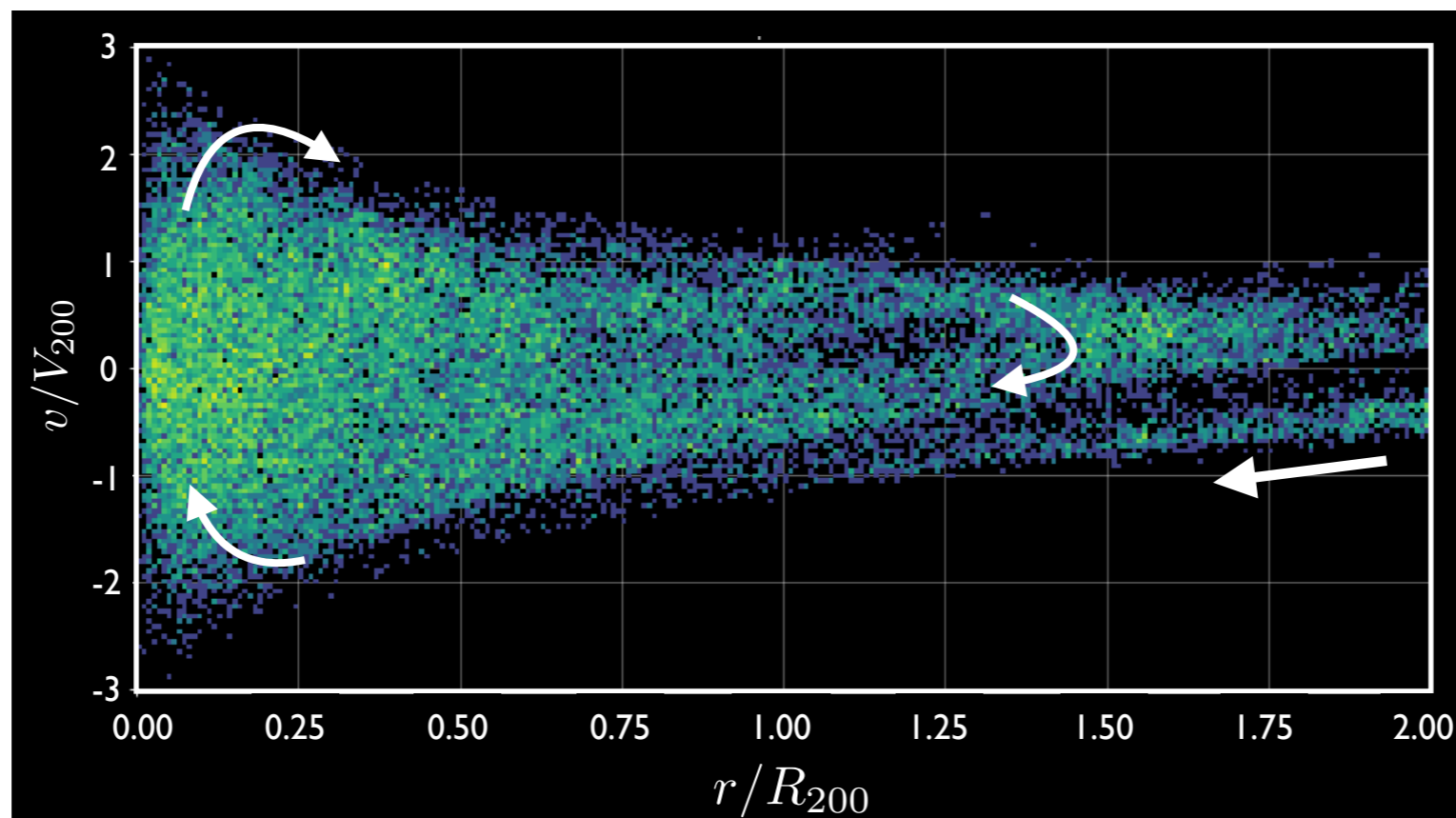


Suto, Kitayama, Osato,
 Sasaki & Suto (16)

Beyond spherical collapse model (SCM)

SCM only describes the onset of halo formation

In particular, SCM fails to describe phase-space structure of halo
(continuous matter accretion)



Tractable analytic
treatment

Self-Similar collapse

e.g., Fillmore & Goldreich ('84)
Bertschinger ('85)

Self-similar collapse

Fillmore & Goldreich ('84)

- Einstein-de Sitter background, $a(t) \propto t^{2/3}$
- Scale-free initial density perturbation, $\delta_i \propto M_i^{-\epsilon}$
- Motion of continuously infall shells at $r < r_*$
turn-around radius

Self-similar
ansatz

$$r(t, t_*) = r_*(t_*) \lambda(t/t_*)$$

EoM

$$\Lambda(\tau) = \tau^{2/3+2/9\epsilon}$$

$$\frac{d^2\lambda}{d\tau^2} = -\frac{\pi^2}{8} \frac{\tau^{2/3\epsilon}}{\lambda^2} \mathcal{M} \left[\frac{\lambda}{\Lambda(\tau)} \right]; \quad \mathcal{M}(x) = \frac{2}{3\epsilon} \int_1^\infty \frac{dy}{y^{1+2/3\epsilon}} \mathcal{H} \left[x - \frac{\lambda(y)}{\Lambda(y)} \right]$$

$\tau \equiv t/t_*$: time normalized by turn-around time

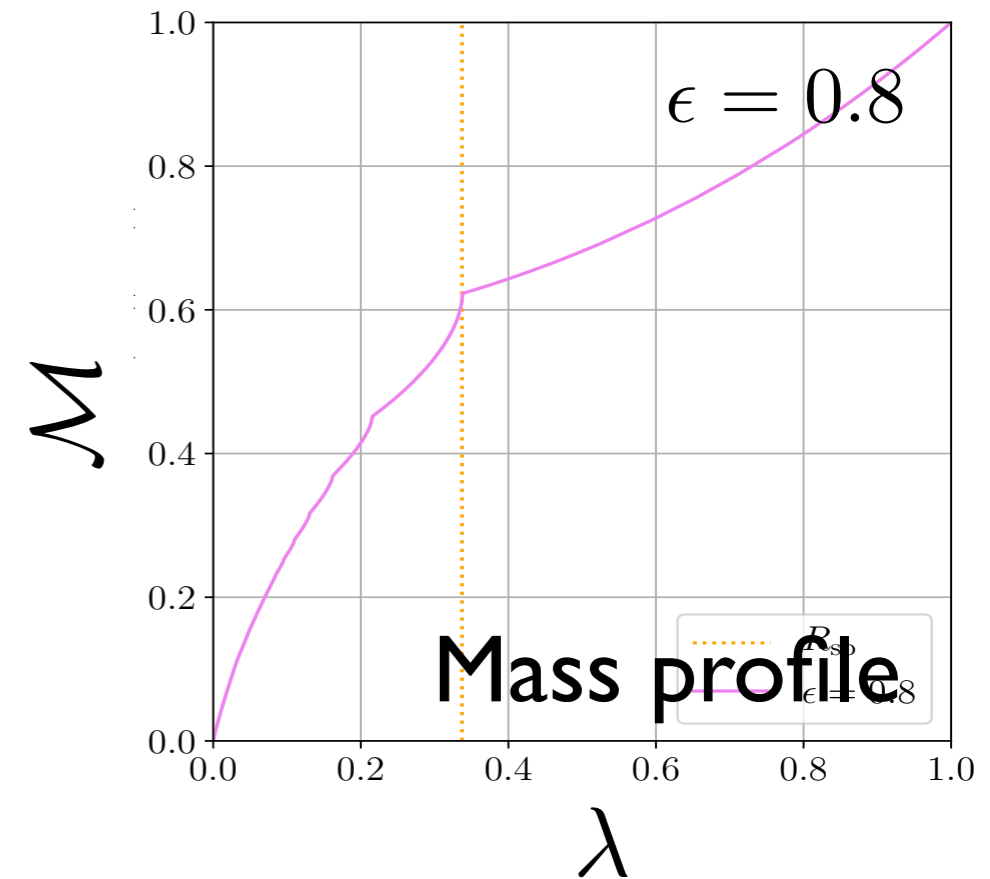
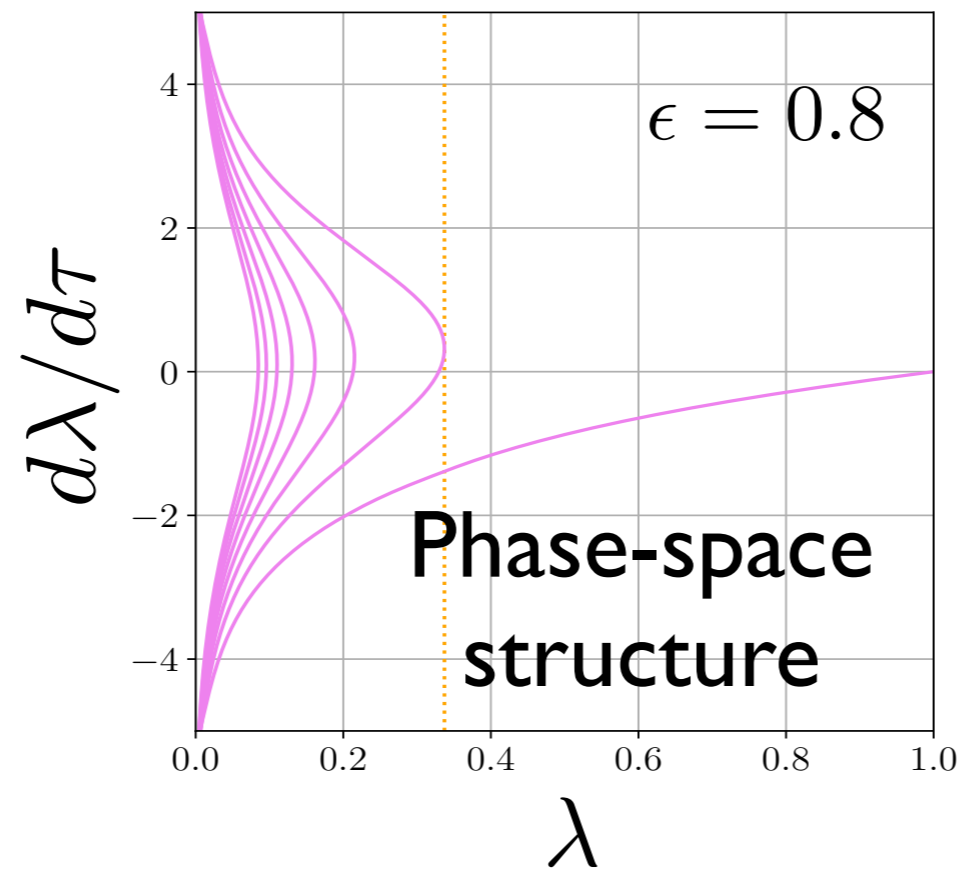
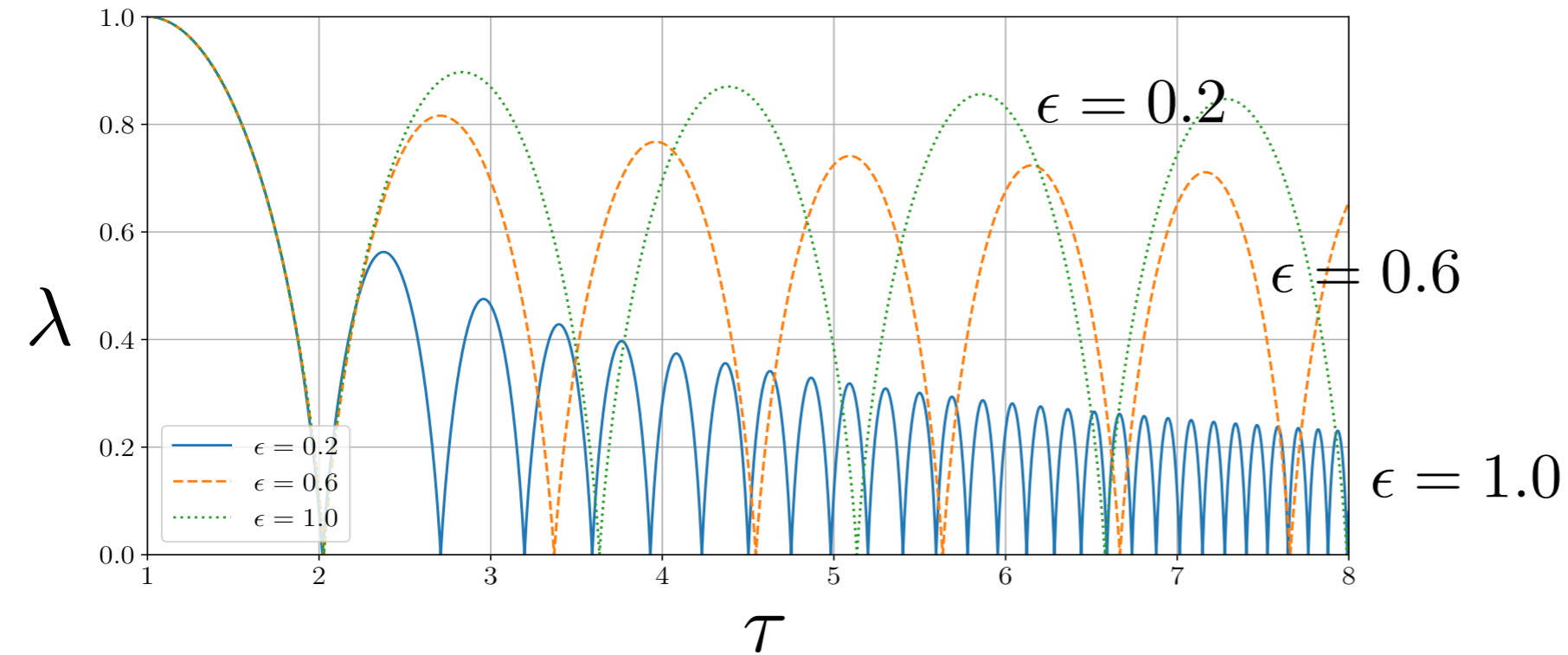
Heaviside step func.

Mass: $M(r, t) = M_t \mathcal{M} \left(\frac{\lambda}{\Lambda(t)} \right); \quad M_t \propto a(t)^{1/\epsilon}$

Solutions

修論 by 杉浦宏夢

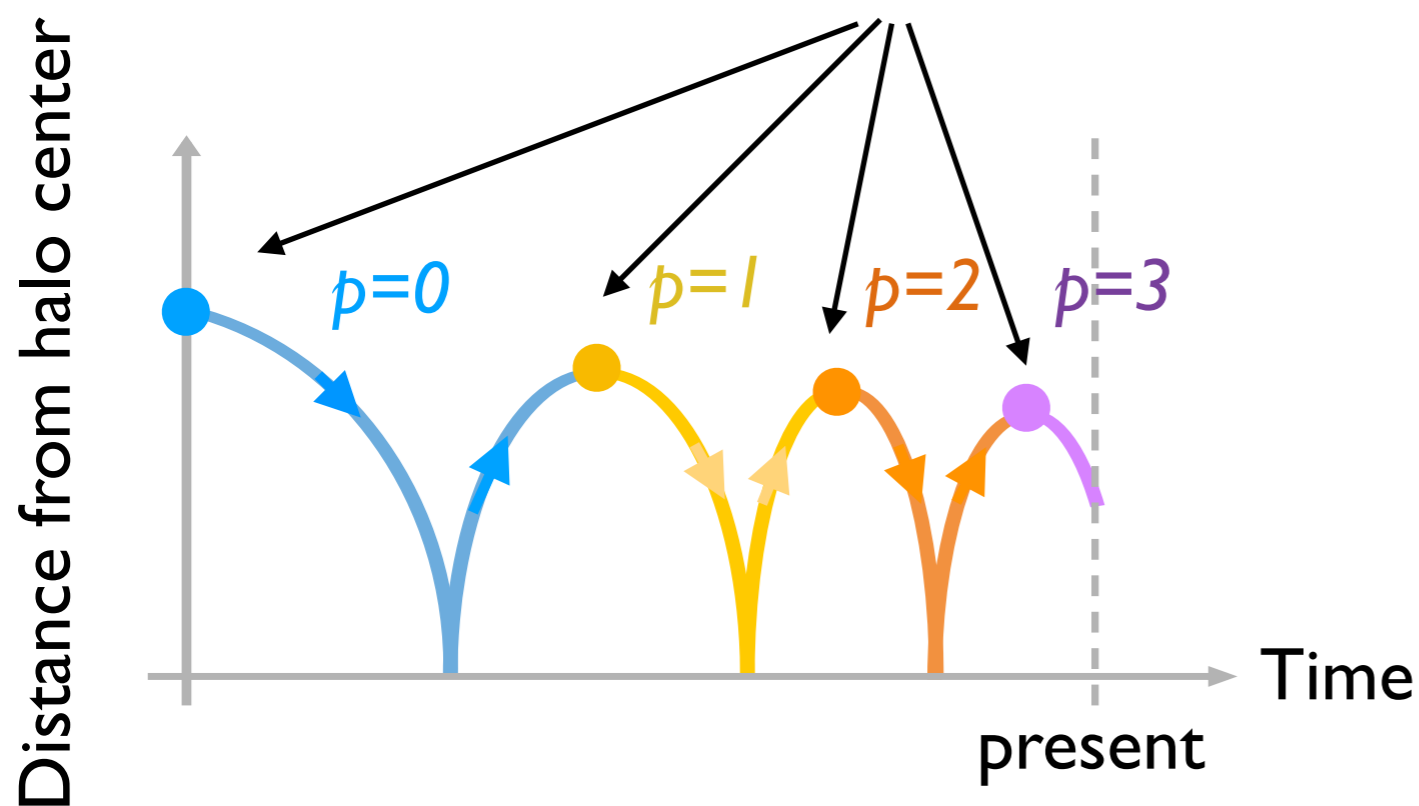
trajectory of
mass shell



Tracing multi-stream flow with particle trajectories in N -body simulation

修論 by 杉浦宏夢

Keeping track of apocenter passage(s) for particle trajectories, number of apocenter passages, p , is stored for each particle



= SPARTA algorithm + α

(Diemer'17; Diemer et al.'17)

Tiling phase-space streams with p

N-body simulation

Y. Rasera@

(Observatoire de Paris)

- $L=316\text{Mpc}/h$, $N=512^3$

- 60 snapshots at $0 < z < 1.43$

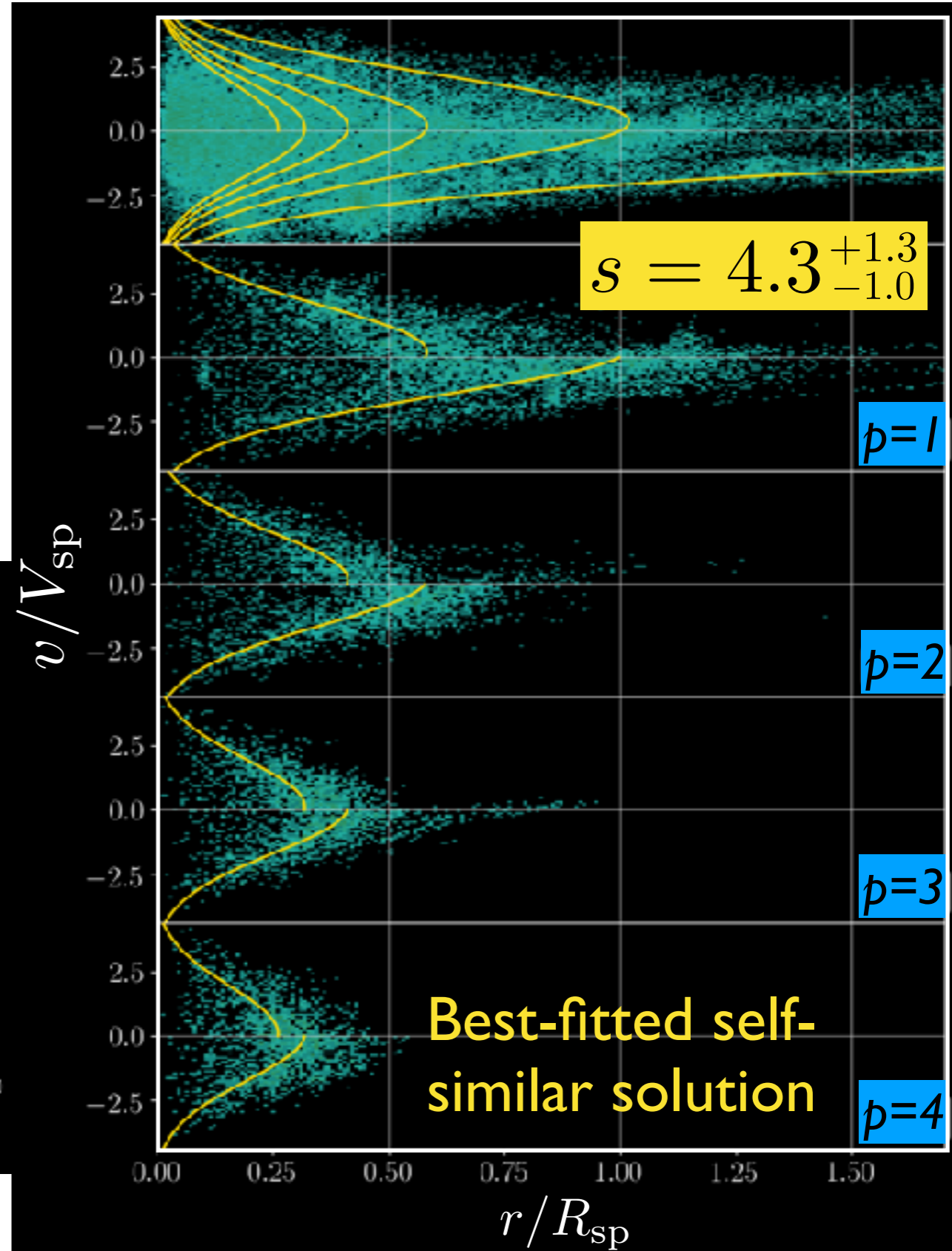
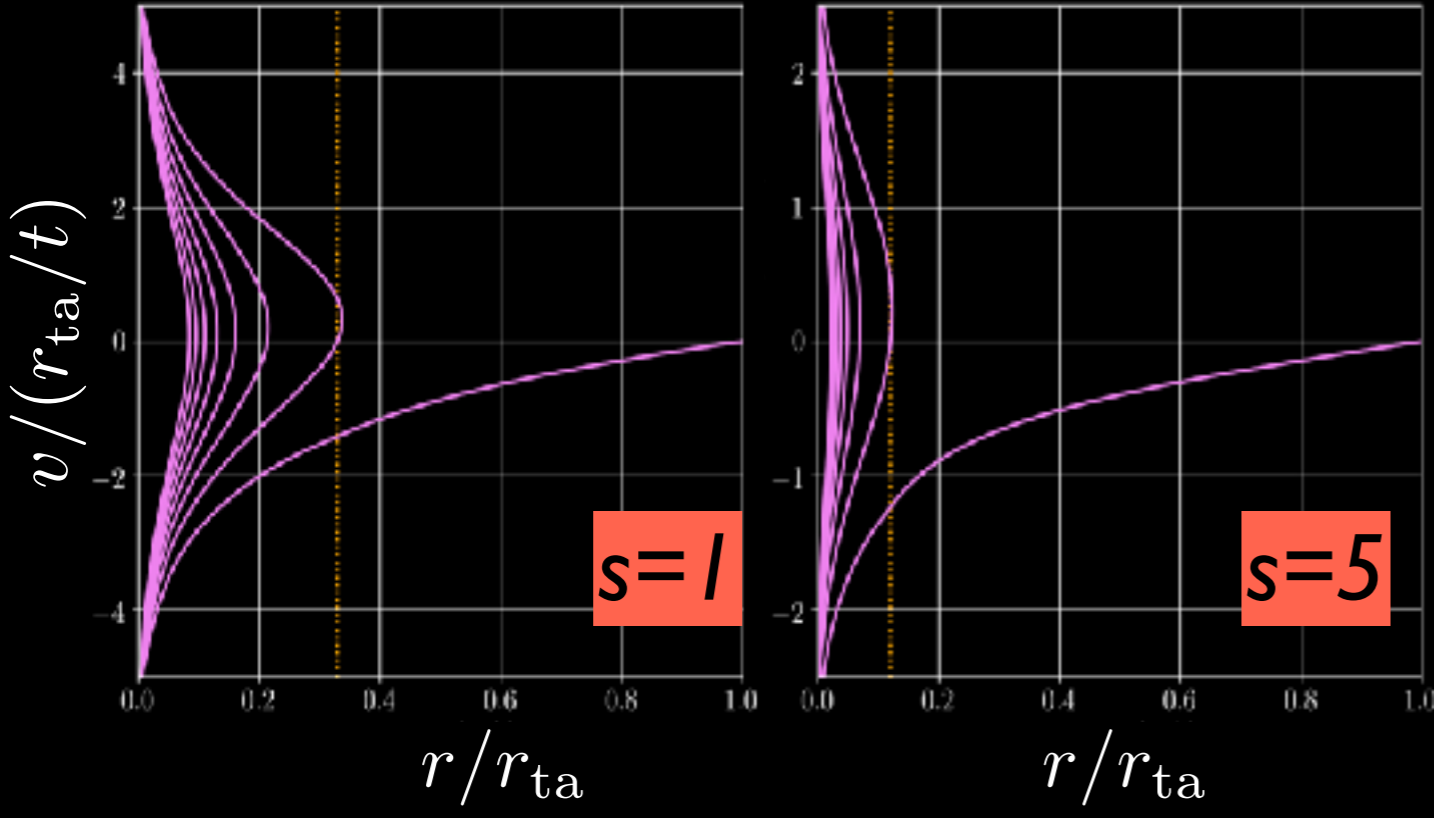
- Einstein-de Sitter universe

11,000 halos
($M_{200} \geq 10^{13} M_{\odot}$)

Comparison with self-similar solution

Use apocenter-passage positions $p=1 \sim 5$ to fit to self-similar solution by Fillmore & Goldreich ('84)

Fitting parameters:
 $s = (1/\epsilon), \quad r_{ta}(t_{ta})$
 accretion rate ($M \propto a^s$) scale radius



(Master thesis by H. Sugiura)

Zel'dovich approximation

Lagrangian PT

Basic equations

$$\ddot{\mathbf{x}} + 2H\dot{\mathbf{x}} = -\frac{1}{a^2} \nabla_{\mathbf{x}} \phi(\mathbf{x}), \quad \swarrow \quad L = \frac{1}{2} m a^2 \dot{\mathbf{x}}^2 - m \phi(\mathbf{x})$$
$$\nabla_{\mathbf{x}}^2 \phi(\mathbf{x}) = 4\pi G a^2 \bar{\rho}_m \delta(\mathbf{x}).$$

Lagrangian coordinate (\mathbf{q}): $\mathbf{x}(\mathbf{q}, t) = \mathbf{q} + \Psi(\mathbf{q}, t)$

In Lagrangian coordinate, mass density is assumed to be uniform:

$$\bar{\rho}_m d^n \mathbf{q} = \rho_m(\mathbf{x}) d^n \mathbf{x} \quad \longrightarrow \quad \delta(\mathbf{x}) = \frac{\rho_m(\mathbf{x})}{\bar{\rho}_m} - 1 = \left| \frac{\partial \mathbf{x}}{\partial \mathbf{q}} \right|^{-1} - 1$$

Rewriting quantities in Eulerian space with those in Lagrangian quantities

Lagrangian PT

Matsubara ('15)

$$\nabla_x \cdot [\ddot{\mathbf{x}} + 2H\dot{\mathbf{x}}] = -4\pi G \bar{\rho}_m \delta,$$

$$\nabla_x \times [\ddot{\mathbf{x}} + 2H\dot{\mathbf{x}}] = \mathbf{0}.$$

$$\hat{\mathcal{T}} f(t) \equiv \ddot{f}(t) + 2H\dot{f}(t)$$

Longitudinal: $(\hat{\mathcal{T}} - 4\pi G \bar{\rho}_m) \Psi_{k,k}$

$$= -\epsilon_{ijk} \epsilon_{ipq} \Psi_{j,p} (\hat{\mathcal{T}} - 2\pi G \bar{\rho}_m) \psi_{k,q}$$

$$- \frac{1}{2} \epsilon_{ijk} \epsilon_{pqr} \Psi_{i,p} \Psi_{j,q} \left(\hat{\mathcal{T}} - \frac{4\pi G}{3} \bar{\rho}_m \right) \Psi_{k,r},$$

Transverse: $\epsilon_{ijk} \hat{\mathcal{T}} \Psi_{j,k} = -\epsilon_{ijk} \Psi_{p,j} \hat{\mathcal{T}} \Psi_{p,k}.$

Levi-Civita symbol

PT expansion: $\Psi(\mathbf{q}, t) = \Psi^{(1)}(\mathbf{q}, t) + \Psi^{(2)}(\mathbf{q}, t) + \Psi^{(3)}(\mathbf{q}, t) + \dots$

Zel'dovich solution: 1st-order LPT

$$\Psi^{(1)} = \Psi^{(1L)} + \Psi^{(1T)} ;$$

$$\eta \equiv \ln D_1(t)$$

$$\left(\frac{\partial^2}{\partial \eta^2} + \frac{1}{2} \frac{\partial}{\partial \eta} - \frac{3}{2} \right) \Psi_{k,k}^{(1L)} = 0$$

$$\left(\frac{\partial^2}{\partial \eta^2} + \frac{1}{2} \frac{\partial}{\partial \eta} \right) \epsilon_{ijk} \Psi_{j,k}^{(1T)} = 0$$

Zel'dovich approximation : $\Psi^{(1T)} = 0$ and take growing-mode only

$$\Psi^{(1)} = \Psi^{(1L)} = -D_1(a) \nabla_{\mathbf{q}} \varphi(\mathbf{q}), \quad \nabla_{\mathbf{q}}^2 \varphi(\mathbf{q}) = \delta_0(\mathbf{q})$$

: initial density field

$$\because 1 + \delta_{\text{m}}(\mathbf{x}) = \left| \frac{\partial \mathbf{x}}{\partial \mathbf{q}} \right|^{-1} \equiv \frac{1}{J} \simeq 1 - \nabla_{\mathbf{q}} \cdot \boldsymbol{\psi}$$

Particle trajectories in ZA

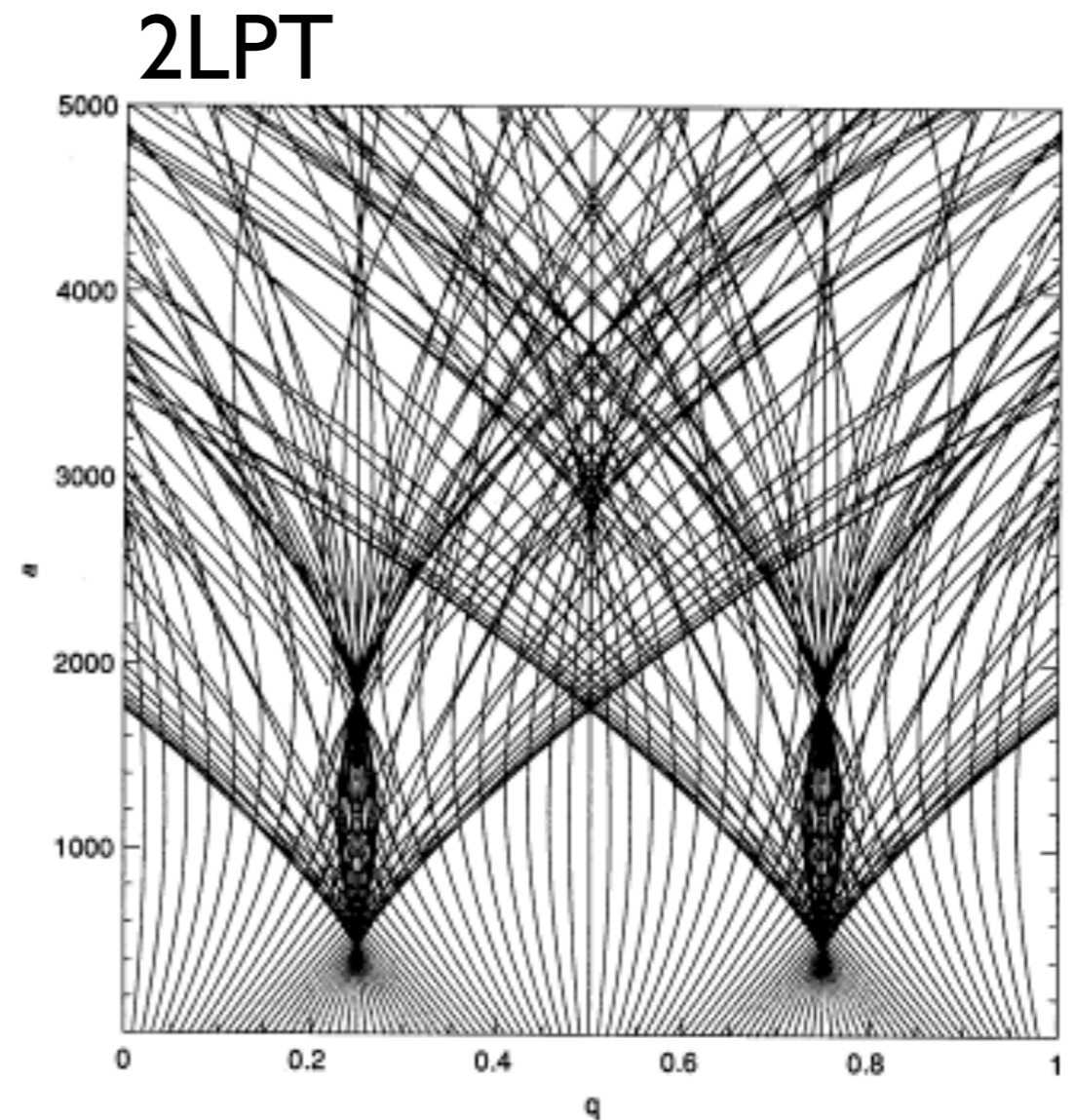
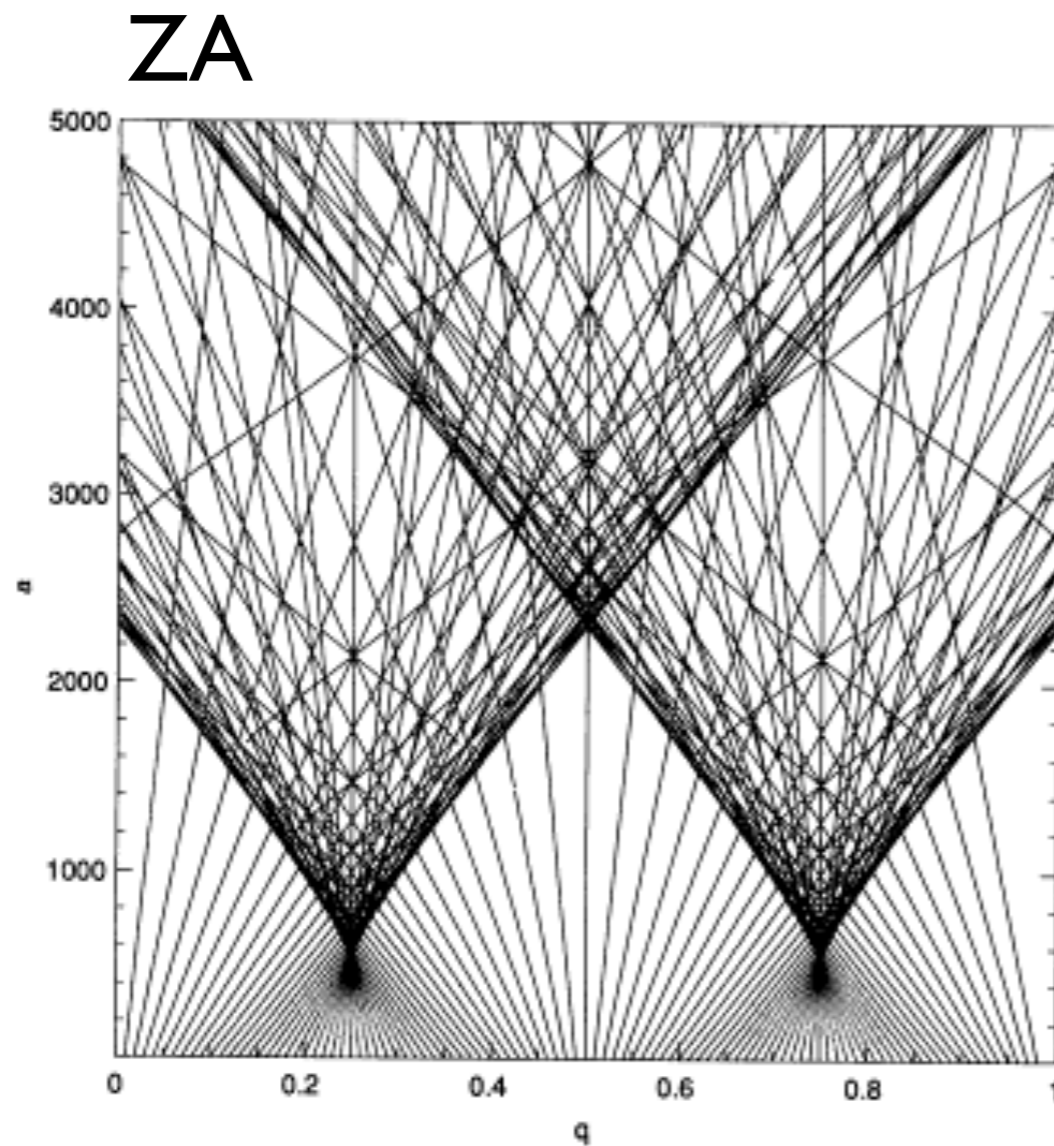
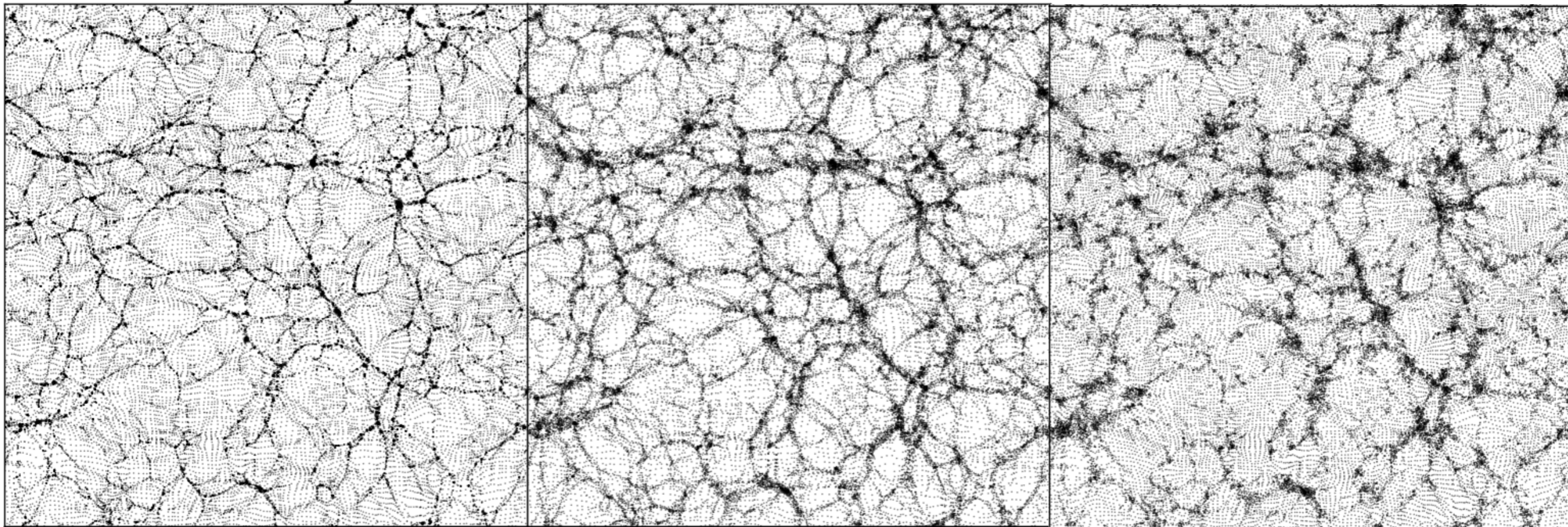


Figure 3. A family of trajectories corresponding to the model presented in Fig. 1 is shown for the first-order (upper panel) and second-order (lower panel) approximations. The trajectories end in the Eulerian space-time section ($y=0.5, t$) centred at a cluster. These plots illustrate that the three-stream system that develops after the first shell-crossing performs a self-oscillation due to the action of self-gravity.

Full N-body

Zel'dovich

2LPT



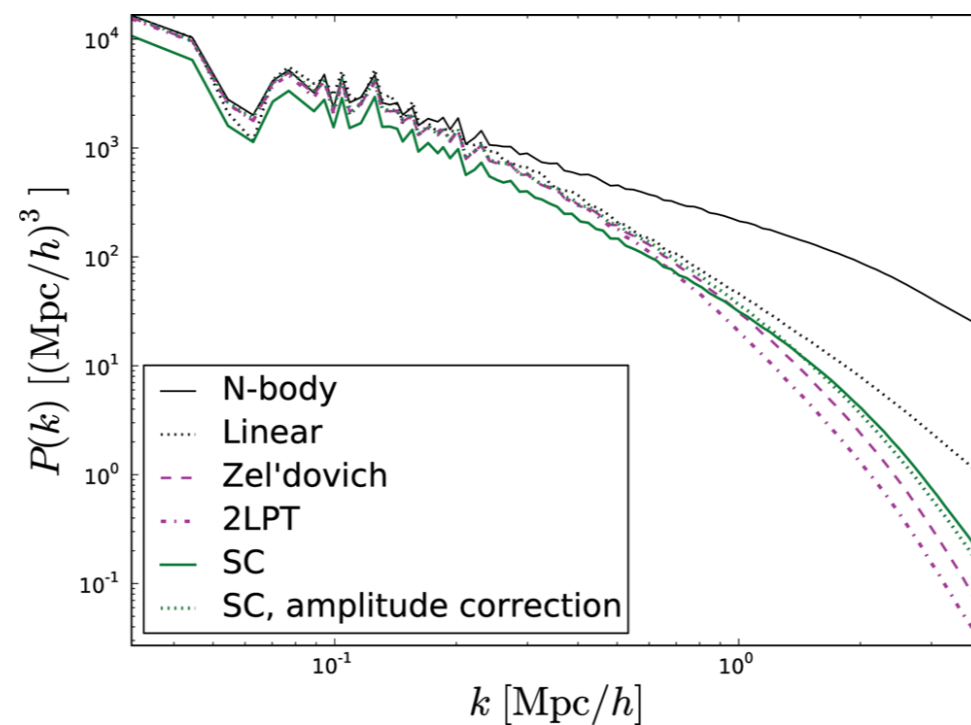
$N_{\text{particle}} = 256^3$

$L = 200 \text{ Mpc}/h$

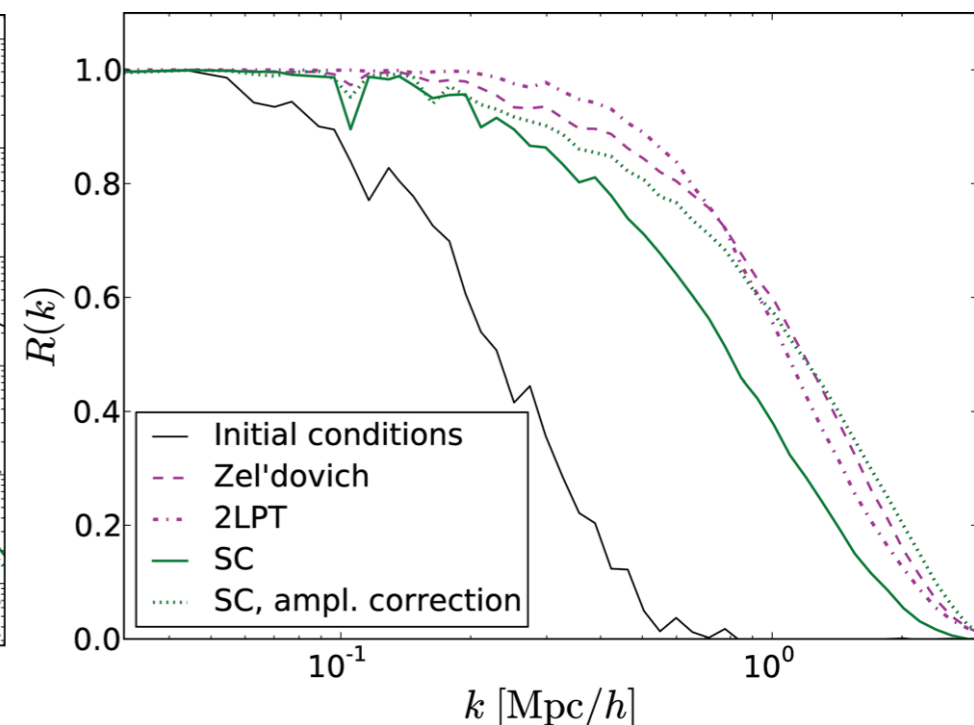
ΛCDM

Neyrink ('13)

power spectrum



cross correlation coeff.



Zel'dovich近似の応用

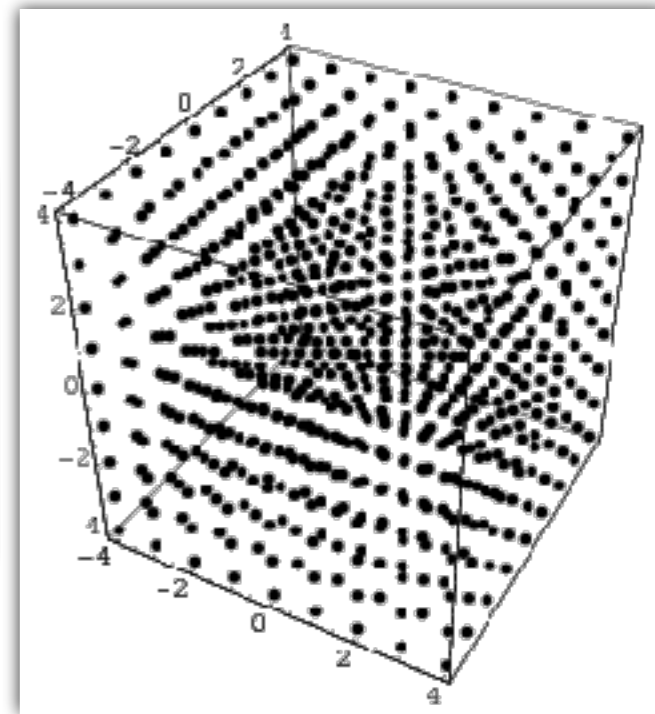
N体シミュレーションの初期条件生成に有用

粒子を格子状に並べてZel'dovich近似ですらす：

$$x = q + \Psi(q) \quad v = a\dot{x} = a\dot{\Psi}(q)$$

格子点の位置

変移場ベクトル



Zel'dovich近似：

$$\Psi(k) \simeq \frac{ik}{k^2} D_+(z) \delta_0(k)$$

初期密度ゆらぎ

計算の流れ

1. フーリエ空間上にランダムな初期密度場を生成 $\delta_0(k)$

2. 変移場ベクトルを計算： $\Psi(k) \xrightarrow{\text{FFT}} \Psi(q)$

3. 変移場ベクトルを使って粒子を移動： $\Psi(q) \quad \dot{\Psi}(q) = \frac{\dot{D}_+(z)}{D_+(z)} \Psi(q)$

Higher-order Lagrangian PT

e.g., Matsubara ('15)

PT expansion: $\Psi(\mathbf{q}, t) = \Psi^{(1)}(\mathbf{q}, t) + \Psi^{(2)}(\mathbf{q}, t) + \Psi^{(3)}(\mathbf{q}, t) + \dots$

Under Einstein-de Sitter approximation: $\Psi_{\text{EdS}}^{(n)}(\mathbf{q}; a(t)) \longrightarrow \Psi^{(n)}(\mathbf{q}; D_1(t))$

Longitudinal: $\left(\frac{\partial^2}{\partial \eta^2} + \frac{1}{2} \frac{\partial}{\partial \eta} - \frac{3}{2}\right) \Psi_{k,k}^{(n)}$

$\eta \equiv \ln D_1(t)$

$$= - \sum_{m_1+m_2=n} \epsilon_{ijk} \epsilon_{ipq} \Psi_{j,p}^{(m_1)} \left(\frac{\partial^2}{\partial \eta^2} + \frac{1}{2} \frac{\partial}{\partial \eta} - \frac{3}{4}\right) \psi_{k,q}^{(m_2)}$$

vanished in 1D

$$- \frac{1}{2} \sum_{m_1+m_2+m_3=n} \epsilon_{ijk} \epsilon_{pqr} \Psi_{i,p}^{(m_1)} \Psi_{j,q}^{(m_2)} \left(\frac{\partial^2}{\partial \eta^2} + \frac{1}{2} \frac{\partial}{\partial \eta} - \frac{1}{2}\right) \Psi_{k,r}^{(m_3)},$$

vanished in 2D

Transverse: $\epsilon_{ijk} \left(\frac{\partial^2}{\partial \eta^2} + \frac{1}{2} \frac{\partial}{\partial \eta}\right) \Psi_{j,k}^{(n)} = - \sum_{m_1+m_2=n} \epsilon_{ijk} \Psi_{p,j}^{(m_1)} \left(\frac{\partial^2}{\partial \eta^2} + \frac{1}{2} \frac{\partial}{\partial \eta}\right) \Psi_{p,k}^{(m_2)}$

vanished in 1D

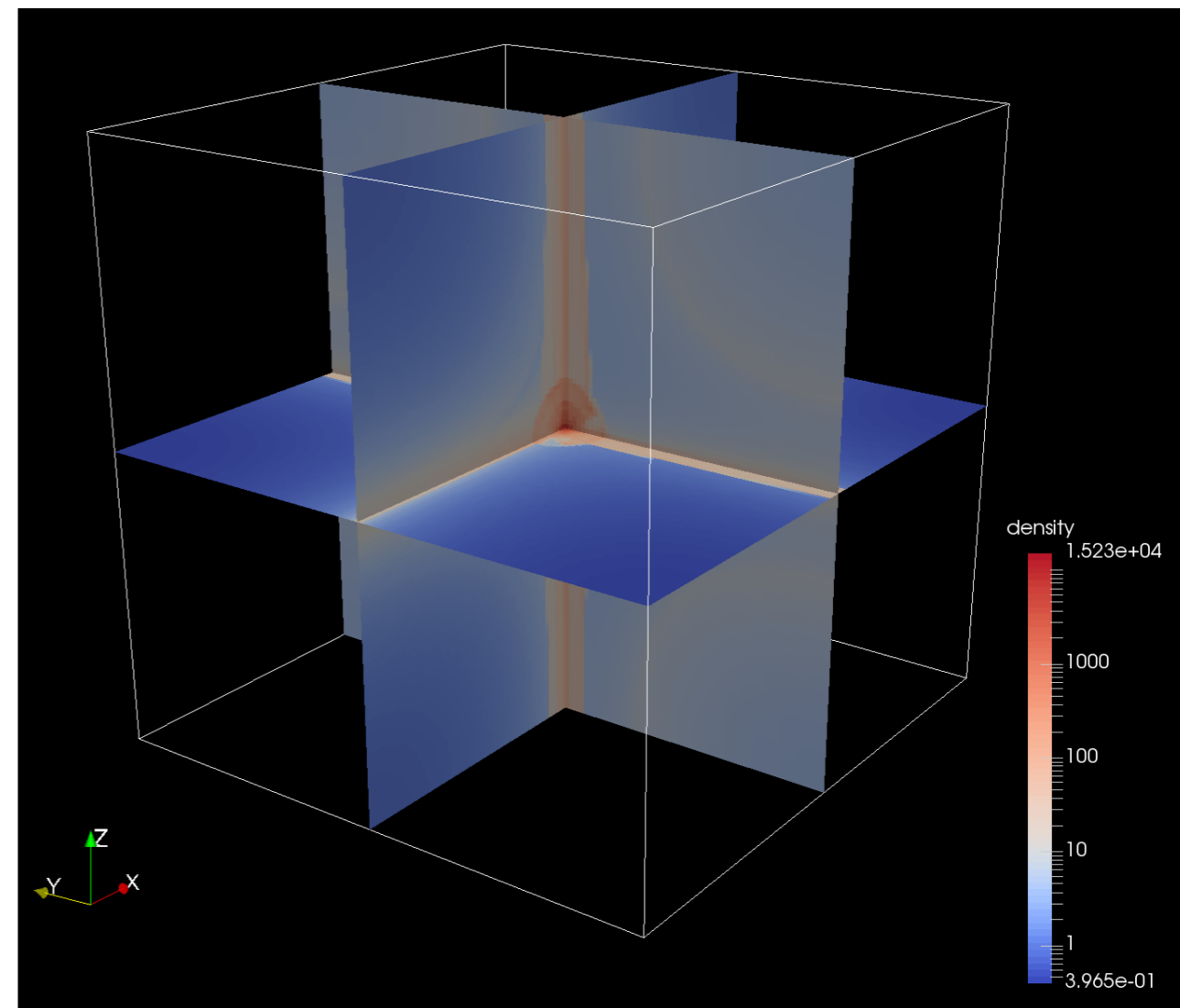
Performance of Lagrangian PT

Saga, AT & Colombi, arXiv:1805.08787

初期条件
(Zel'dovich近似解)

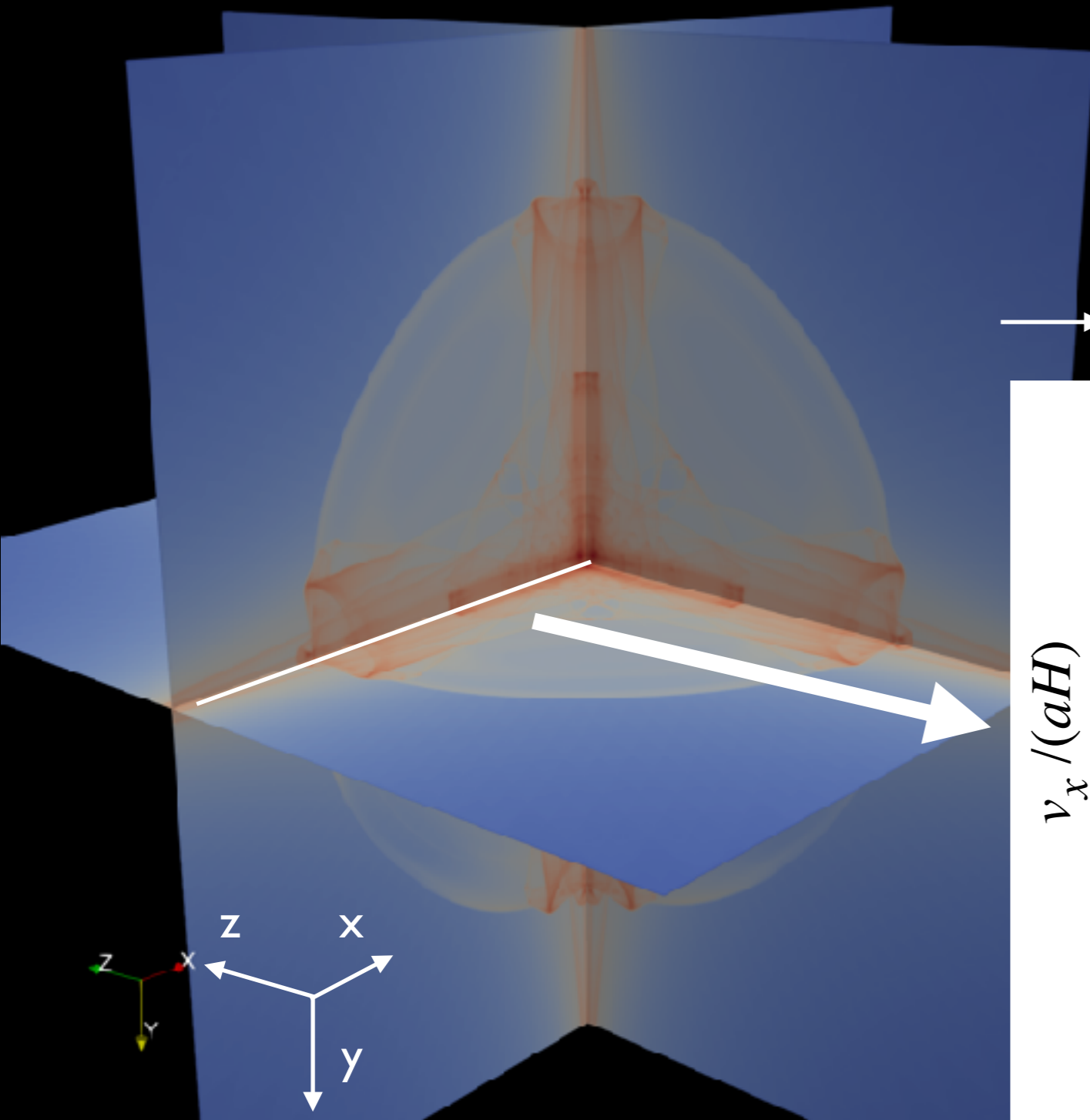
$$\Psi(\mathbf{q}) = a_{\text{init}} \begin{pmatrix} \epsilon_x \sin q_x \\ \epsilon_y \sin q_y \\ \epsilon_z \sin q_z \end{pmatrix}$$

10次まで計算



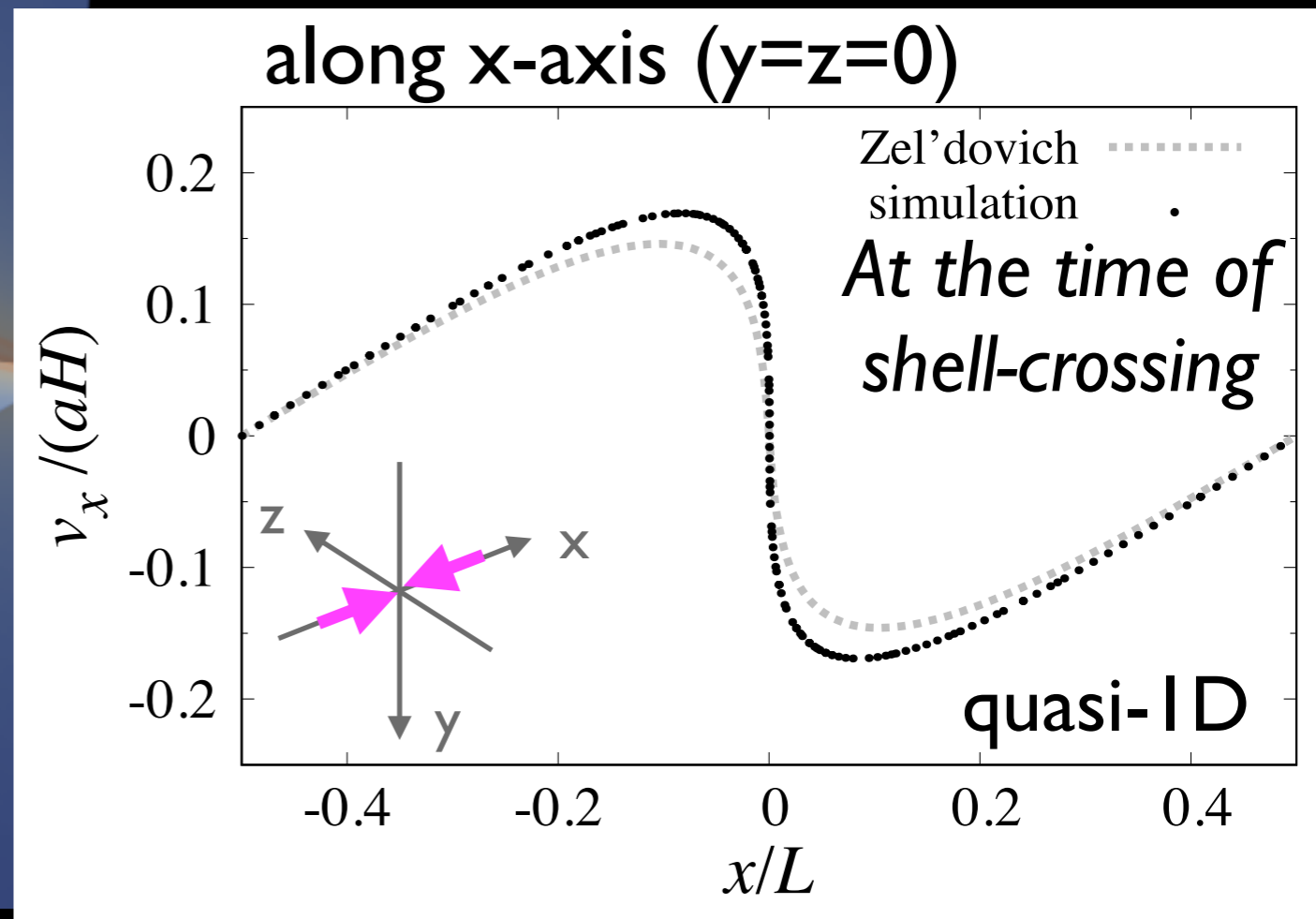
Results

Saga, AT & Colombi, arXiv:1805.08787

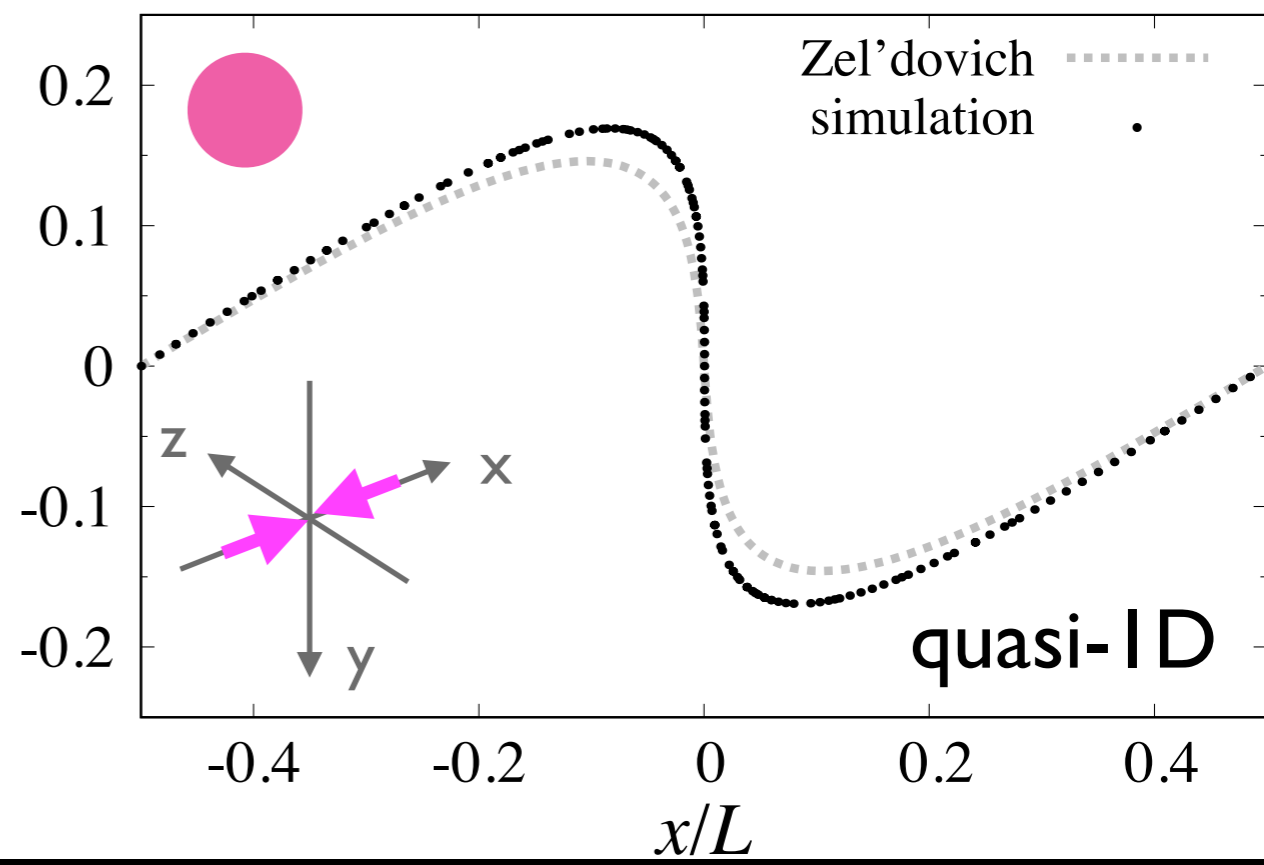
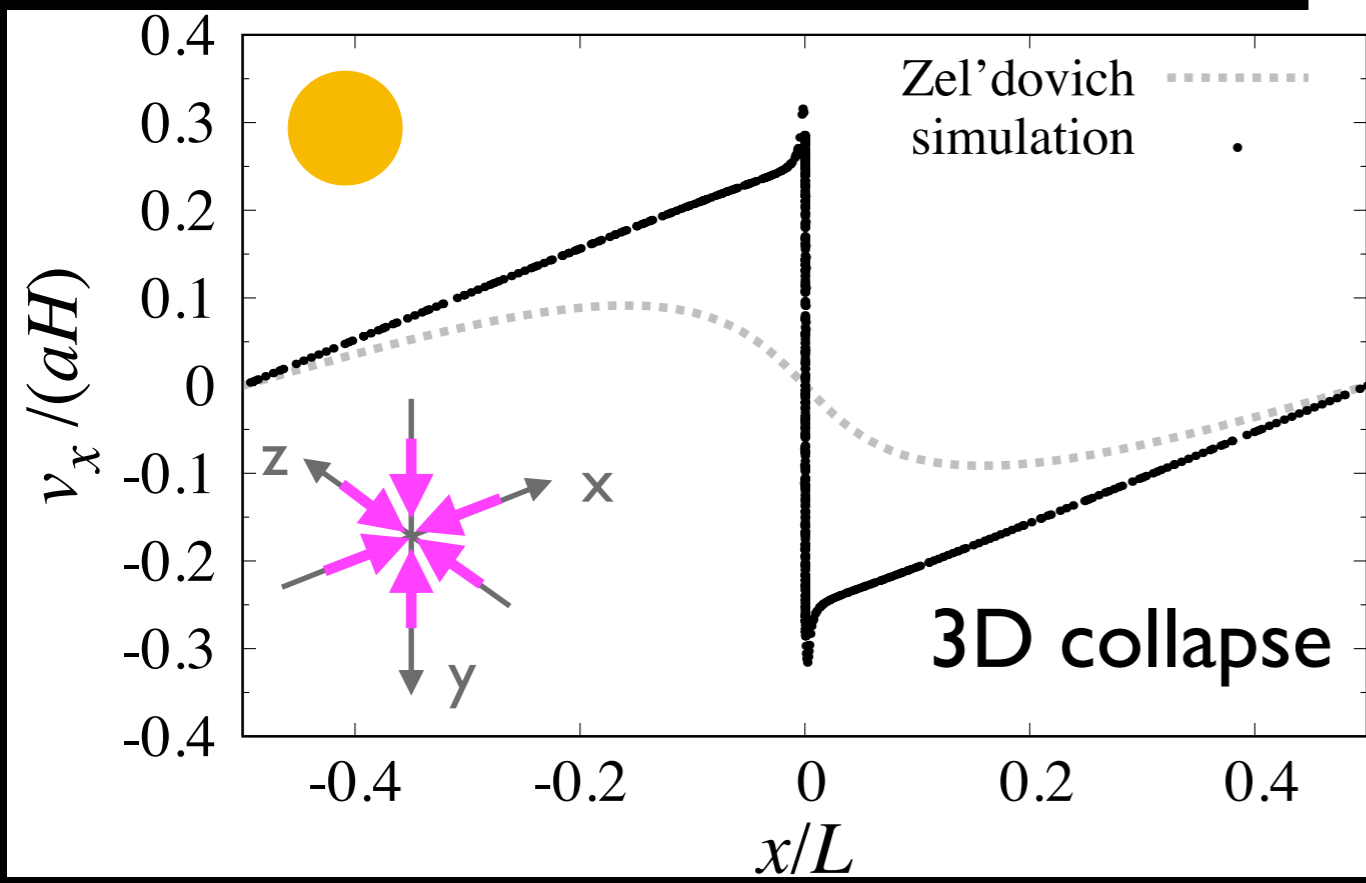
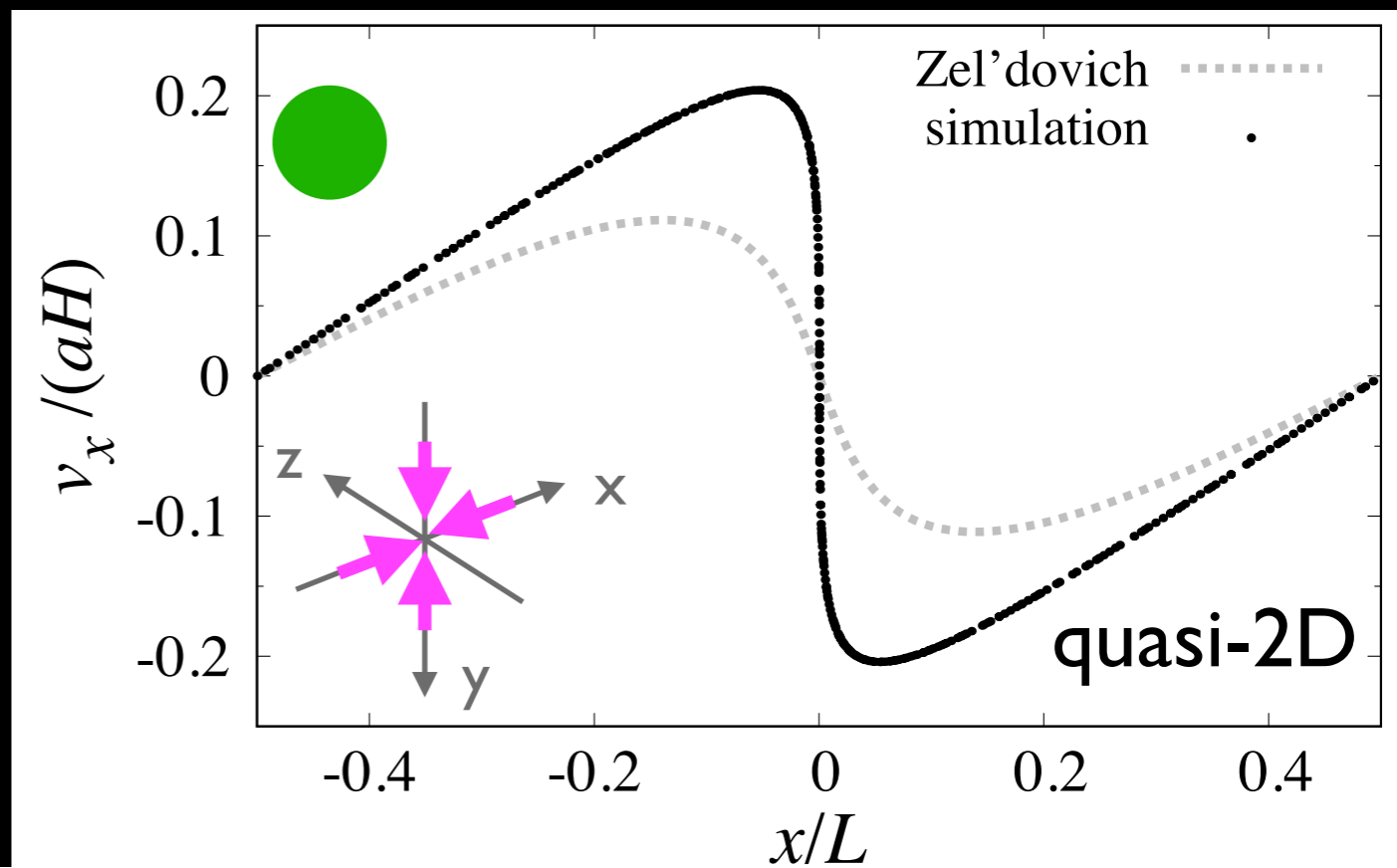
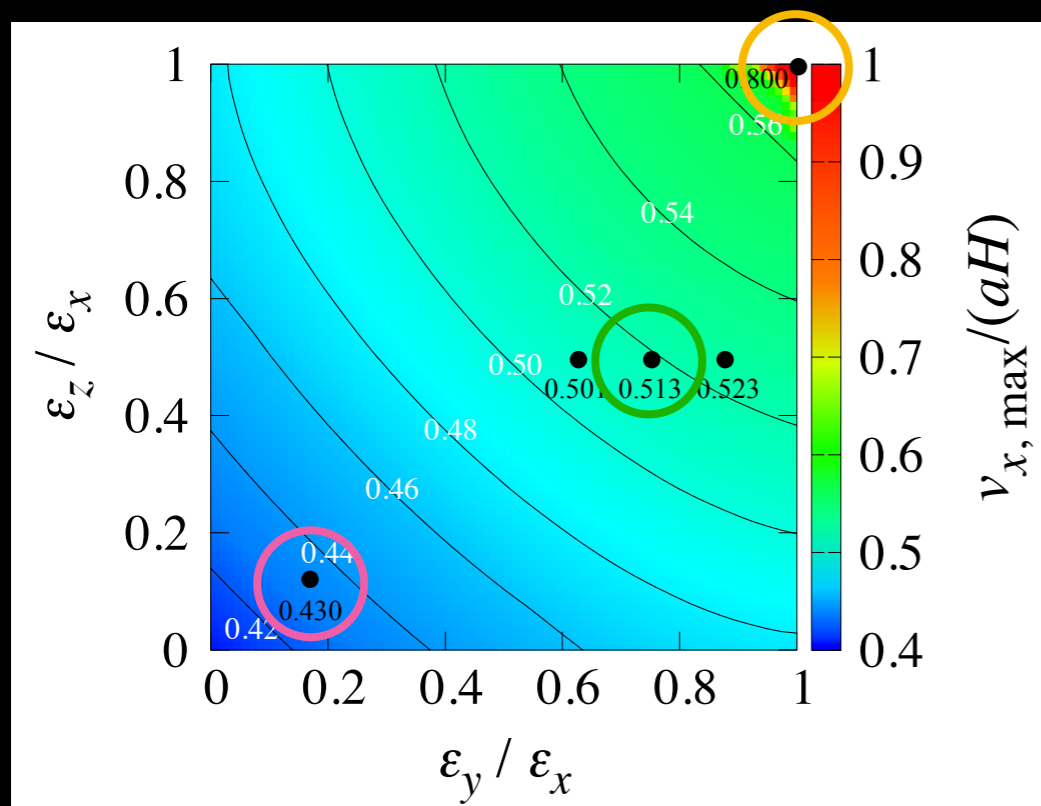


Single density peak in a periodic boundary box
(sinusoidal function)

→ Shell-crossing happens at origin

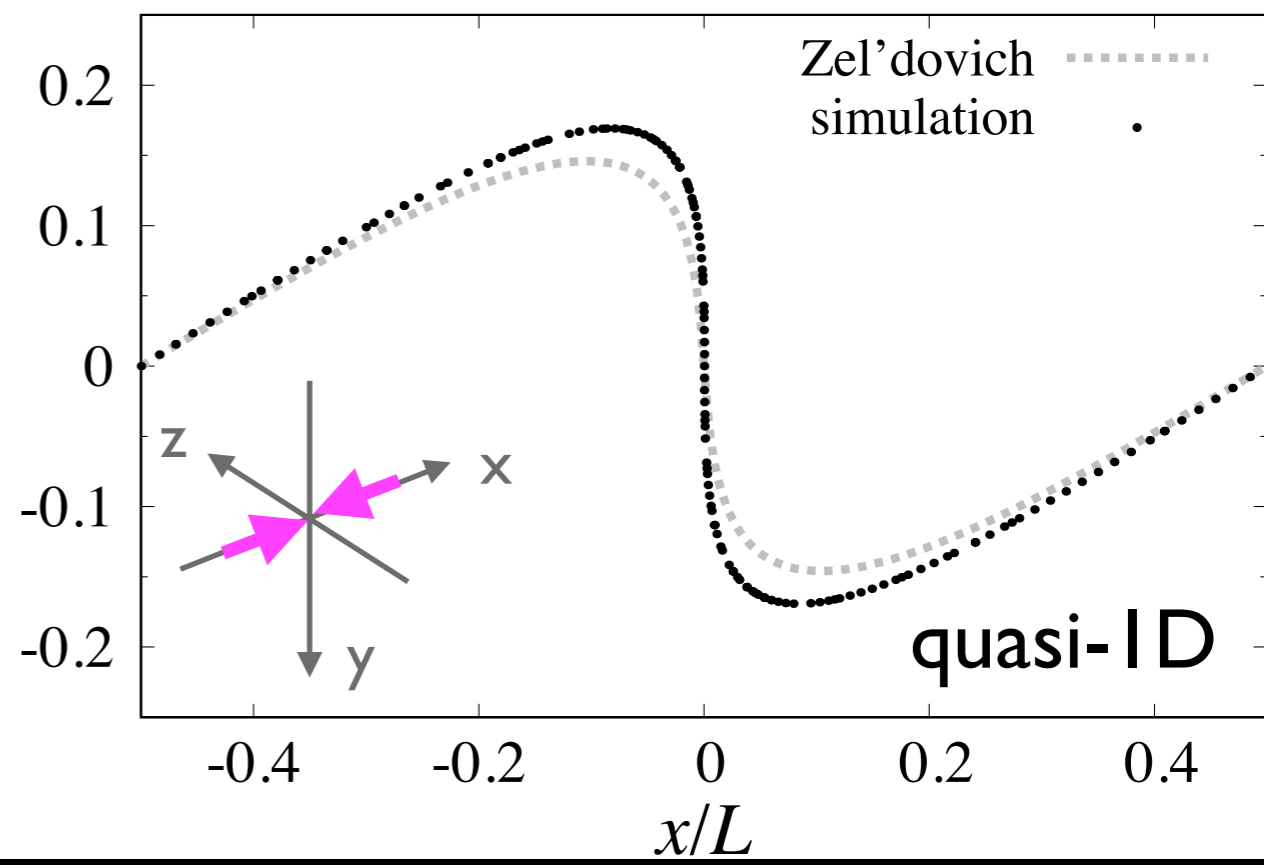
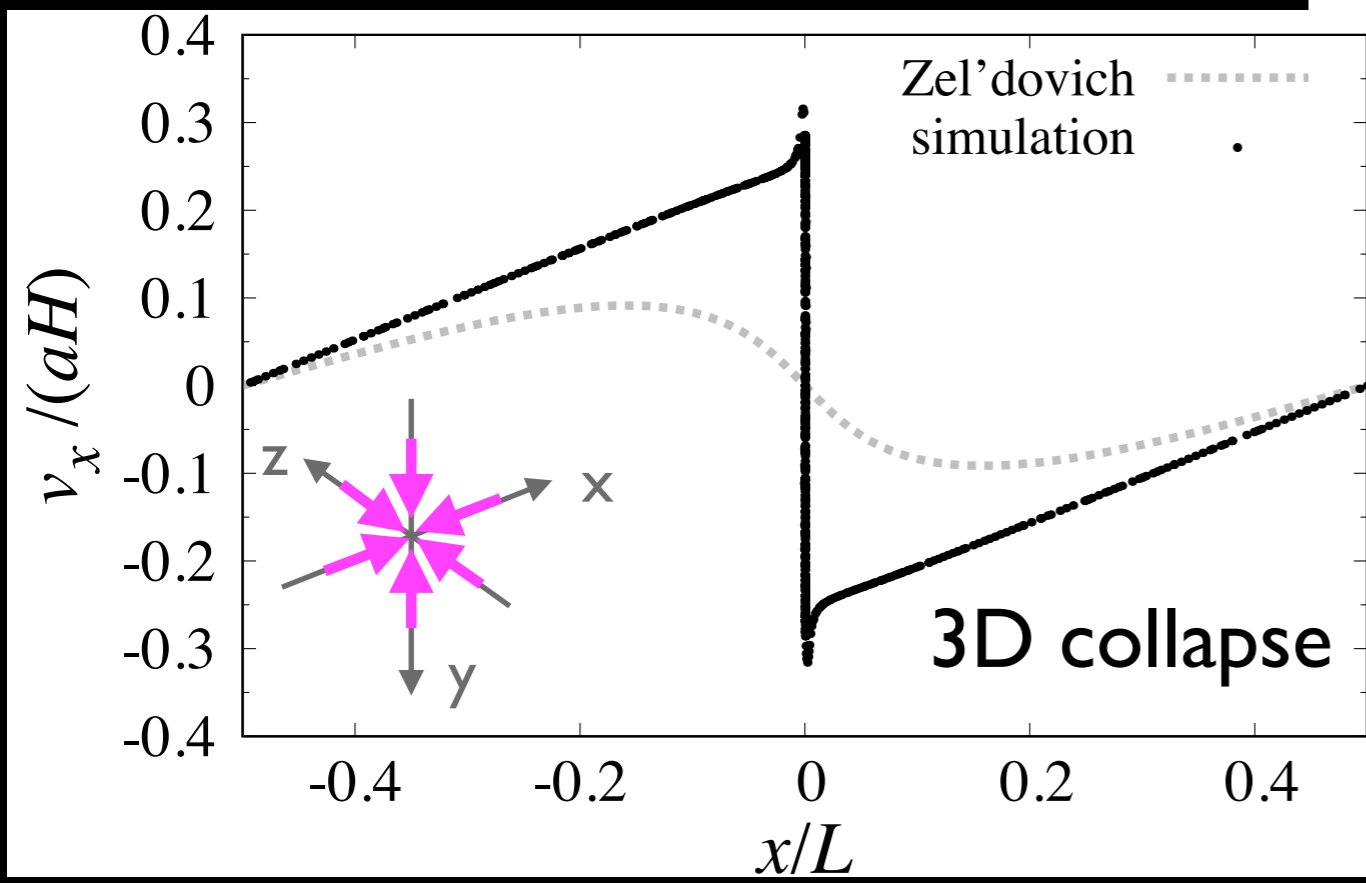
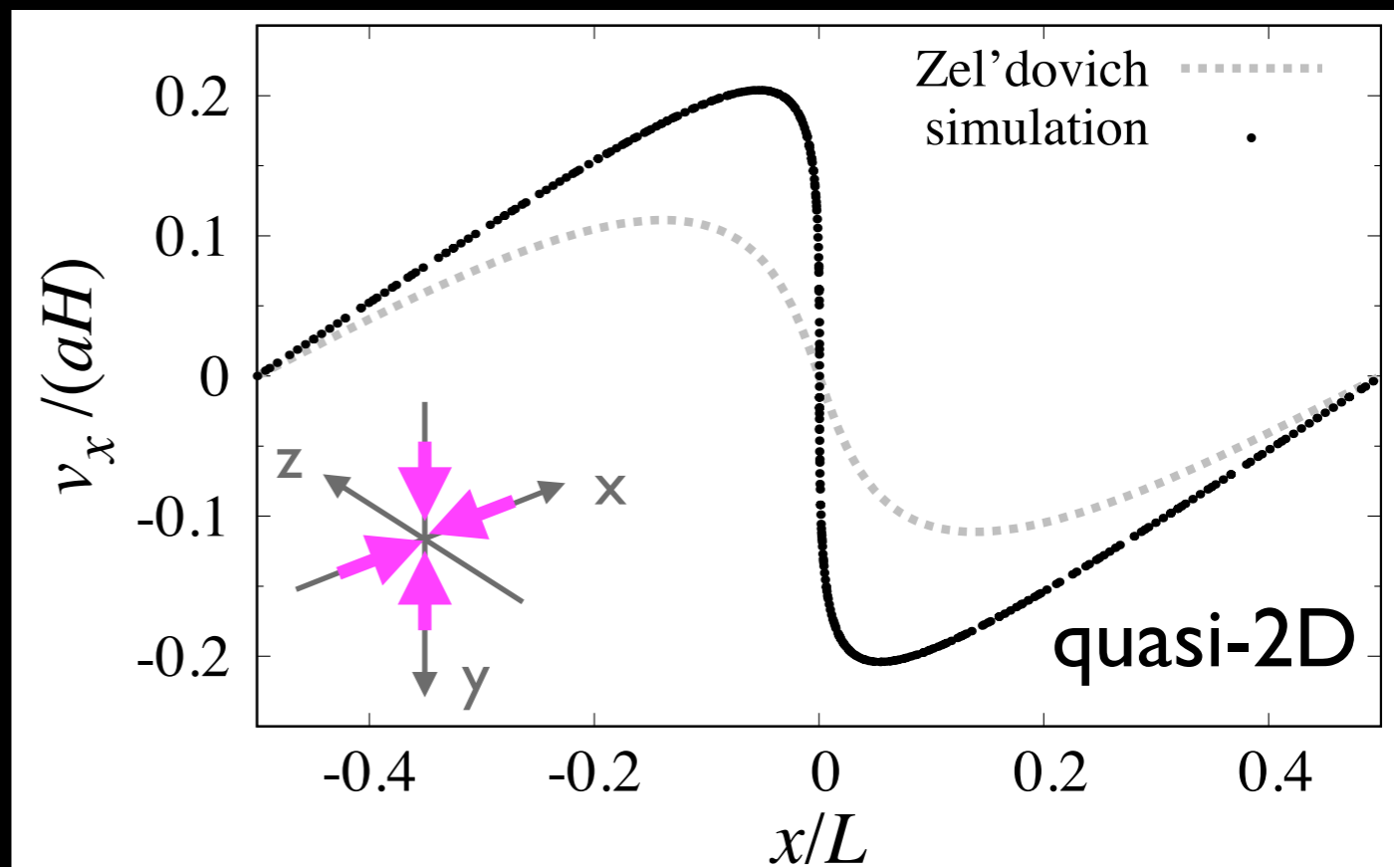


Vlasov simulation vs LPT



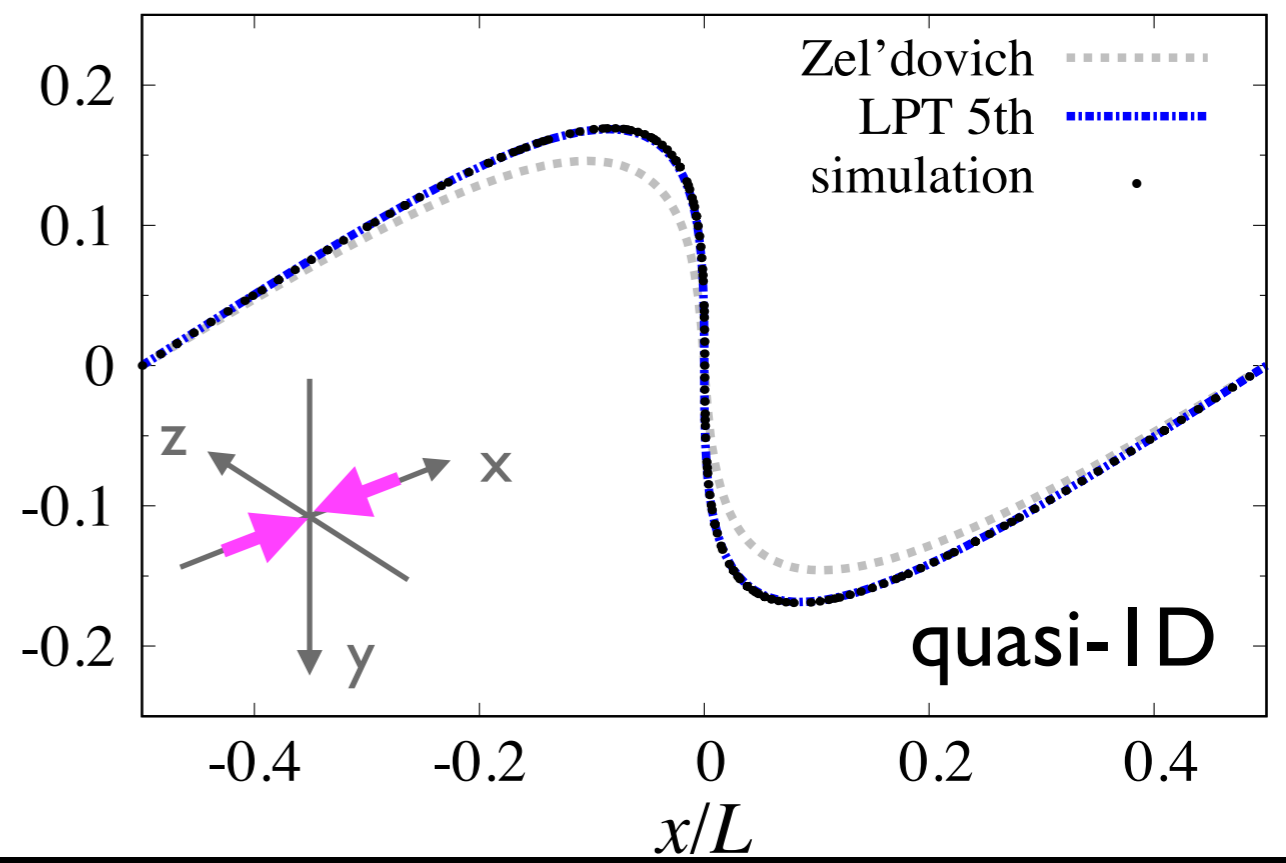
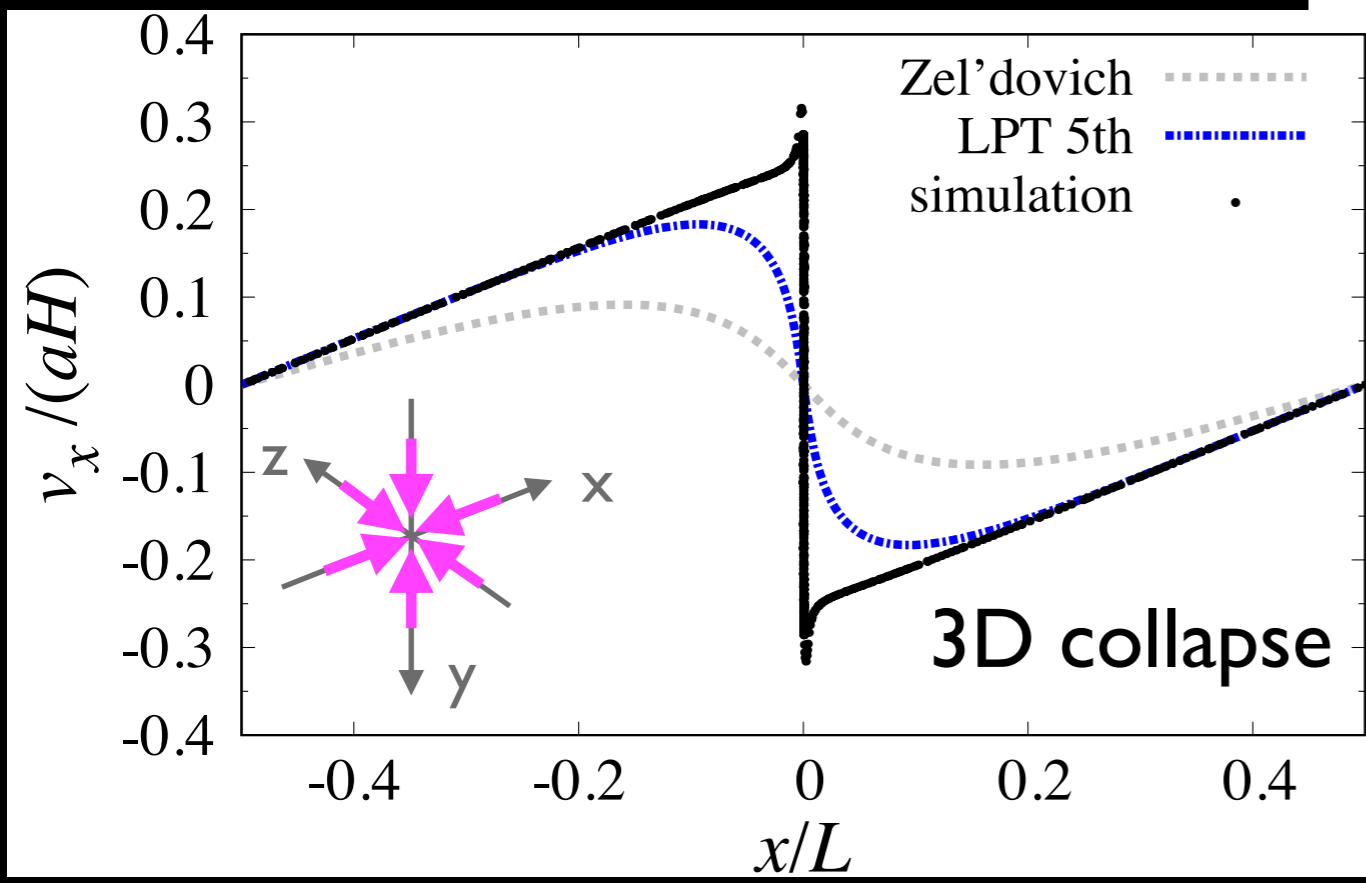
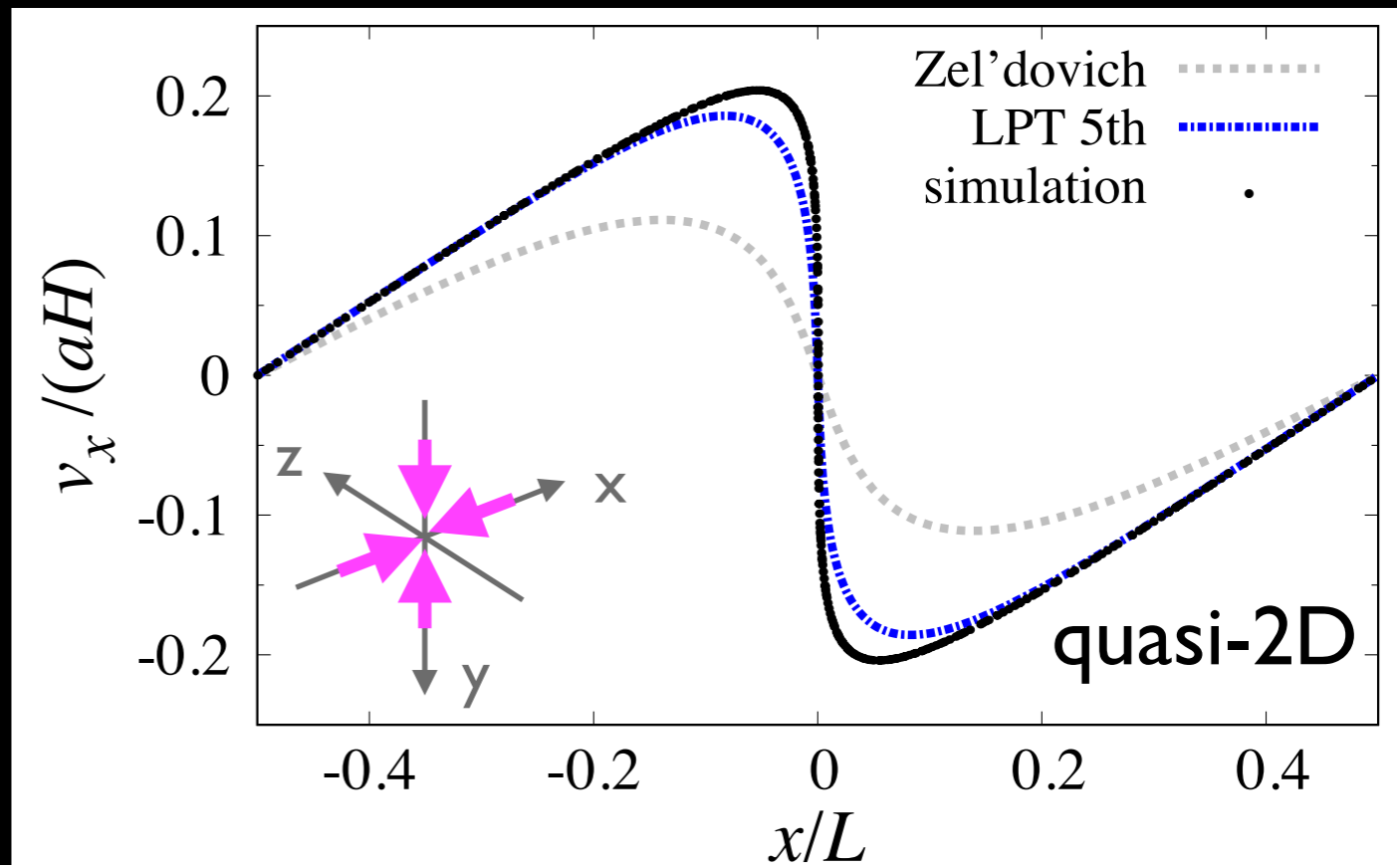
Vlasov simulation vs LPT

シェクルロツシング
時における比較
(原点で密度場発散)

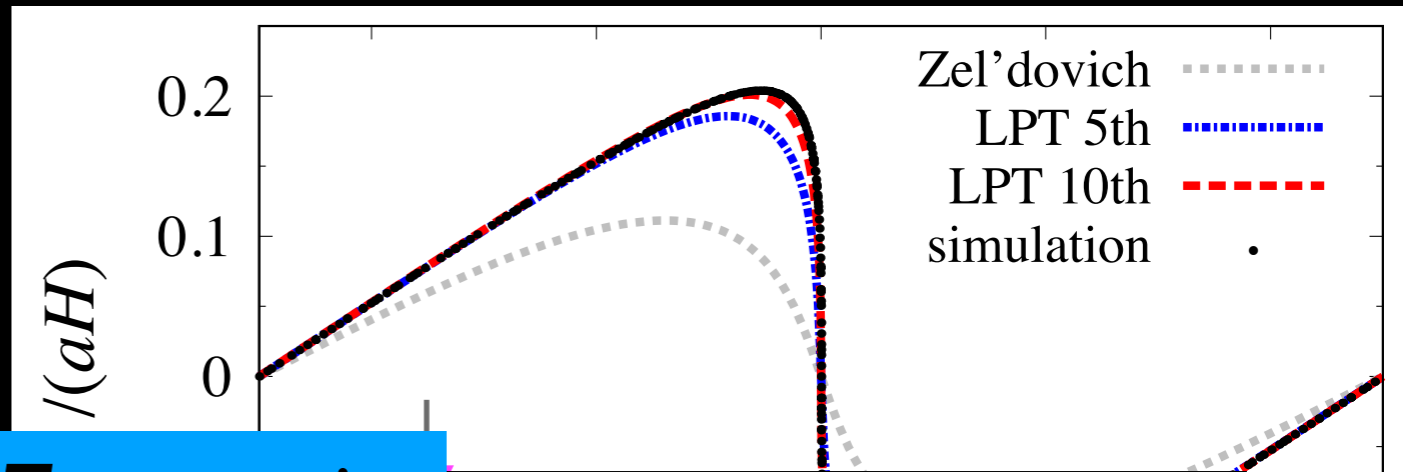


Vlasov simulation vs LPT

5th-order Lagrangian PT



Vlasov simulation vs LPT



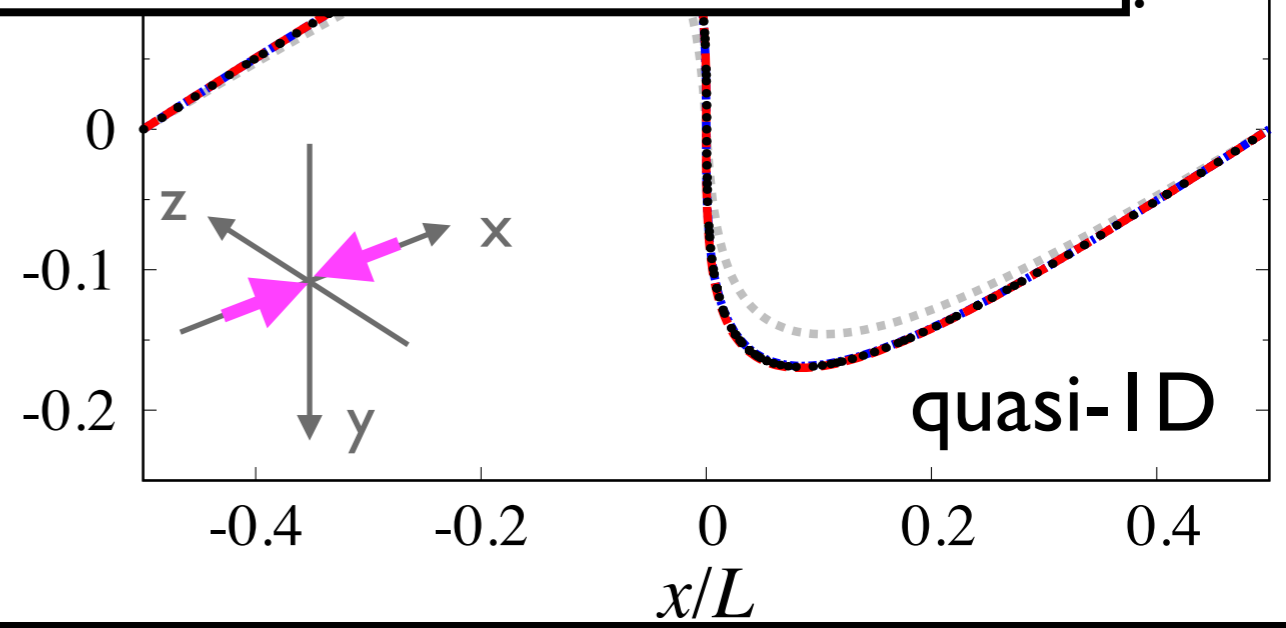
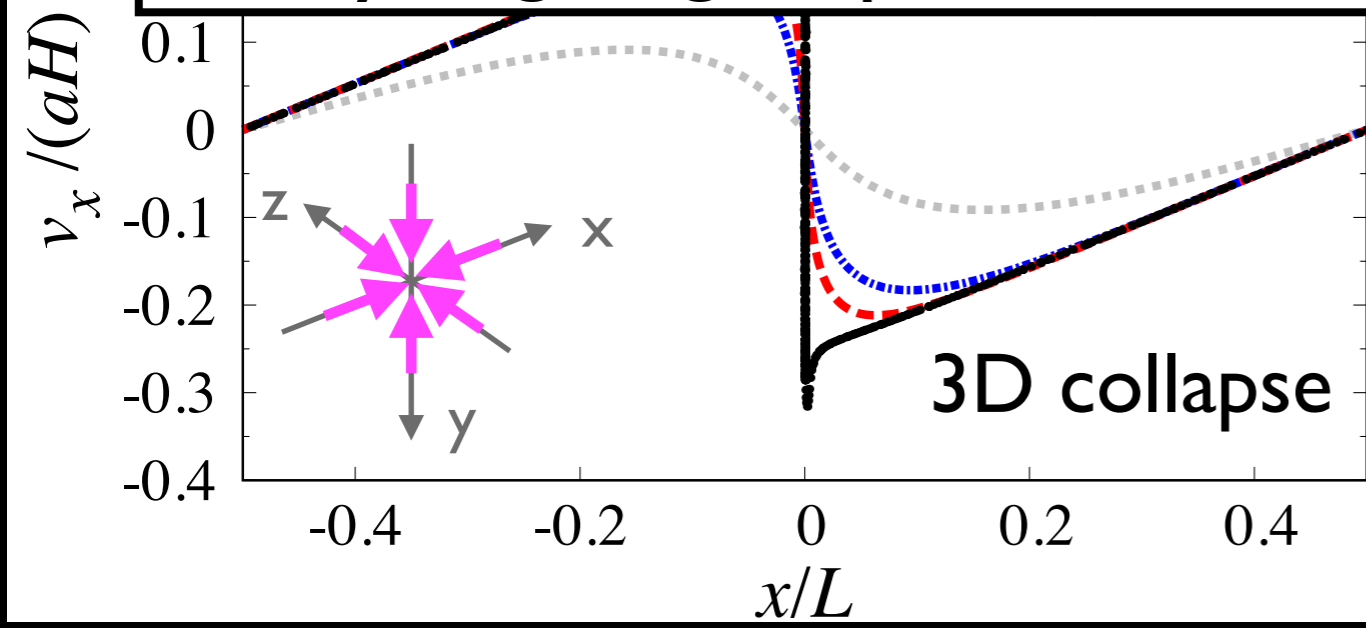
Making use of convergence of LPT expansion

$x_{\text{LPT}}(q)$ at n -th order is found to be accurately fitted to

$$a + \frac{1}{b + c \exp[dn^e]} \xrightarrow{n \rightarrow \infty} a \quad \text{Extrapolation}$$

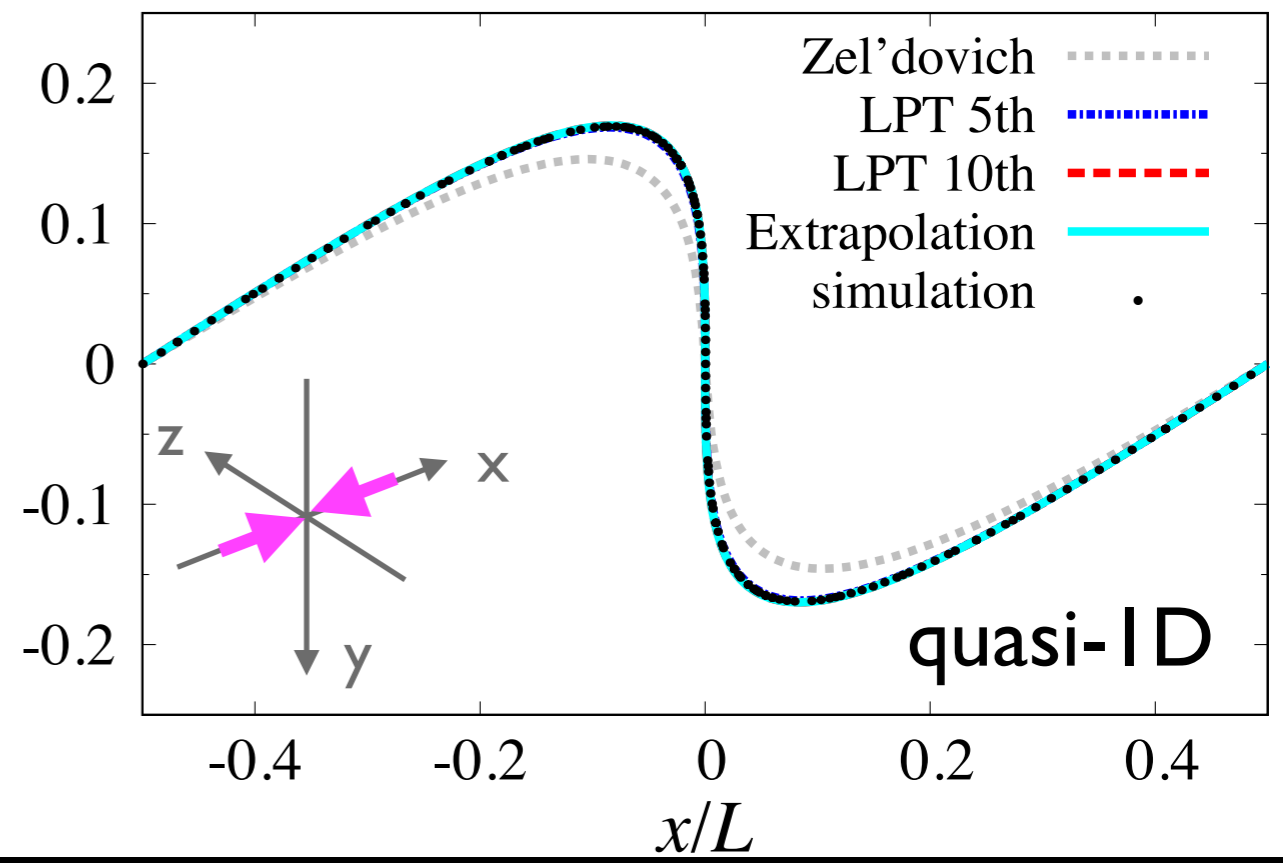
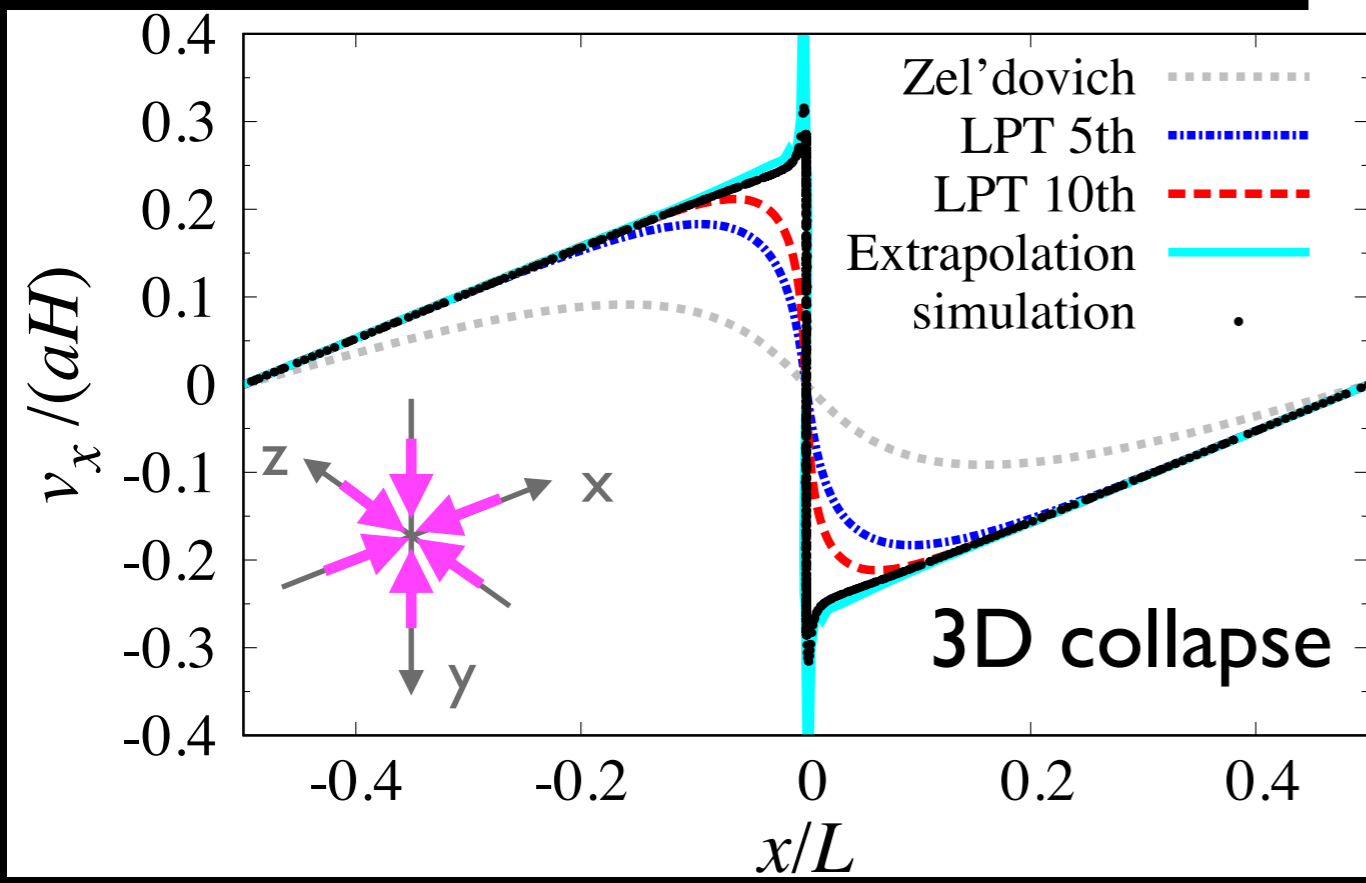
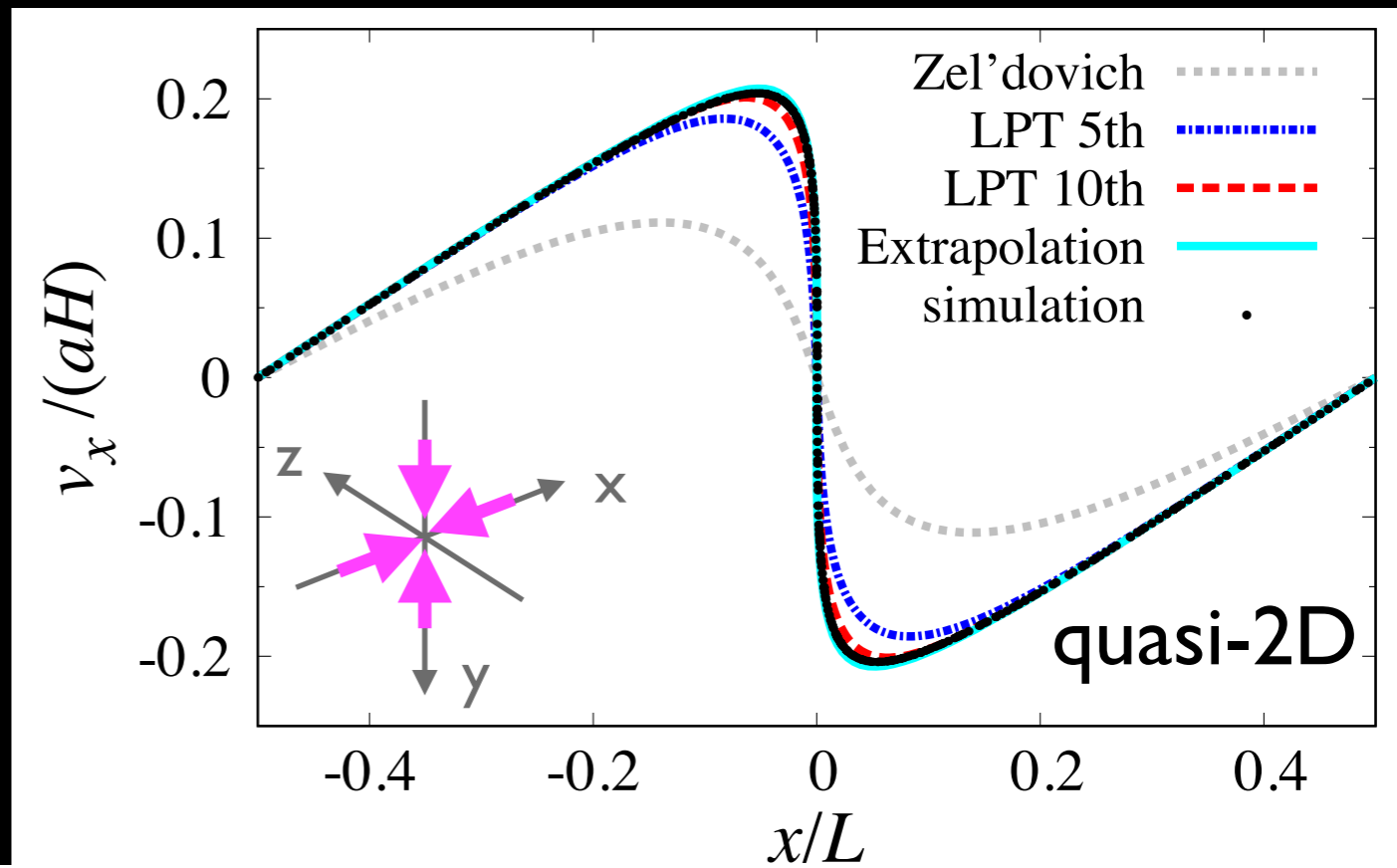
(a, \dots, e : fitting parameter)

at any Lagrangian position



Vlasov simulation vs LPT

Extrapolation based on LPT

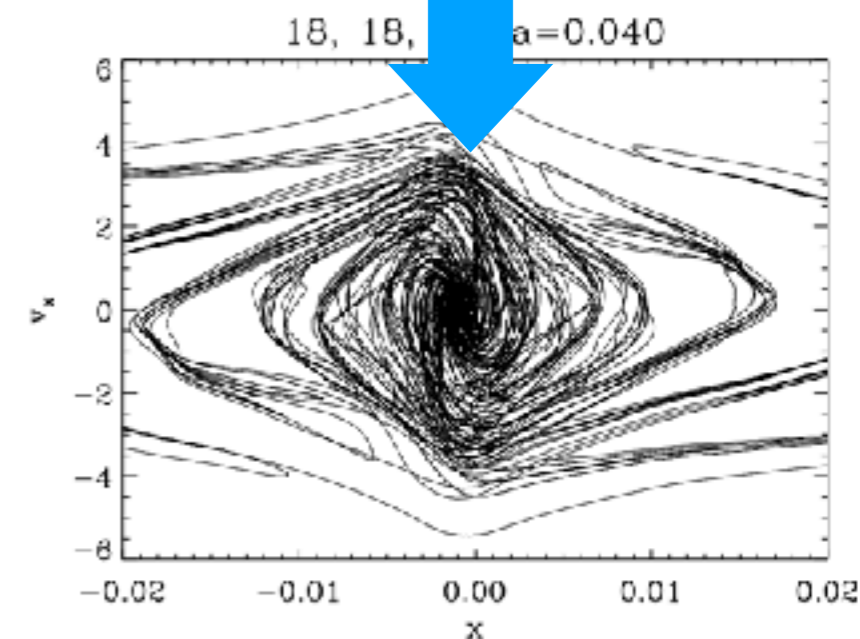
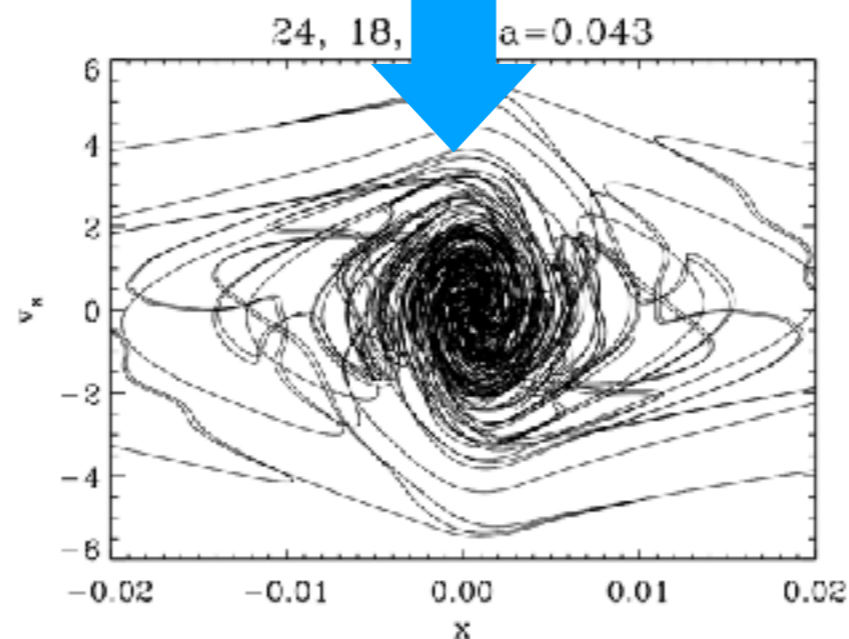
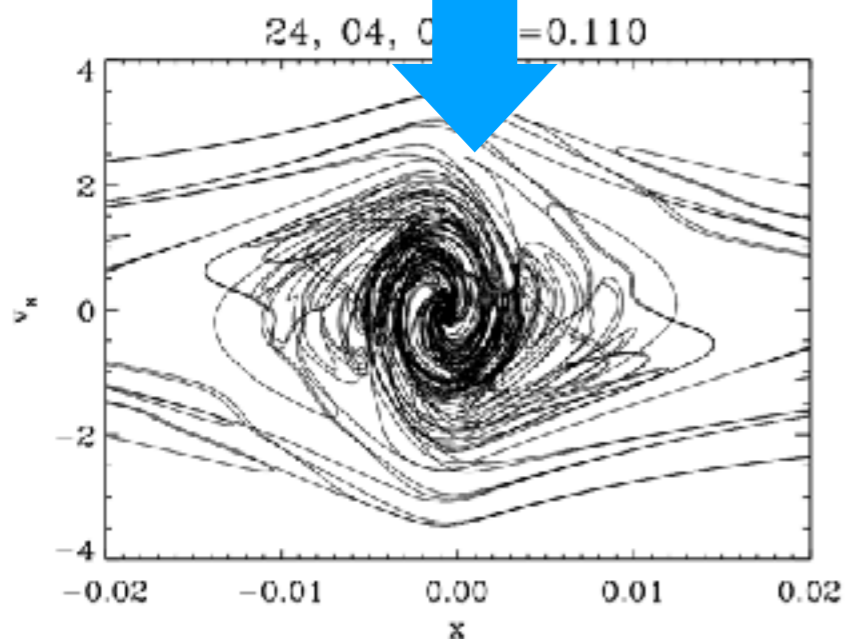
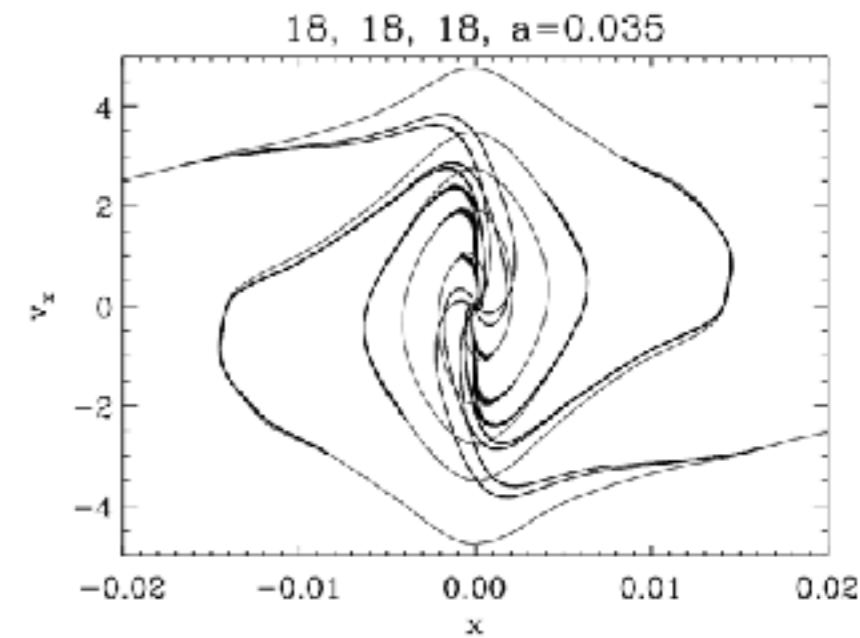
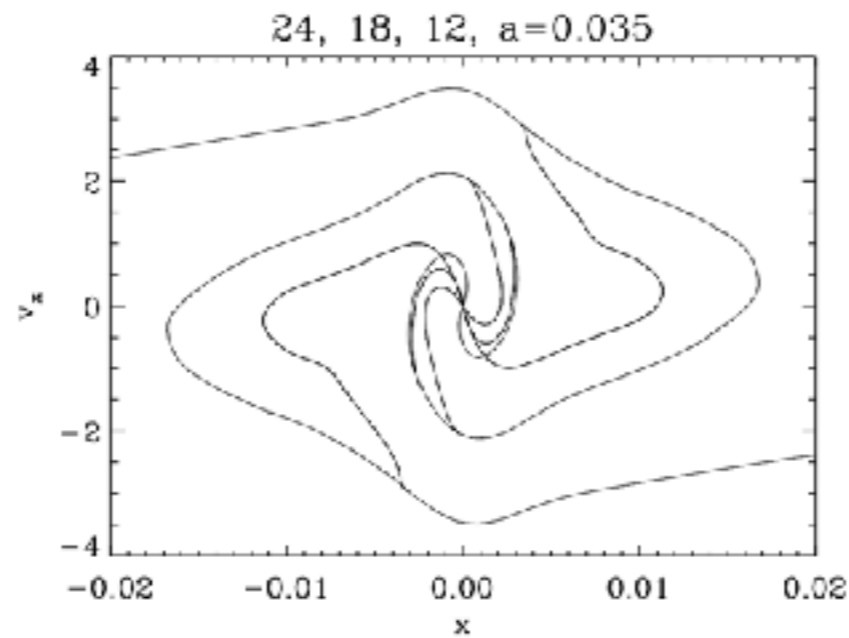
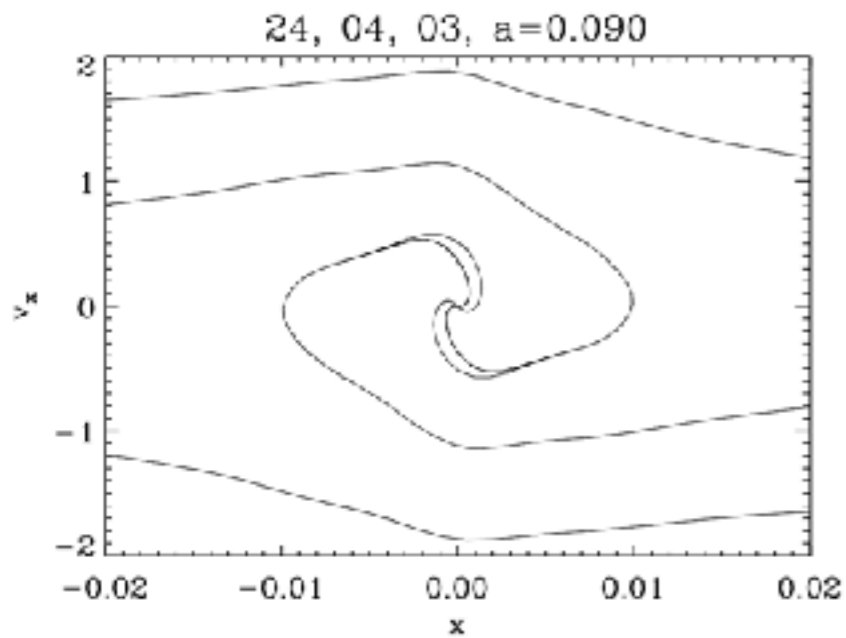


After shell-crossing,

quasi-1D collapse

quasi-2D collapse

3D collapse

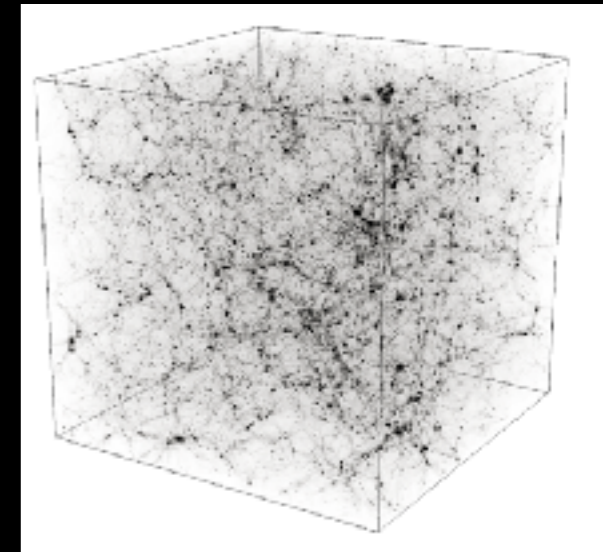


マルチストリーム構造が発達 (ハローが形成)

Cosmological N -body simulations

Directly solve equation of motion for N particles

→ Run N -body simulation many times with a large number of particles in a huge box



To reduce $O(N^2)$ operation for force calculation,

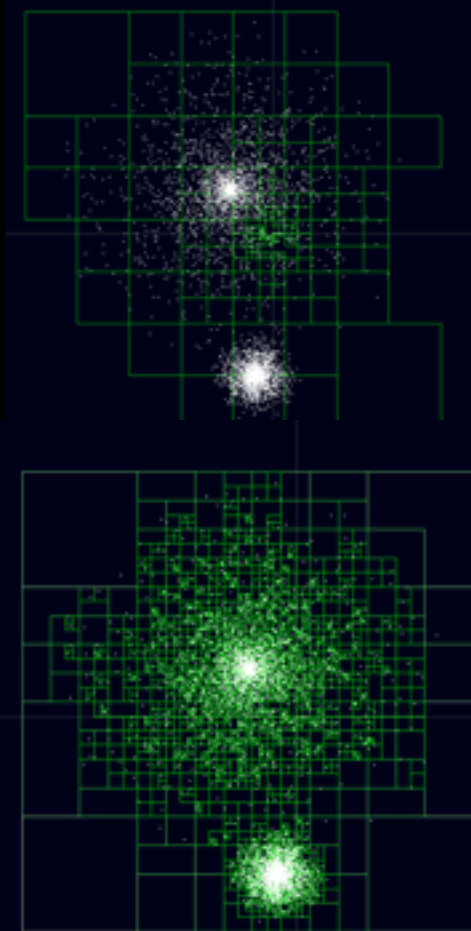
- $O(N \log N)$
- Tree algorithm
 - Particle-Mesh algorithm (using FFT)

For cosmological study

$N \sim 1,000^3$, $L \sim 1,000$ Mpc, >50 runs

Still extensive but very useful for practical purposes :

mock data analysis, locating 'galaxies' in dark matter halo, ...



Tree-PM method for force calculation

In Fourier space,

$$\phi_k = \phi_k^{\text{long}} + \phi_k^{\text{short}}$$

$$\phi_k^{\text{long}} = \phi_k \exp(-k^2 r_s^2)$$

$$\phi_k^{\text{short}} = \phi_k [1 - \exp(-k^2 r_s^2)] \longrightarrow \phi^{\text{short}}(\mathbf{x}) = -G \sum_i \frac{m_i}{r_i} \operatorname{erfc}\left(\frac{r_i}{2r_s}\right)$$

$r_i = \min(|\mathbf{x} - \mathbf{r}_i - \mathbf{n}L|)$

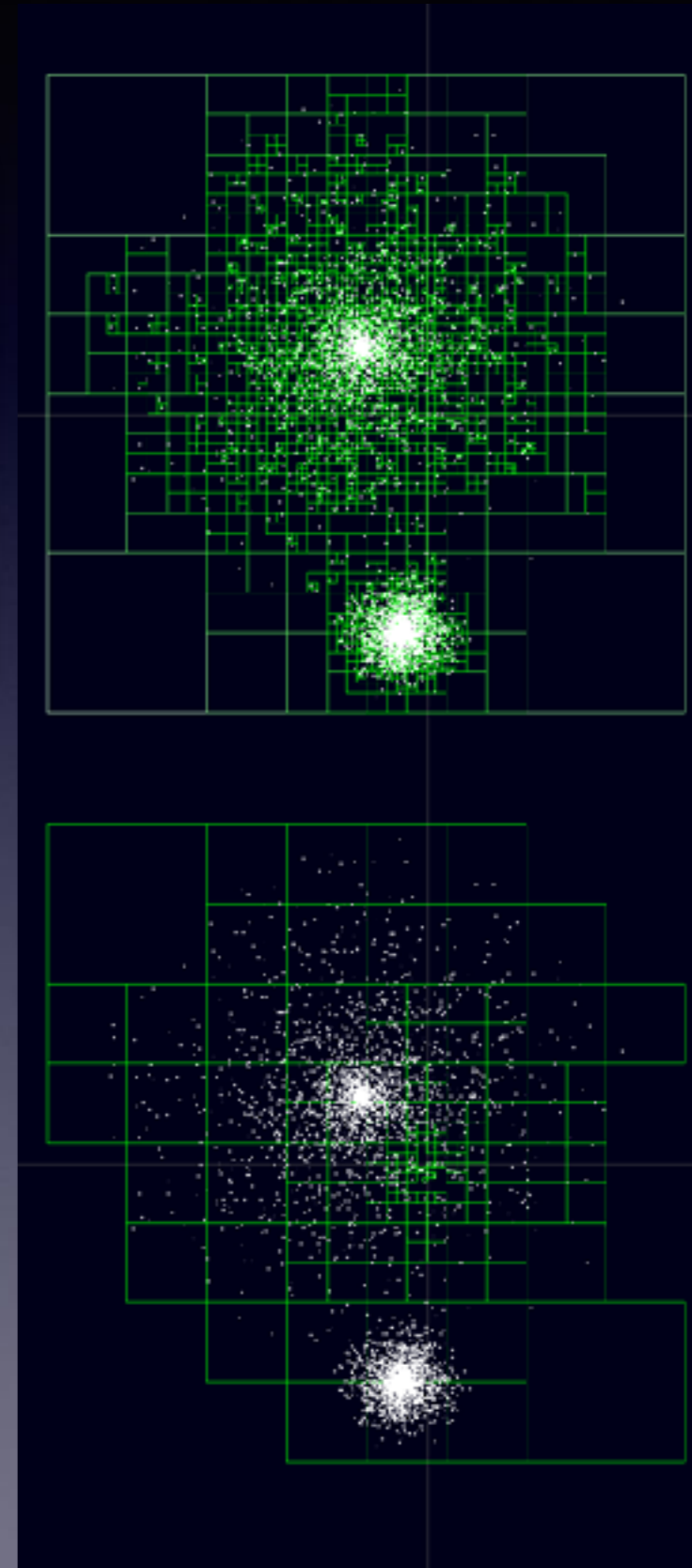
- long-range: PM method with FFT

- short-range: Tree algorithm

(Barnes-Hut oct-tree)

<http://arborjs.org/docs/barnes-hut>

Performance of each method is $O(N \log N)$



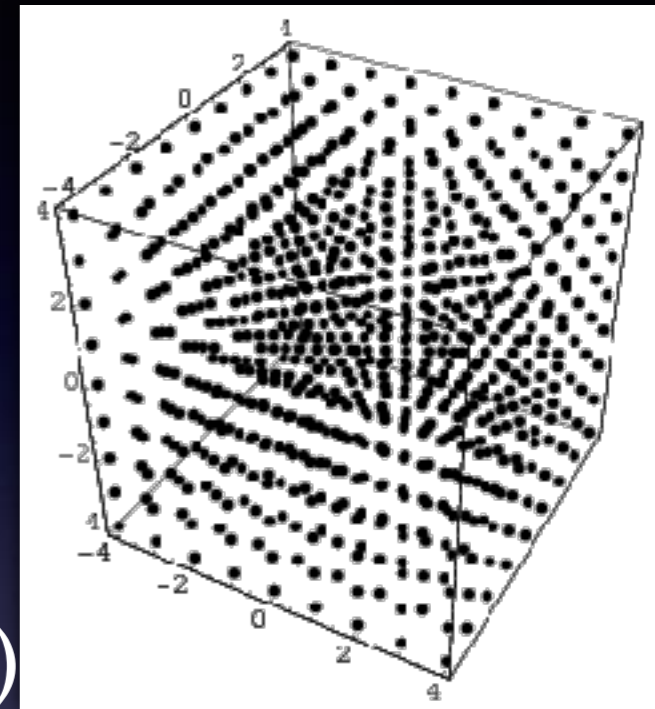
Cosmological initial condition

For particle assigned on each grid:

$$x = q + \Psi(q)$$

initial position
Lagrangian displacement

Note $v = a\dot{x} = a\dot{\Psi}(q)$



'q' is called Lagrangian coordinate (homogeneous mass dist)

leading order (Zel'dovich approx.) $\Psi(k) \simeq \frac{ik}{k^2} D_+(z) \delta_0(k)$ initial density field (random)

General procedure

Improved initial condition generator with Lagrangian PT (2LPT code)

1. generate random field $\delta_0(k)$

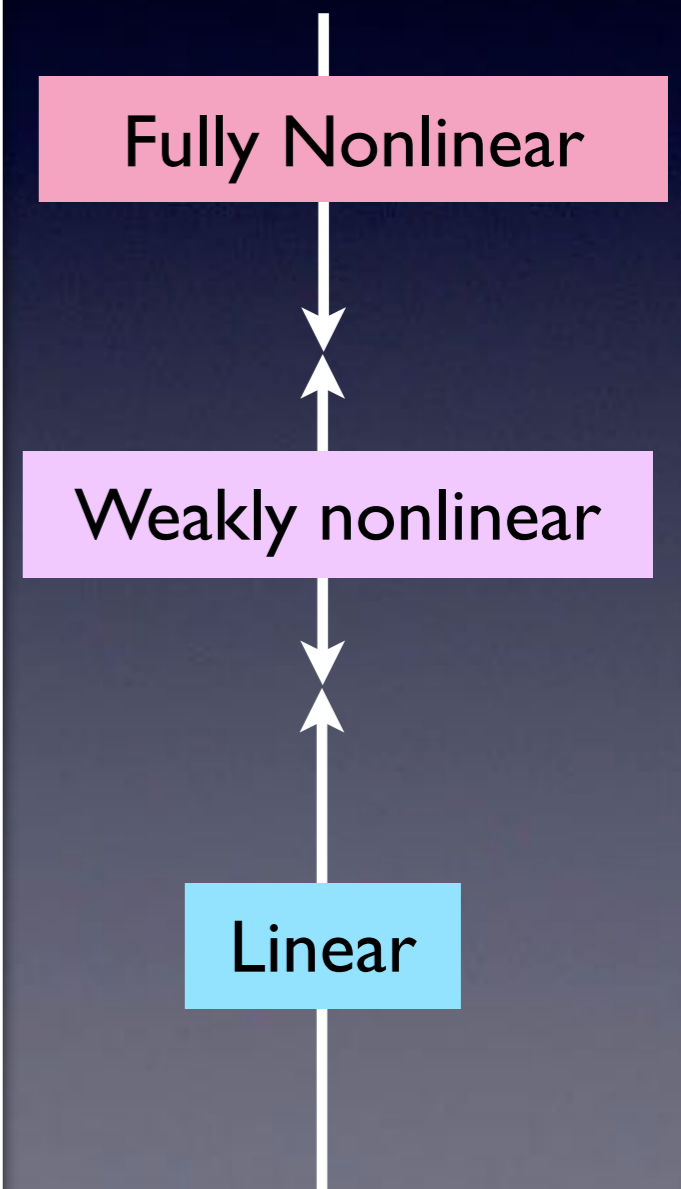
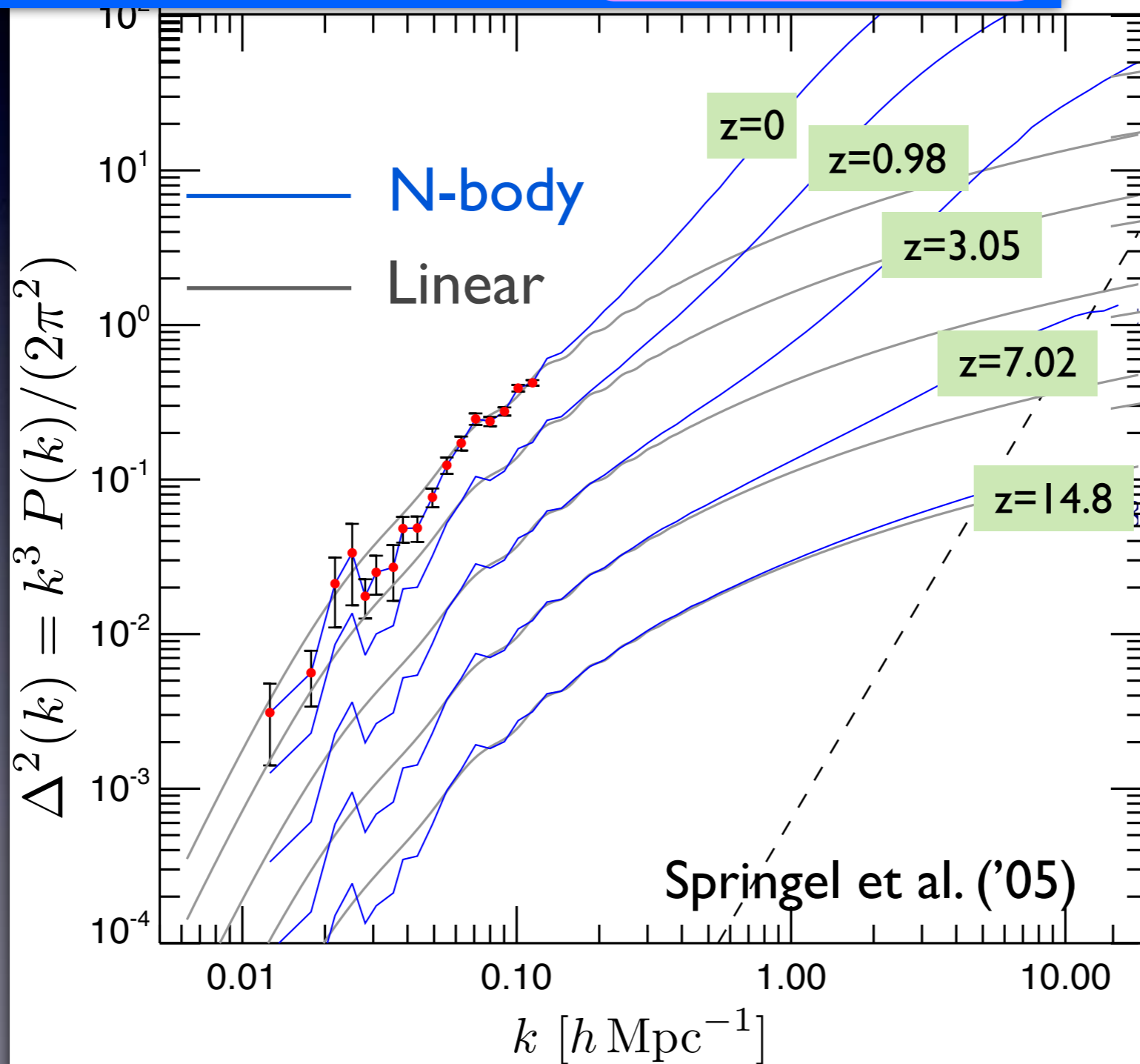
2. calculate displacement field $\Psi(k) \xrightarrow{\text{FFT}} \Psi(q)$

3. move particles according to displacement field $\Psi(q) \quad \dot{\Psi}(q) = \frac{\dot{D}_+(z)}{D_+(z)} \Psi(q)$

Perturbation theory of large-scale structure

Nonlinear gravitational evolution

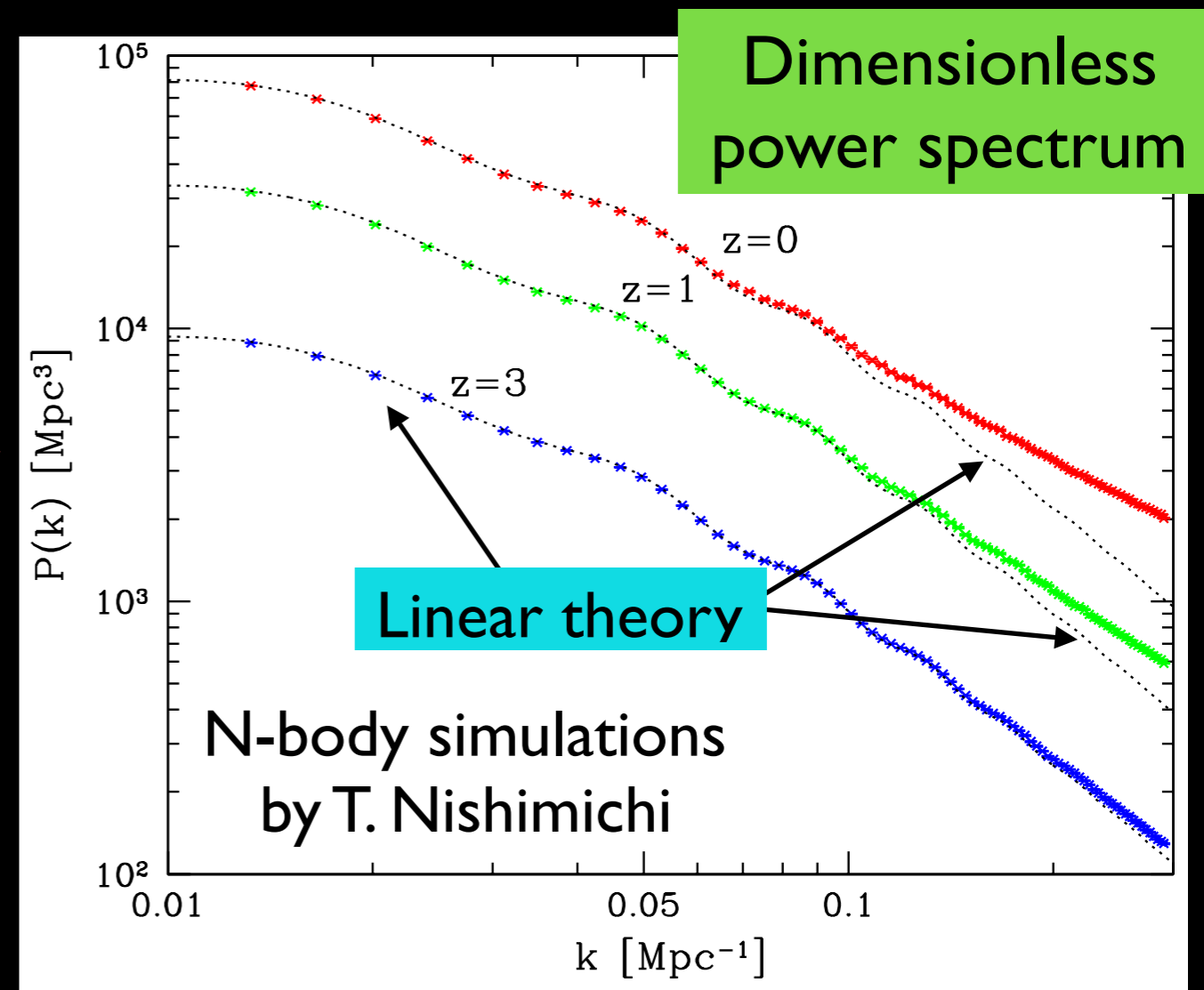
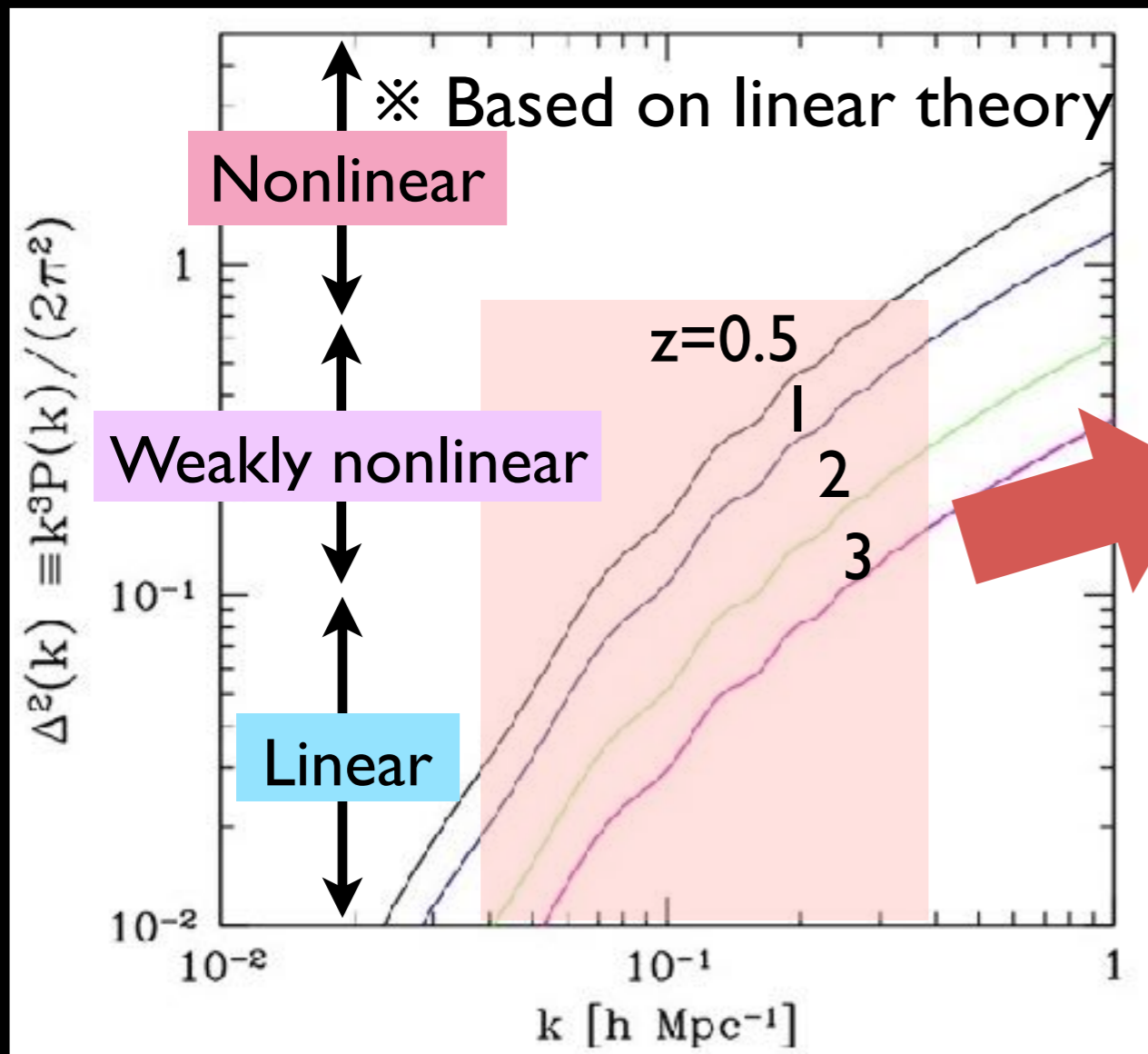
$$\delta(\vec{x}) \equiv \frac{\delta\rho_m(\vec{x})}{\bar{\rho}_m} = \frac{1}{\sqrt{V}} \sum_{\vec{k}} \delta(\vec{k}) e^{i\vec{k}\cdot\vec{x}} \quad \longrightarrow \quad P(k) = \frac{1}{N_k} \sum_{|\vec{k}|=k} |\delta(\vec{k})|^2$$



Regime of our interest

Most of interesting cosmological information (BAO, RSD, signature of massive neutrinos, ...) lies at $k < 0.2-0.3 \text{ h/Mpc}$

-----> Weakly nonlinear regime



Range of applicability

Methods (Gravitational evolution)

Other systematics

Fully nonlinear
($\Delta^2 > 1$)

N-body simulation

most powerful, but extensive
& time-consuming
(c.f. fitting formula)

weakly nonlinear
($\Delta^2 \lesssim 1$)

Perturbation theory

limited range of application, but
analytical & very fast

linear
($\Delta^2 \ll 1$)

Linear theory
(CMB Boltzmann code)

very difficult

Baryon physics
(weak lensing)

- Galaxy bias
- Redshift-space distortion
(galaxy surveys)

relatively easy

Perturbation theory (PT)

Theory of large-scale structure based on gravitational instability

Juszkiewicz ('81), Vishniac ('83), Goroff et al. ('86),
Suto & Sasaki ('91), Jain & Bertschinger ('94), ...

Cold dark matter + baryons = pressureless & irrotational fluid

Basic
eqs.

$$\frac{\partial \delta}{\partial t} + \frac{1}{a} \vec{\nabla} \cdot [(1 + \delta) \vec{v}] = 0$$

$$\frac{\partial \vec{v}}{\partial t} + \frac{\dot{a}}{a} \vec{v} + \frac{1}{a} (\vec{v} \cdot \vec{\nabla}) \vec{v} = -\frac{1}{a} \vec{\nabla} \Phi$$

$$\frac{1}{a^2} \nabla^2 \Phi = 4\pi G \bar{\rho}_m \delta$$

*Single-stream approx. of
collisionless Boltzmann eq.*

standard PT

$$|\delta| \ll 1$$

$$\delta = \delta^{(1)} + \delta^{(2)} + \delta^{(3)} + \dots$$

$$\langle \delta(\mathbf{k}; t) \delta(\mathbf{k}'; t) \rangle = (2\pi)^3 \delta_D(\mathbf{k} + \mathbf{k}') P(|\mathbf{k}|; t)$$

Equations of motion

$$\partial_\tau \delta + \partial_i [(1 + \delta)v^i] = 0 ,$$

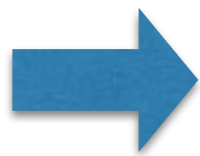
$$\partial_\tau v^i + \mathcal{H} v_l^i + \partial^i \phi + v_l^j \partial_j v^i = 0$$

$$\Delta \phi = \frac{3}{2} \mathcal{H}^2 \Omega_m \delta .$$

τ : conformal time
($a d\tau = dt$)

$$\int_{\mathbf{q}} \equiv \int \frac{d^3 \mathbf{q}}{(2\pi)^3}$$

Fourier
expansion



$$\theta \equiv \nabla \cdot \mathbf{v}$$

$$\partial_\tau \delta(\mathbf{k}, \tau) + \theta(\mathbf{k}, \tau) = - \int_{\mathbf{q}} \alpha(\mathbf{q}, \mathbf{k} - \mathbf{q}) \theta(\mathbf{q}, \tau) \delta(\mathbf{k} - \mathbf{q}, \tau) ,$$

$$\partial_\tau \theta(\mathbf{k}, \tau) + \mathcal{H} \theta(\mathbf{k}, \tau) + \frac{3}{2} \Omega_m \mathcal{H}^2 \delta(\mathbf{k}, \tau)$$

$$= - \int_{\mathbf{q}} \beta(\mathbf{q}, \mathbf{k} - \mathbf{q}) \theta(\mathbf{q}, \tau) \theta(\mathbf{k} - \mathbf{q}, \tau)$$

$$\alpha(\mathbf{q}_1, \mathbf{q}_2) \equiv \frac{\mathbf{q}_1 \cdot (\mathbf{q}_1 + \mathbf{q}_2)}{q_1^2} ,$$

$$\beta(\mathbf{q}_1, \mathbf{q}_2) \equiv \frac{1}{2} (\mathbf{q}_1 + \mathbf{q}_2)^2 \frac{\mathbf{q}_1 \cdot \mathbf{q}_2}{q_1^2 q_2^2} .$$

Standard perturbation theory

$$\delta(\mathbf{k}, a) = \sum_{i=1}^{\infty} \delta_{(i)}(\mathbf{k}, a), \quad \theta(\mathbf{k}, a) = -\mathcal{H} f(a) \sum_{i=1}^{\infty} \theta_{(i)}(\mathbf{k}, a)$$

$$f(a) \equiv d \ln D_1 / d \ln a$$

$D_1(a)$: Linear growth factor

Adopting the E-dS approximation,

$$\delta_{(n)}(\mathbf{k}, a) = \underline{D_1^n(a)} \delta_n(\mathbf{k}), \quad \theta_{(n)}(\mathbf{k}, a) = \underline{D_1^n(a)} \theta_n(\mathbf{k}).$$

$$\delta_n(\mathbf{k}) = \int_{\mathbf{q}_1} \dots \int_{\mathbf{q}_n} (2\pi)^3 \delta_D^{(3)}(\mathbf{k} - \mathbf{q}_1 \dots - \mathbf{q}_n) F_n(\mathbf{q}_1, \dots, \mathbf{q}_n) \delta_0(\mathbf{q}_1) \dots \delta_0(\mathbf{q}_n),$$

$$\theta_n(\mathbf{k}) = \int_{\mathbf{q}_1} \dots \int_{\mathbf{q}_n} (2\pi)^3 \delta_D^{(3)}(\mathbf{k} - \mathbf{q}_1 \dots - \mathbf{q}_n) G_n(\mathbf{q}_1, \dots, \mathbf{q}_n) \delta_0(\mathbf{q}_1) \dots \delta_0(\mathbf{q}_n),$$

standard PT kernel ($F_1 = G_1 = 1$)

Linear density field
(Gaussian)

Recursion relation for PT kernels

$$\mathcal{F}_a^{(n)}(\mathbf{k}_1, \dots, \mathbf{k}_n) \equiv \begin{bmatrix} F_n(\mathbf{k}_1, \dots, \mathbf{k}_n) \\ G_n(\mathbf{k}_1, \dots, \mathbf{k}_n) \end{bmatrix}$$

$$\mathcal{F}_a^{(n)}(\mathbf{k}_1, \dots, \mathbf{k}_n) = \sum_{m=1}^{n-1} \sigma_{ab}^{(n)} \gamma_{bcd}(\mathbf{q}_1, \mathbf{q}_2) \mathcal{F}_c^{(m)}(\mathbf{k}_1, \dots, \mathbf{k}_m) \mathcal{F}_d^{(n-m)}(\mathbf{k}_{m+1}, \dots, \mathbf{k}_n)$$

$$\mathbf{q}_1 = \mathbf{k}_1 + \dots + \mathbf{k}_m$$

$$\mathbf{q}_2 = \mathbf{k}_{m+1} + \dots + \mathbf{k}_n$$

$$\sigma_{ab}^{(n)} = \frac{1}{(2n+3)(n-1)} \begin{pmatrix} 2n+1 & 2 \\ 3 & 2n \end{pmatrix}$$

$$\gamma_{abc}(\mathbf{k}_1, \mathbf{k}_2) = \begin{cases} \frac{1}{2} \left\{ 1 + \frac{\mathbf{k}_2 \cdot \mathbf{k}_1}{|\mathbf{k}_2|^2} \right\}; & (a, b, c) = (1, 1, 2) \\ \frac{1}{2} \left\{ 1 + \frac{\mathbf{k}_1 \cdot \mathbf{k}_2}{|\mathbf{k}_1|^2} \right\}; & (a, b, c) = (1, 2, 1) \\ \frac{(\mathbf{k}_1 \cdot \mathbf{k}_2) |\mathbf{k}_1 + \mathbf{k}_2|^2}{2|\mathbf{k}_1|^2 |\mathbf{k}_2|^2}; & (a, b, c) = (2, 2, 2) \\ 0; & \text{otherwise.} \end{cases}$$

Note—. repetition of the same subscripts (a,b,c) indicates the sum over all multiplet components

PT kernels constructed from recursion relation should be *symmetrized*

Power spectrum

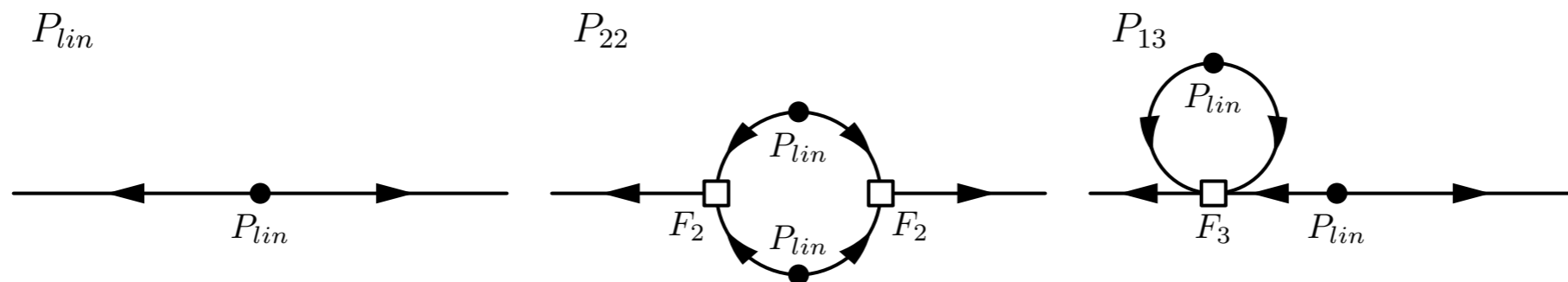
$$\langle \delta(\mathbf{k}_1, a) \delta(\mathbf{k}_2, a) \rangle \equiv (2\pi)^3 \delta_D^{(3)}(\mathbf{k}_1 + \mathbf{k}_2) P(k_1, a)$$



$$P_{SPT}(k) = \underbrace{P_{lin}(k)}_{\text{linear}} + \underbrace{P_{22}(k)}_{\text{1-loop}} + P_{13}(k) + \text{higher order loops .}$$

$$P_{22}(k) = 2 \int_{\mathbf{q}} P_{lin}(q) P_{lin}(|\mathbf{k} - \mathbf{q}|) F_2^2(\mathbf{q}, \mathbf{k} - \mathbf{q}) ,$$

$$P_{13}(k) = 6 P_{lin}(k) \int_{\mathbf{q}} P_{lin}(q) F_3(\mathbf{k}, \mathbf{q}, -\mathbf{q}) ,$$



Next-to-next-to leading order

up to 2-loop order

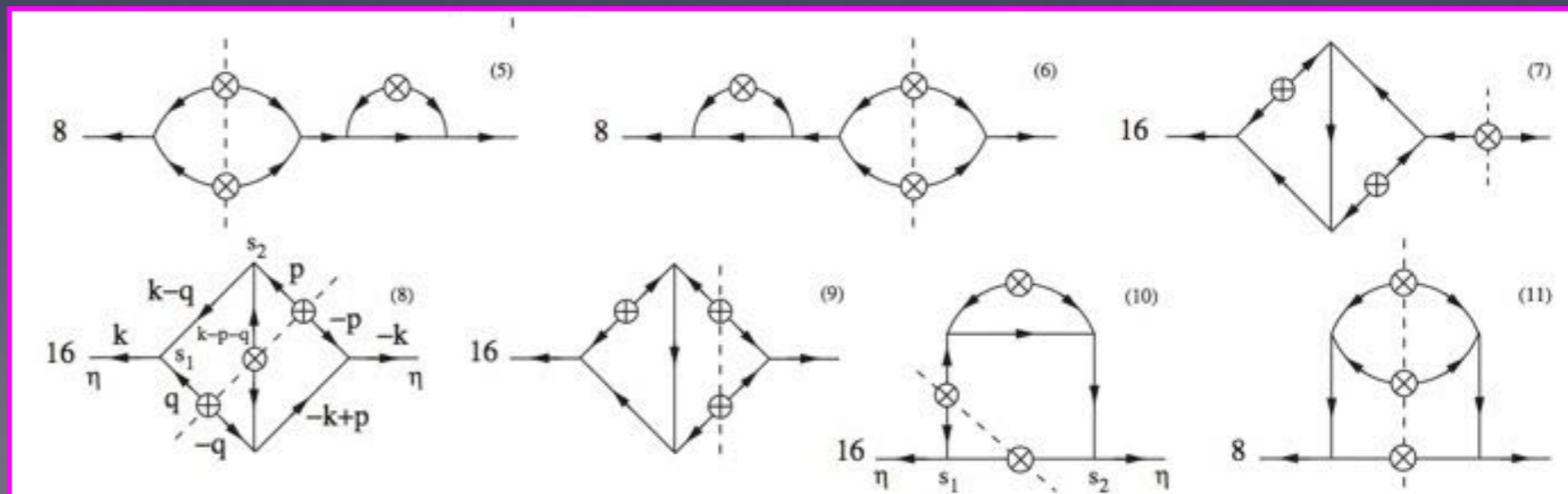
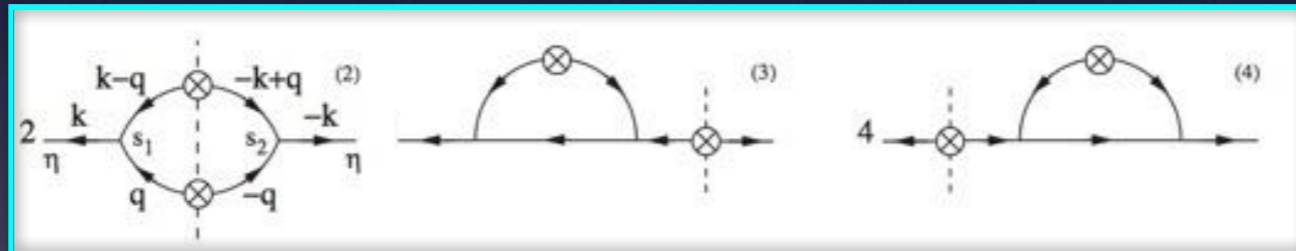
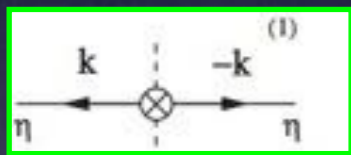
$$P^{(mn)} \simeq \langle \delta^{(m)} \delta^{(n)} \rangle$$

$$P(k) = \underbrace{P^{(11)}(k)}_{\text{Linear (tree)}} + \underbrace{\left(P^{(22)}(k) + P^{(13)}(k) \right)}_{\text{1-loop}} + \underbrace{\left(P^{(33)}(k) + P^{(24)}(k) + P^{(15)}(k) \right)}_{\text{2-loop}} + \dots$$

Linear (tree)

1-loop

2-loop



Crocce & Scoccimarro ('06)

Calculation involves multi-dimensional numerical integration
(time-consuming)

Comparison with simulations

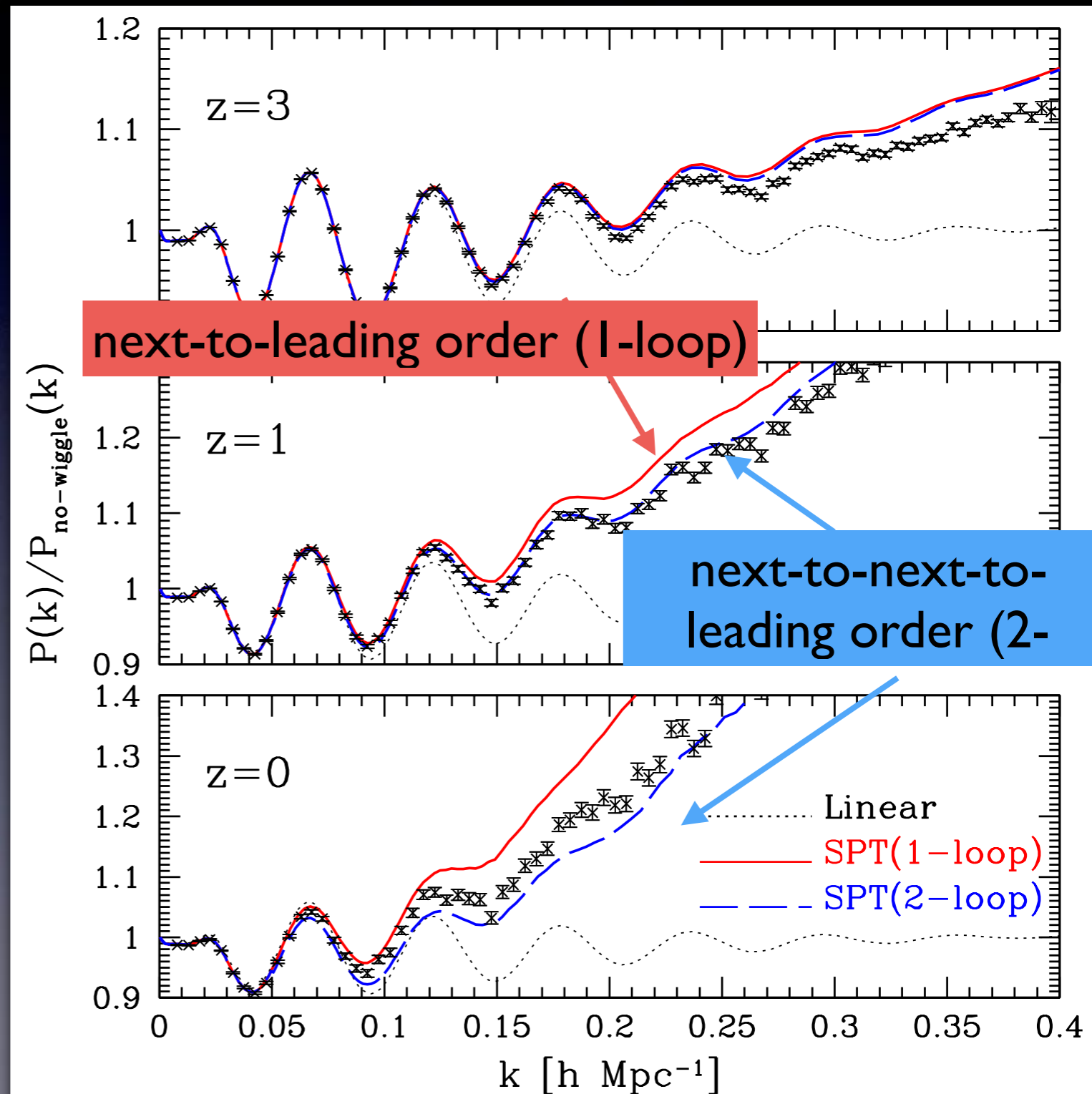
Standard PT qualitatively explains scale-dependent nonlinear growth, however,

1-loop :
overestimates simulations

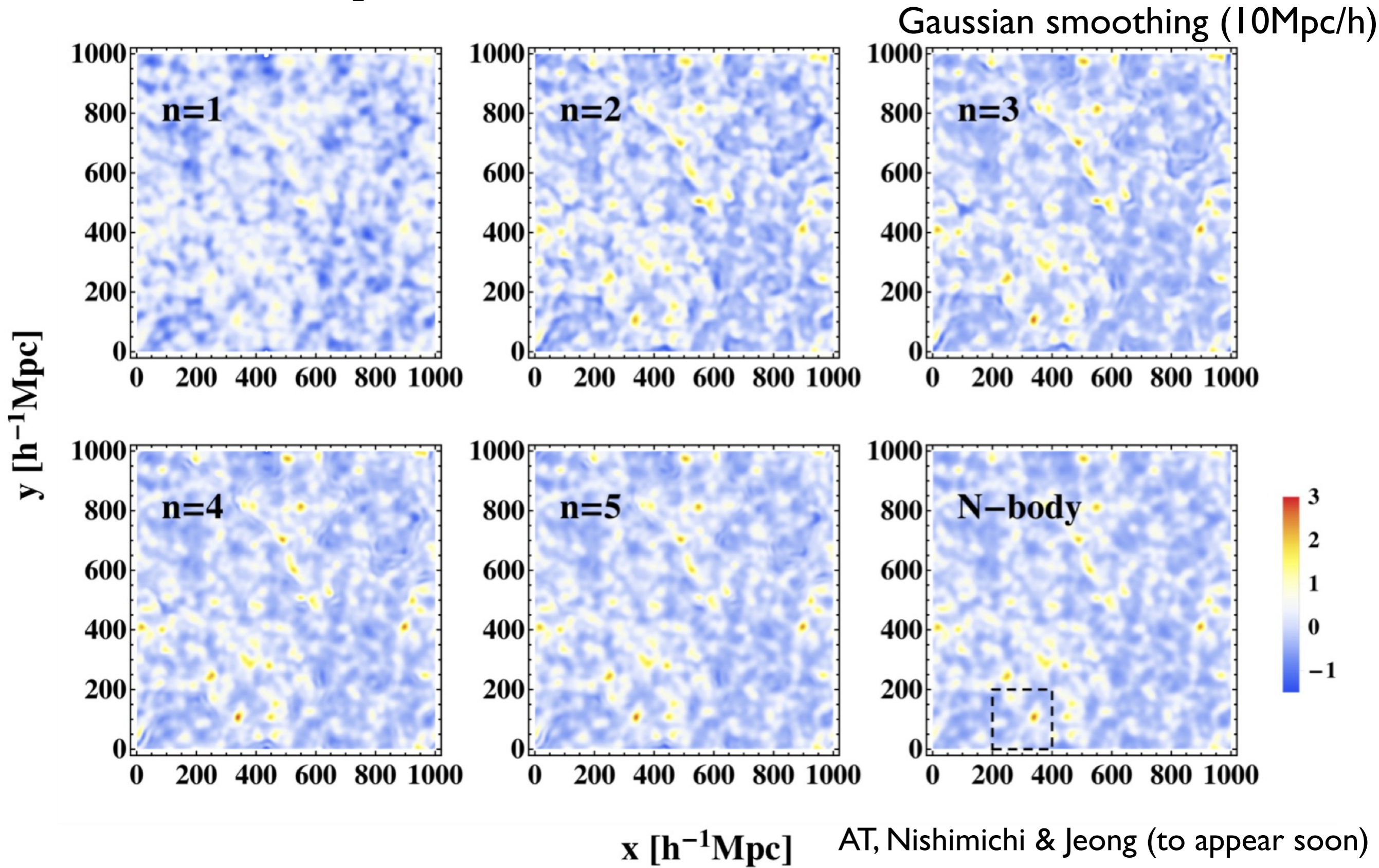
2-loop :
overestimates at high-z, while it turn to underestimate at low-z

Standard PT produces ill-behaved PT expansion !!

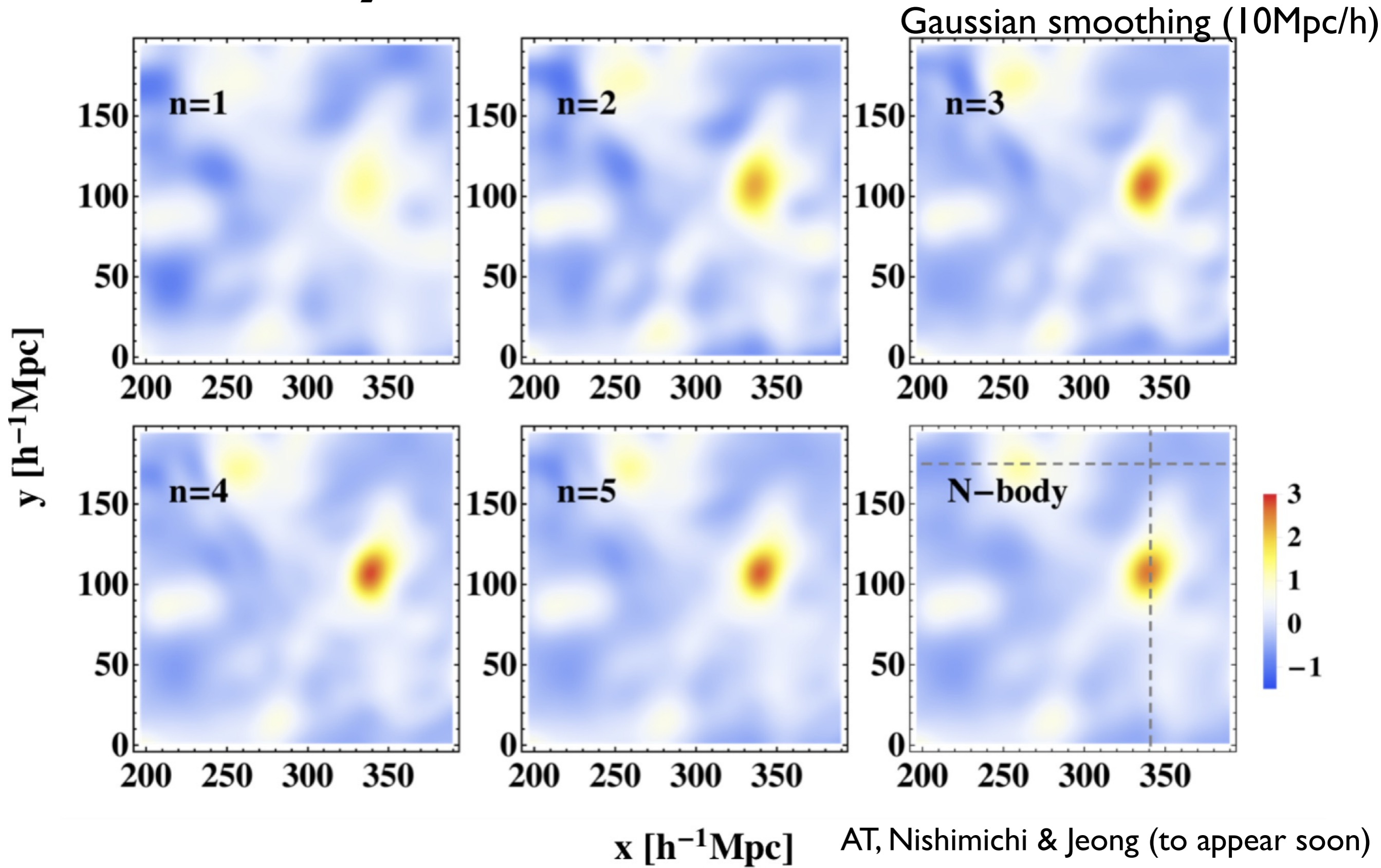
... need to be improved



Density field in standard PT



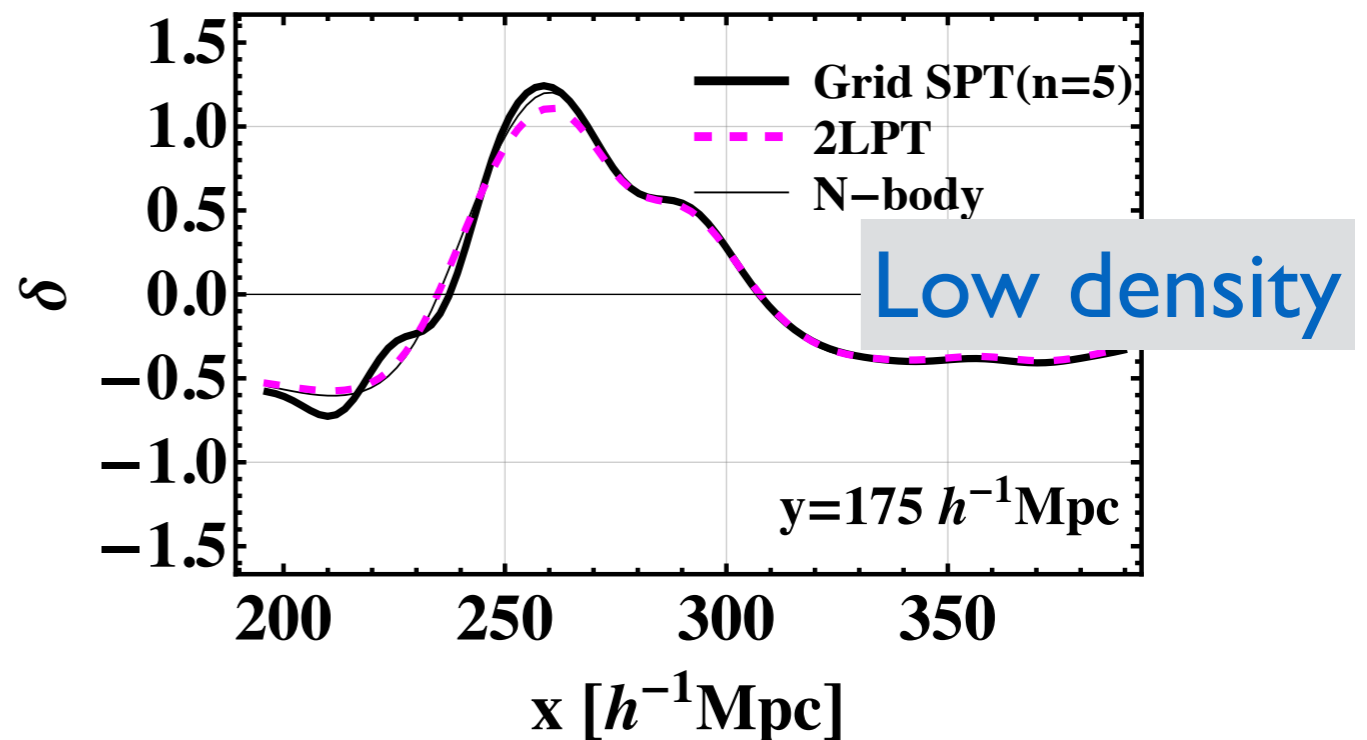
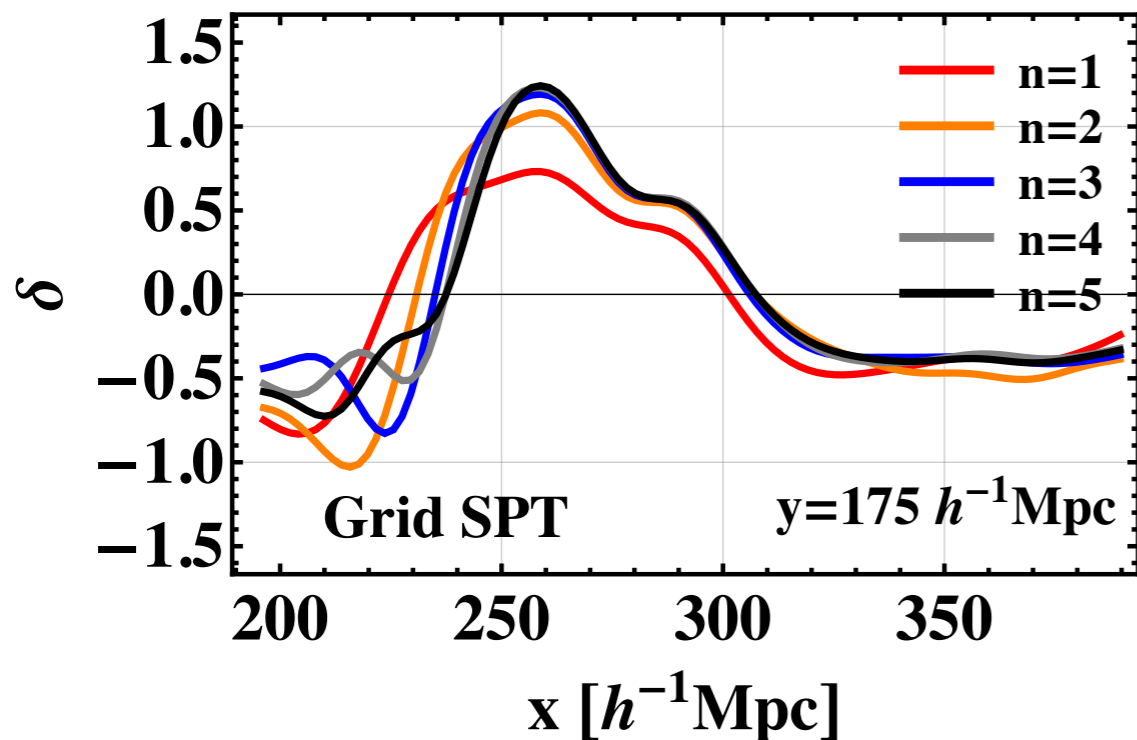
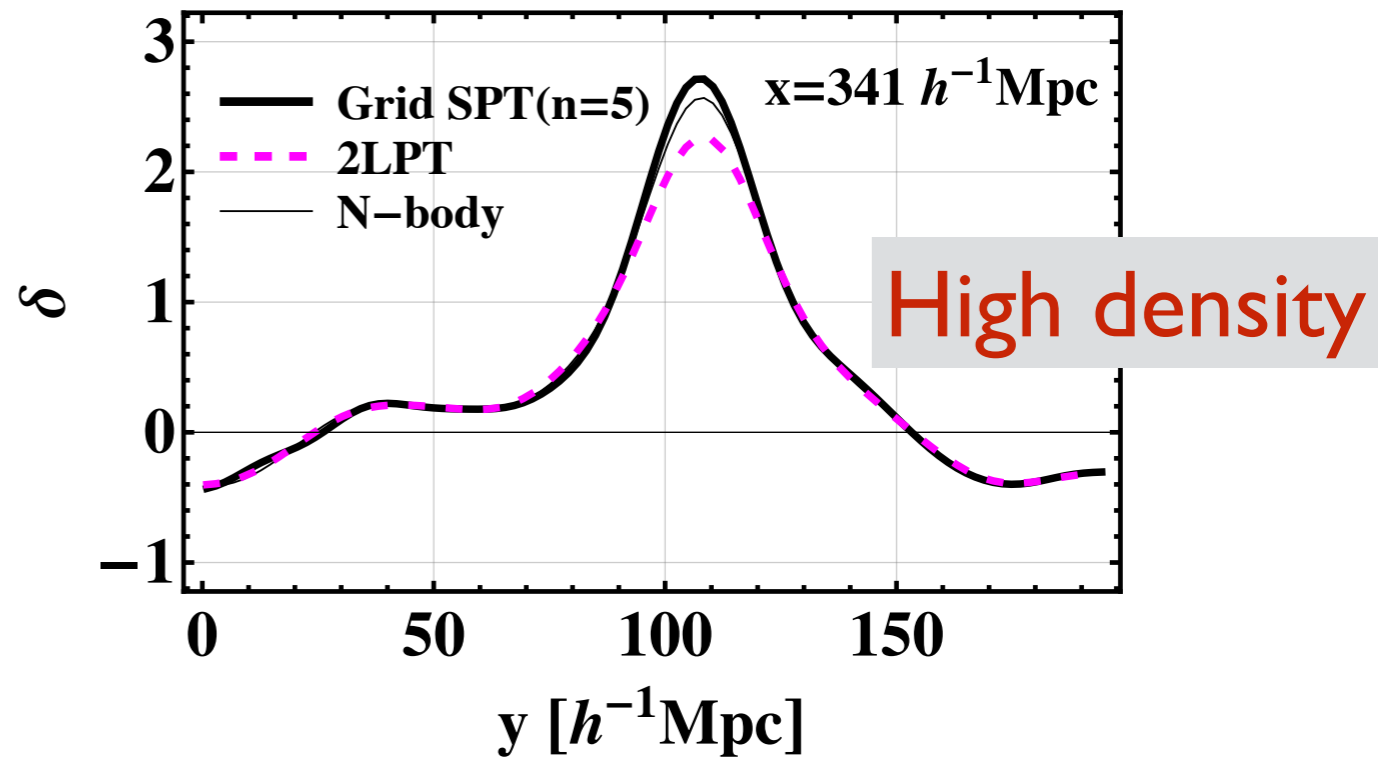
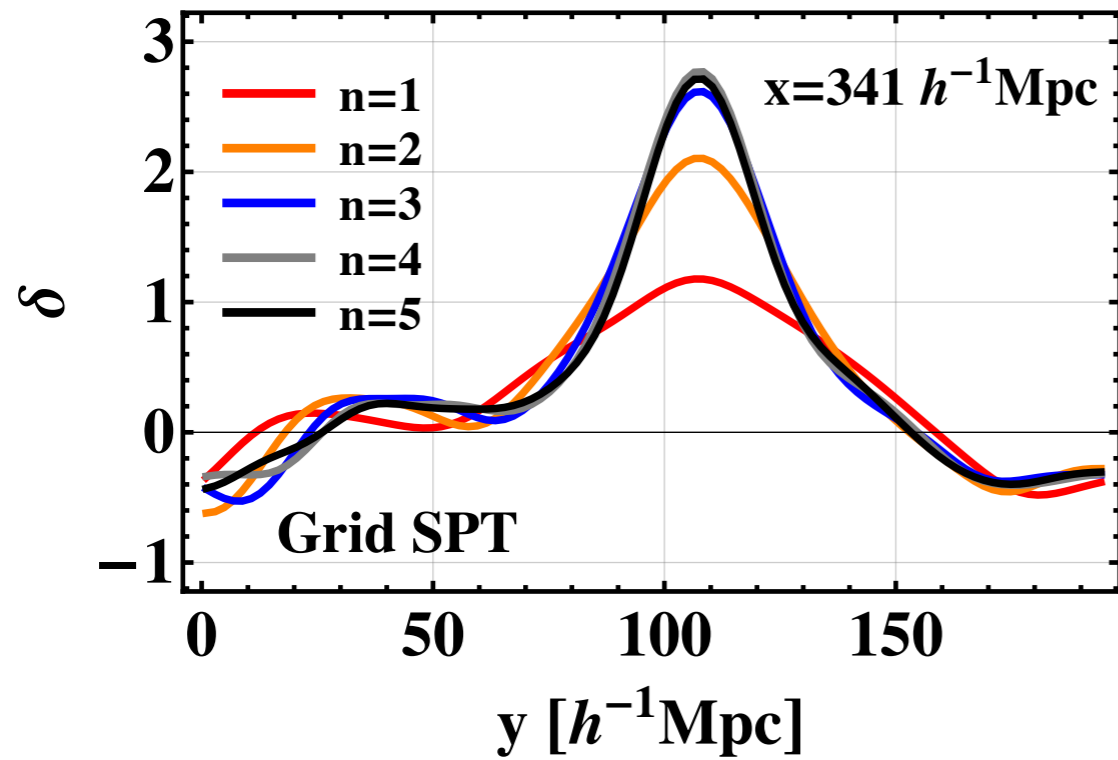
Density field in standard PT



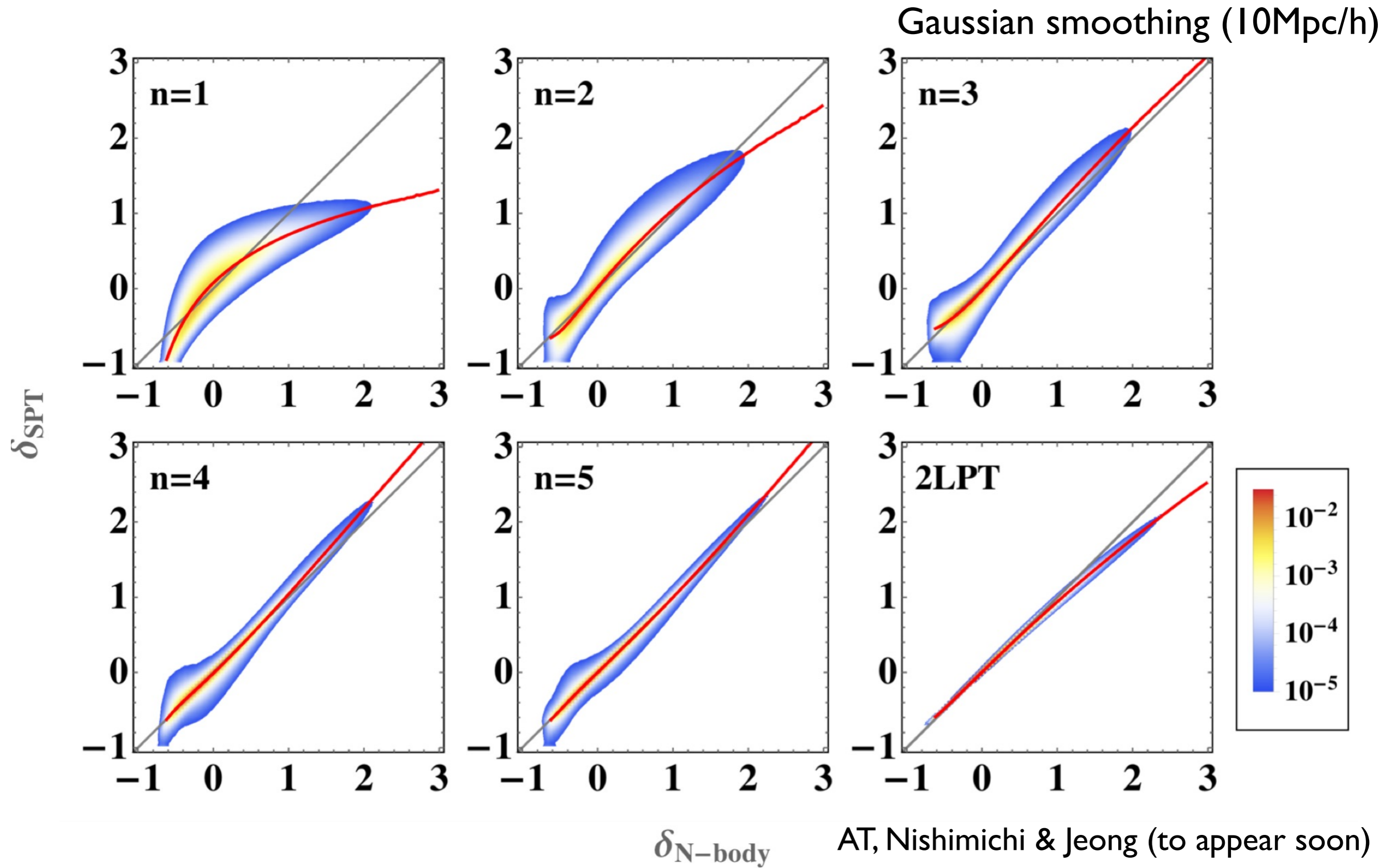
ID density field in standard PT

Gaussian smoothing ($10\text{Mpc}/h$)

AT, Nishimichi & Jeong (to appear soon)



Correlation between N-body and SPT



Improving PT predictions

Basic
idea

Reorganizing standard PT expansion by introducing
non-perturbative statistical quantities

$$\delta_0(\mathbf{k})$$

initial density field (Gaussian)

Initial power spectrum

$$P_0(k)$$

from linear theory
(CMB Boltzmann code)



Nonlinear
mapping

$$\delta(\mathbf{k}; z)$$

Evolved density field (non-Gaussian)

Observables

$$P(k; z)$$

$$B(k_1, k_2, k_3; z)$$

$$T(k_1, k_2, k_3, k_4; z)$$

⋮

of dark matter/galaxies/halos

Concept of '*propagator*' in physics/mathematics may be useful

Propagator in physics


- ◆ Green's function in linear differential equations
- ◆ Probability amplitude in quantum mechanics

Schrödinger Eq.

$$\left(-i\hbar\frac{\partial}{\partial t} + H_x\right)\psi(x, t) = 0$$

$$G(x, t; x', t') \equiv \frac{\delta\psi(x, t)}{\delta\psi(x', t')}$$

$$\left(-i\hbar\frac{\partial}{\partial t} + H_x\right)G(x, t; x', t') = -i\hbar\delta_D(x - x')\delta_D(t - t')$$


$$\psi(x, t) = \int_{-\infty}^{+\infty} dx' G(x, t; x', t') \psi(x', t') ; \quad t > t'$$

Cosmic propagators

Propagator should carry information on
non-linear evolution & statistical properties

Evolved (non-linear) density field

Crocce & Scoccimarro ('06)

$$\left\langle \frac{\delta \delta_m(\mathbf{k}; t)}{\delta \delta_0(\mathbf{k}')} \right\rangle \equiv \delta_D(\mathbf{k} - \mathbf{k}') \Gamma^{(1)}(k; t) \text{ Propagator}$$

Initial density field

Ensemble w.r.t randomness of initial condition

Contain statistical information on *full-nonlinear* evolution
(Non-linear extension of Green's function)

Multi-point propagators

Bernardeau, Crocce & Scoccimarro ('08)

Matsubara ('11) \longrightarrow *integrated PT*

As a natural generalization,

$$\left\langle \frac{\delta^n \delta_{\mathbf{m}}(\mathbf{k}; t)}{\delta \delta_0(\mathbf{k}_1) \cdots \delta \delta_0(\mathbf{k}_n)} \right\rangle = (2\pi)^{3(1-n)} \delta_{\mathbf{D}}(\mathbf{k} - \mathbf{k}') \Gamma^{(n)}(\mathbf{k}_1, \cdots, \mathbf{k}_n; t)$$

Multi-point propagator

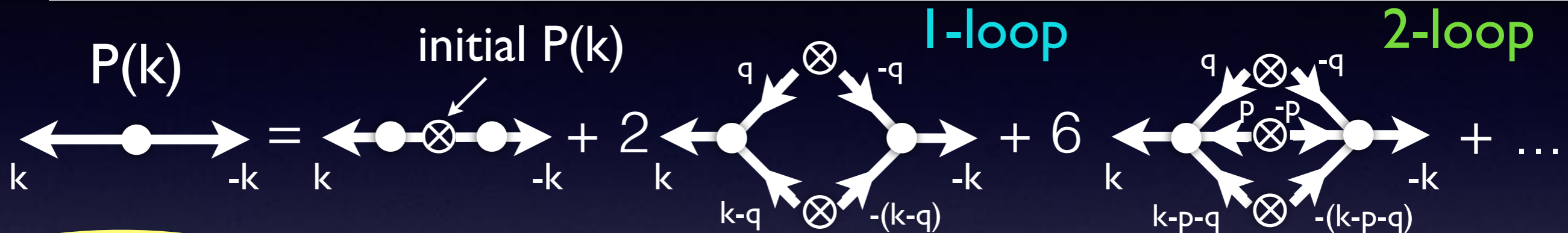
With this multi-point prop.

- Building blocks of a new perturbative theory (PT) expansion
..... Γ -expansion or Wiener-Hermite expansion
- A good convergence of PT expansion is expected
(c.f. standard PT)

Power spectrum

Initial power spectrum

$$P(k; t) = \left[\Gamma^{(1)}(k; t) \right]^2 P_0(k) + 2 \int \frac{d^3 \mathbf{q}}{(2\pi)^3} \left[\Gamma^{(2)}(\mathbf{q}, \mathbf{k} - \mathbf{q}; t) \right]^2 P_0(q) P_0(|\mathbf{k} - \mathbf{q}|) + 6 \int \frac{d^6 \mathbf{p} d^3 \mathbf{q}}{(2\pi)^6} \left[\Gamma^{(3)}(\mathbf{p}, \mathbf{q}, \mathbf{k} - \mathbf{p} - \mathbf{q}; t) \right]^2 P_0(p) P_0(q) P_0(|\mathbf{k} - \mathbf{p} - \mathbf{q}|) + \dots$$



Bispectrum

$$B(k_1, k_2, k_3) = 2 \Gamma^{(2)}(\mathbf{k}_1, \mathbf{k}_2) \Gamma^{(1)}(k_1) \Gamma^{(1)}(k_2) P_0(k_1) P_0(k_2) + \text{cyc.} + \left[8 \int d^3 q \Gamma^{(2)}(\mathbf{k}_1 - \mathbf{q}, \mathbf{q}) \Gamma^{(2)}(\mathbf{k}_2 + \mathbf{q}, -\mathbf{q}) \Gamma^{(2)}(\mathbf{q} - \mathbf{k}_1, -\mathbf{k}_2 - \mathbf{q}) P_0(|\mathbf{k}_1 - \mathbf{q}|) P_0(|\mathbf{k}_2 + \mathbf{q}|) P_0(q) + 6 \int d^3 q \Gamma^{(3)}(-\mathbf{k}_3, -\mathbf{k}_2 + \mathbf{q}, -\mathbf{q}) \Gamma^{(2)}(\mathbf{k}_2 - \mathbf{q}, \mathbf{q}) \Gamma^{(1)}(\mathbf{k}_3) P_0(|\mathbf{k}_2 - \mathbf{q}|) P_0(q) P_0(k_3) + \text{cyc.} \right]$$

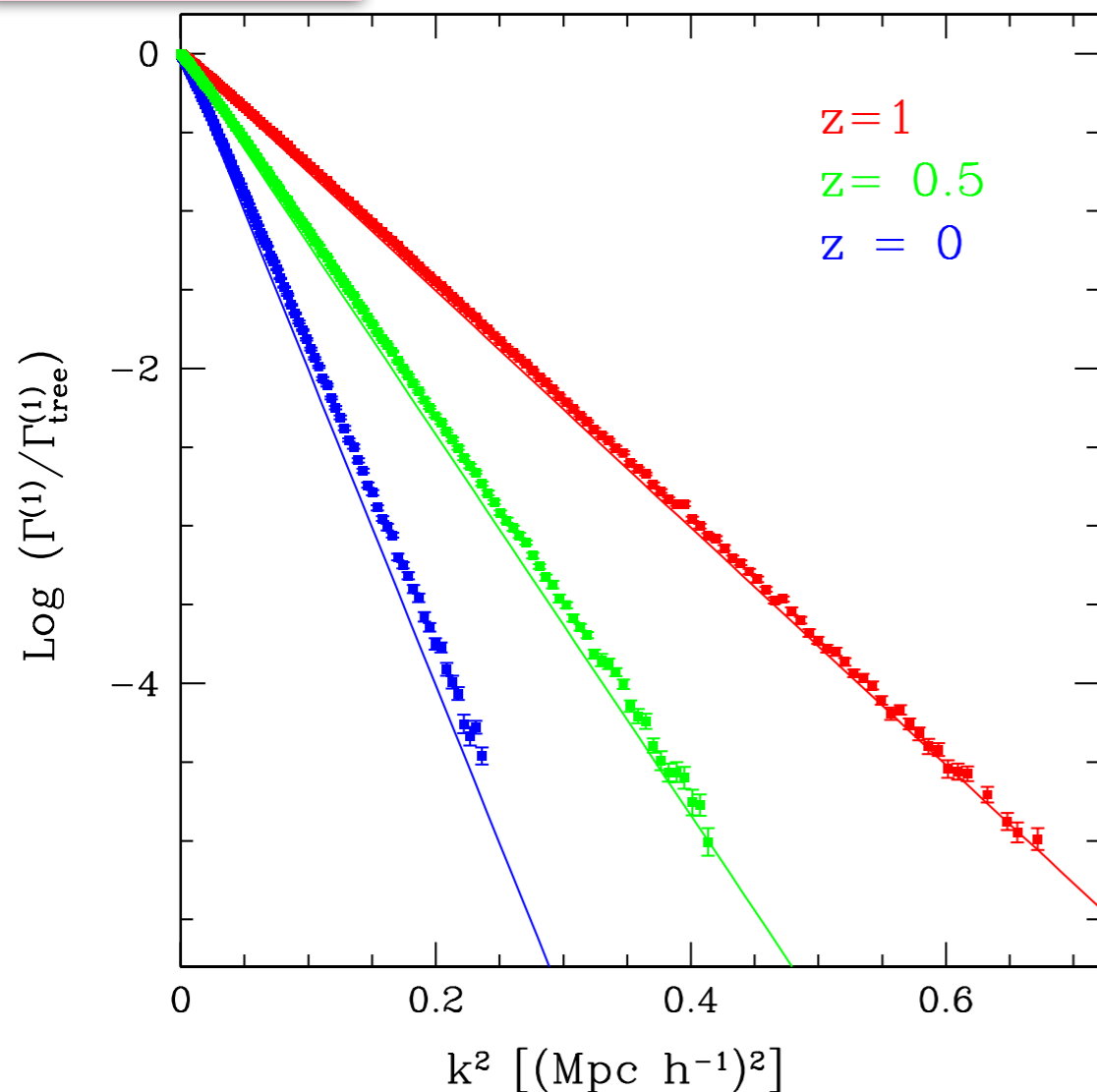


Generic property of propagators

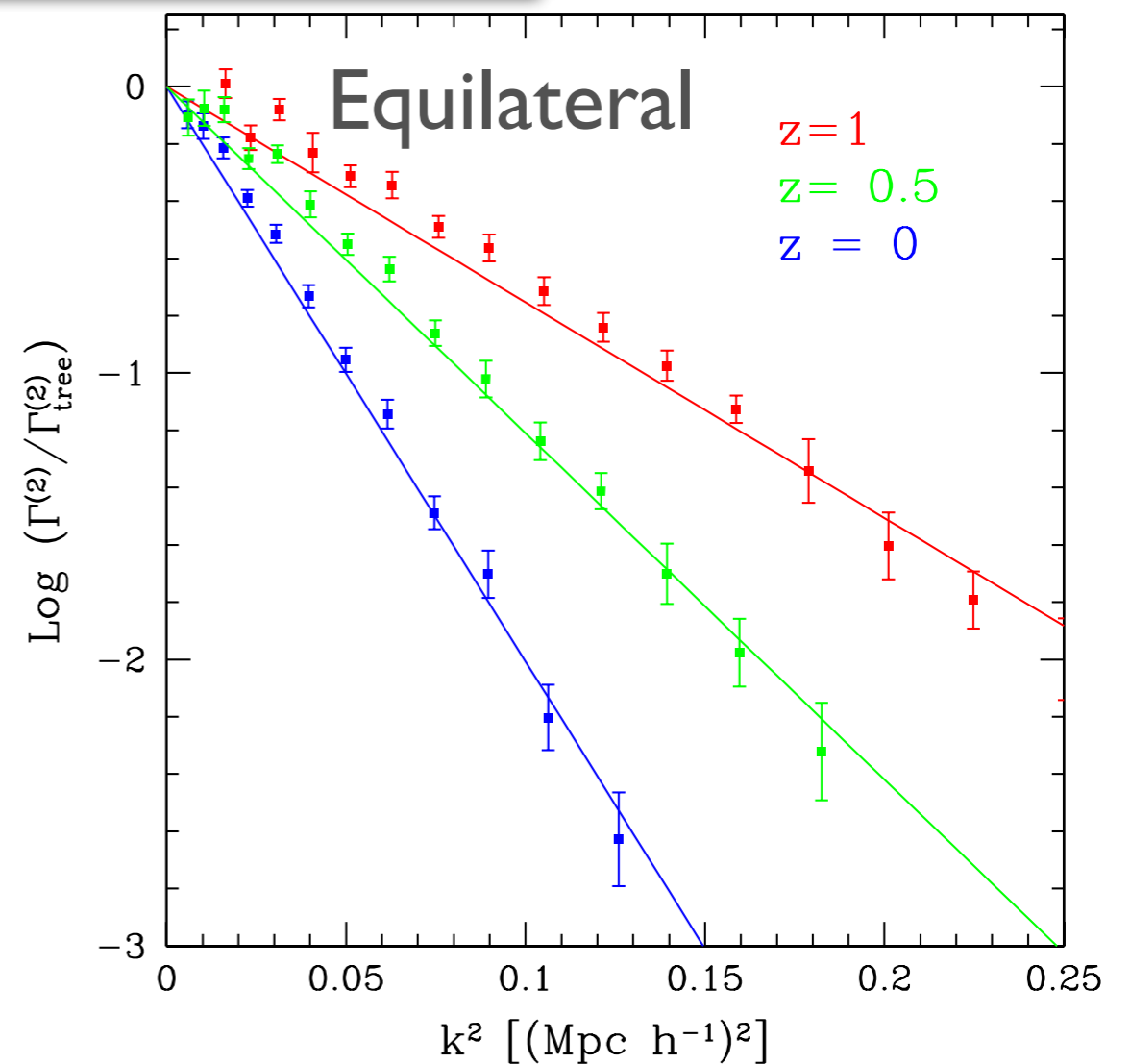
Crocce & Scoccimarro '06, Bernardeau et al. '08

$$\Gamma^{(n)} \xrightarrow{k \rightarrow +\infty} {}^s F_n(\mathbf{k}_1, \dots, \mathbf{k}_n) e^{-k^2 \sigma_v^2 / 2} ; \quad \sigma_v^2 = \int \frac{dq}{6\pi^2} P_{\theta\theta}(q)$$

$\Gamma^{(1)}(k)$



$\Gamma^{(2)}(k_1, k_2, k_3)$



Constructing regularized propagators

- UV property ($k \gg 1$) :

$$\Gamma^{(n)} \xrightarrow{k \rightarrow +\infty} \Gamma_{\text{tree}}^{(n)} e^{-k^2 \sigma_v^2 / 2} \quad ; \quad \sigma_v^2 = \int \frac{dq}{6\pi^2} P_{\theta\theta}(q)$$

Bernardeau, Crocce & Scoccimarro ('08), Bernardeau, Van de Rijt, Vernizzi ('11)

- IR behavior ($k \ll 1$) can be described by standard PT calculations :

$$\Gamma^{(n)} = \Gamma_{\text{tree}}^{(n)} + \Gamma_{\text{1-loop}}^{(n)} + \Gamma_{\text{2-loop}}^{(n)} + \dots$$

Importantly, each term behaves like $\Gamma_{p\text{-loop}}^{(n)} \xrightarrow{k \rightarrow +\infty} \frac{1}{p!} \left(-\frac{k^2 \sigma_v^2}{2} \right)^p \Gamma_{\text{tree}}^{(n)}$

 A regularization scheme that reproduces both UV & IR behaviors

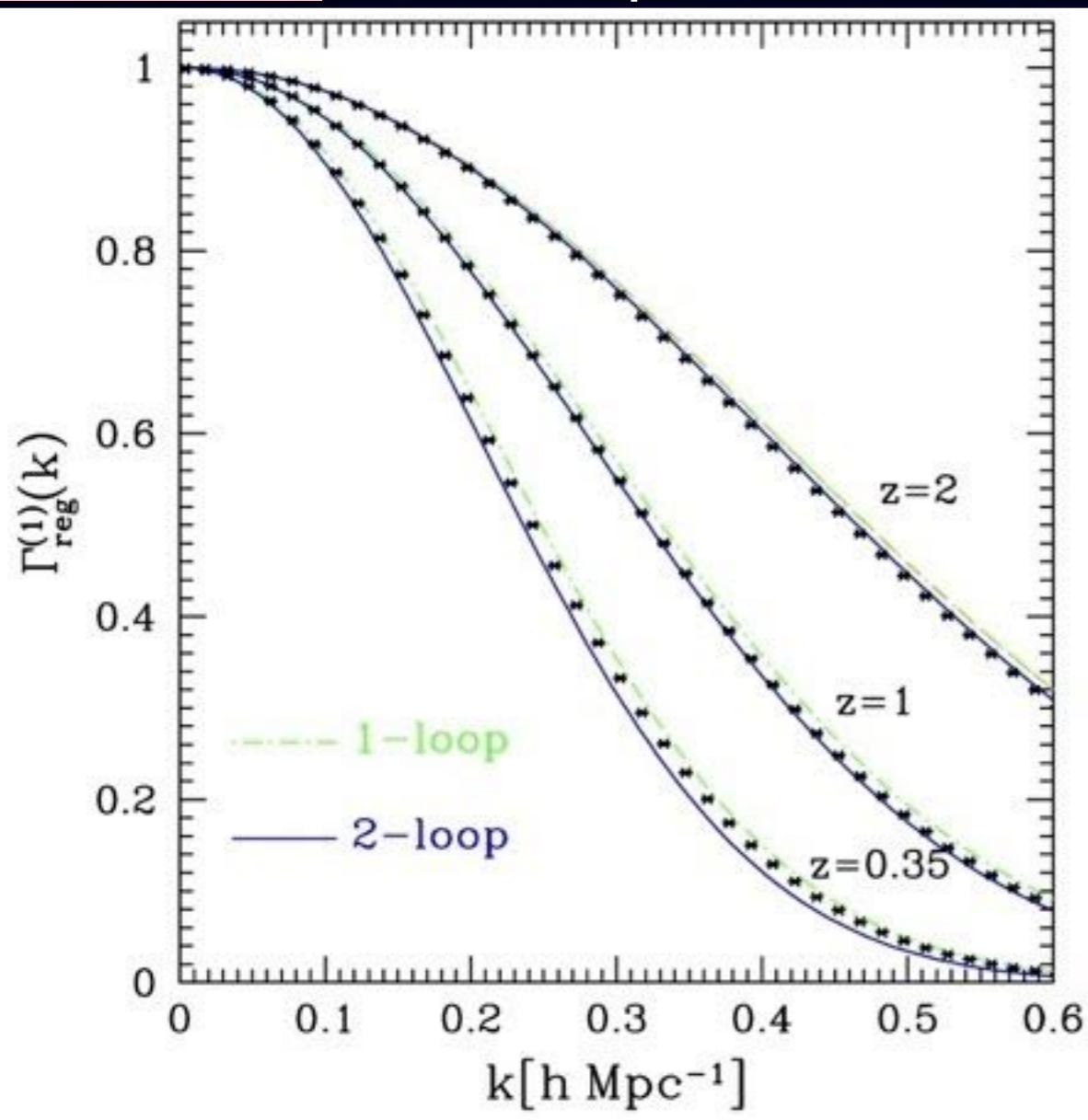
Bernardeau, Crocce & Scoccimarro ('12)

Propagators in N-body simulations

compared with '*Regularized*' propagators constructed analytically

$$\Gamma^{(1)}(k)$$

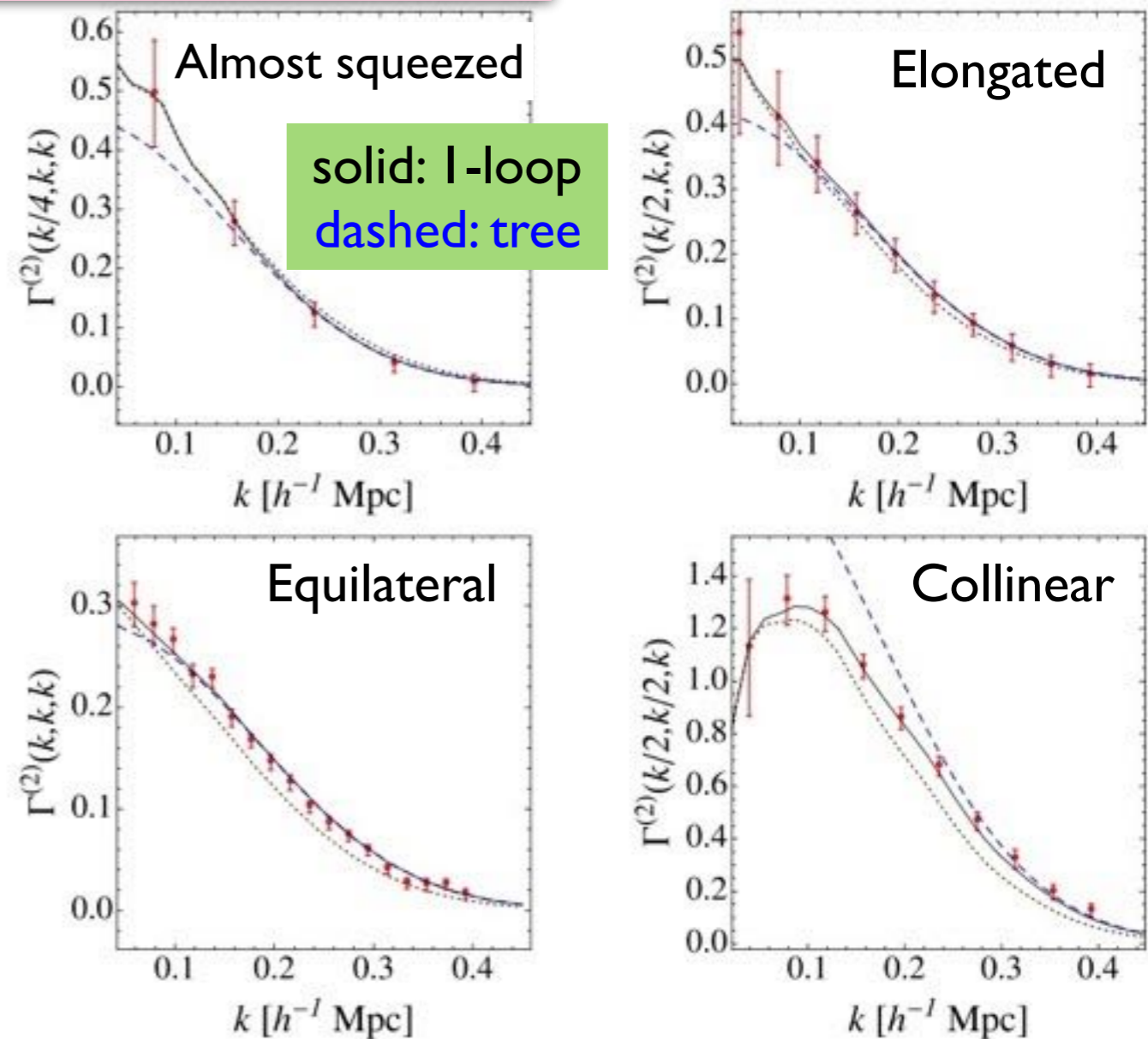
predictions up to
2-loop order



Bernardeau, AT & Nishimichi ('12)

$$\Gamma^{(2)}(k_1, k_2, k_3)$$

predictions up to
1-loop order



Bernardeau et al. ('12)

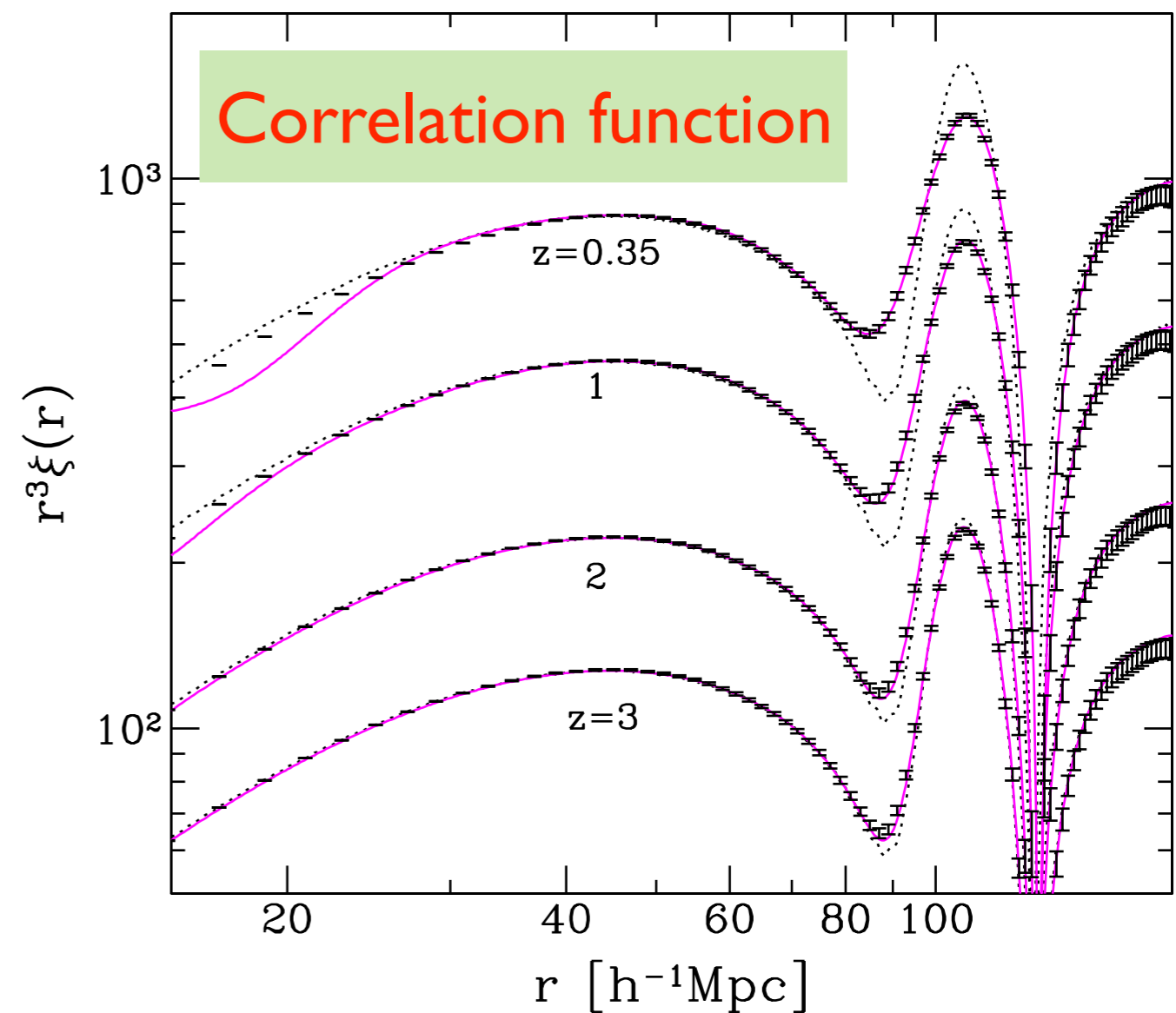
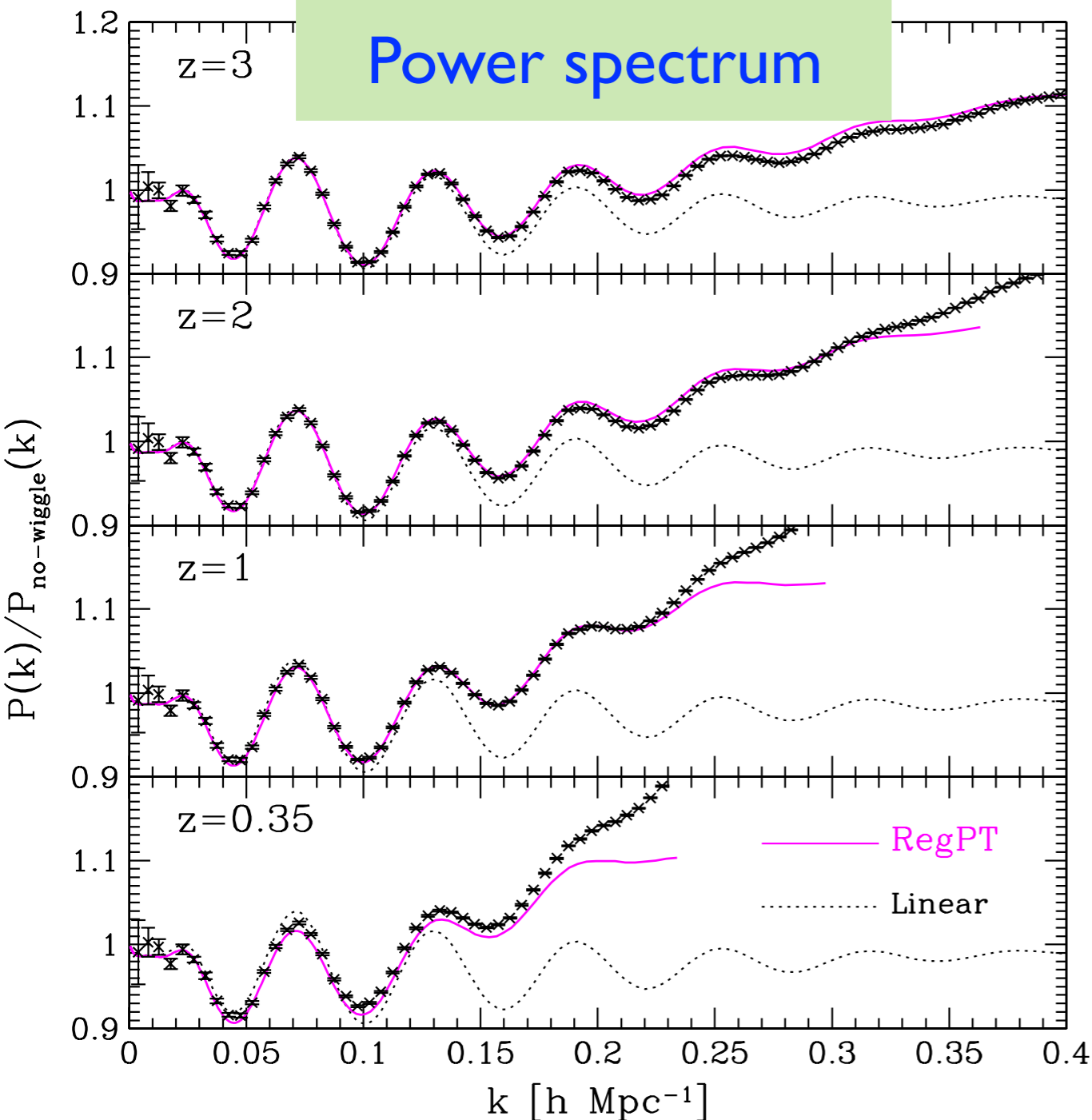
RegPT: fast PT code for $P(k)$ & $\xi(r)$

few sec.

(regularized)

A public code based on multi-point propagators at 2-loop order

http://www2.yukawa.kyoto-u.ac.jp/~atsushi.taruya/regpt_code.html



AT, Bernardeau, Nishimichi & Codis ('12)

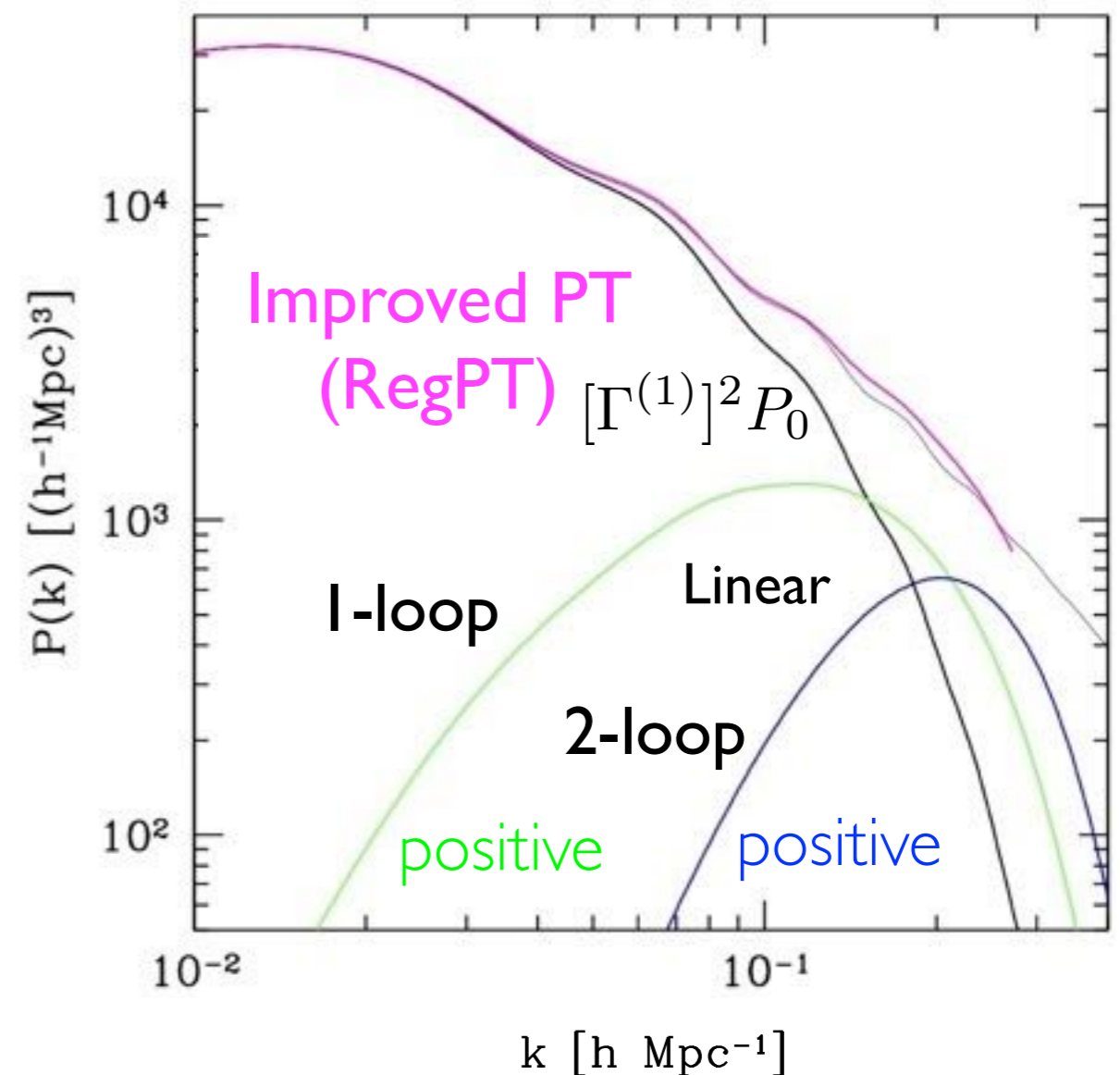
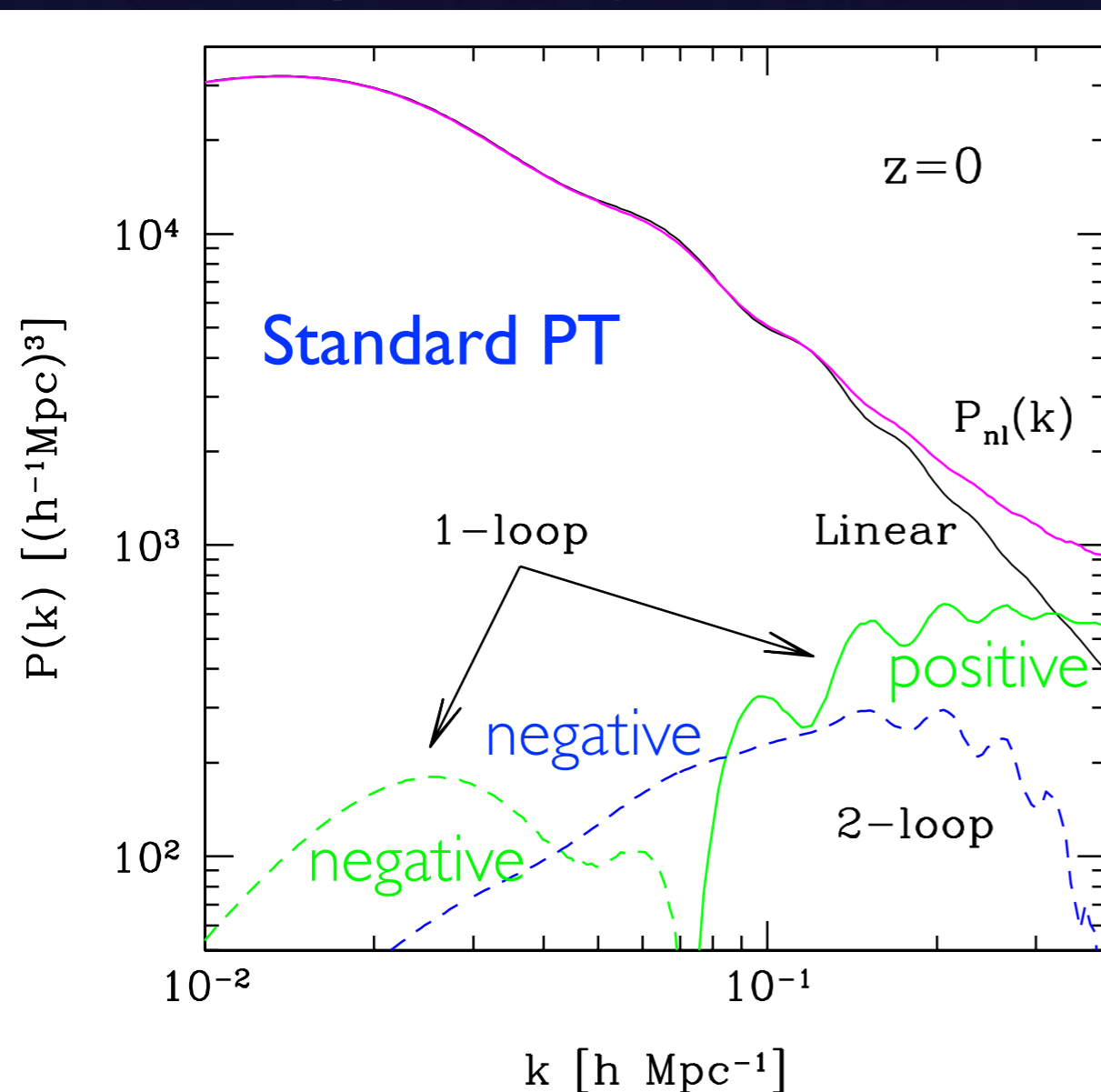
Why improved PT works well?

AT, Bernardeau, Nishimichi, Codis ('12)

AT et al. ('09)

- All corrections become comparable at low- z .
- Positivity is not guaranteed.

Corrections are positive & localized, shifted to higher- k for higher-loop



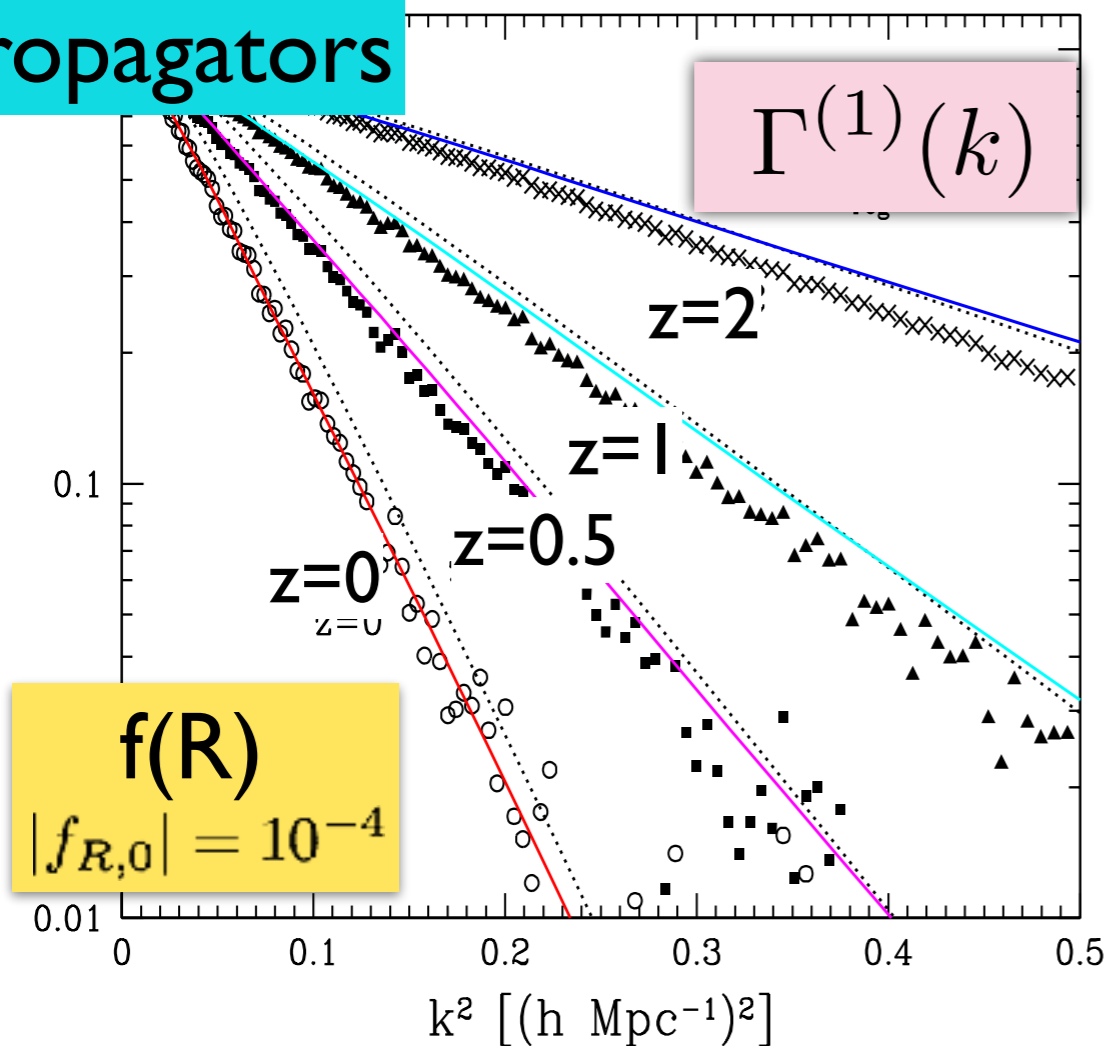
RegPT in modified gravity

Good convergence is ensured by

a *generic* damping behavior in propagators $\Gamma^{(n)} \xrightarrow{k \rightarrow \infty} \Gamma_{\text{tree}}^{(n)} e^{-k^2 \sigma_d^2/2}$

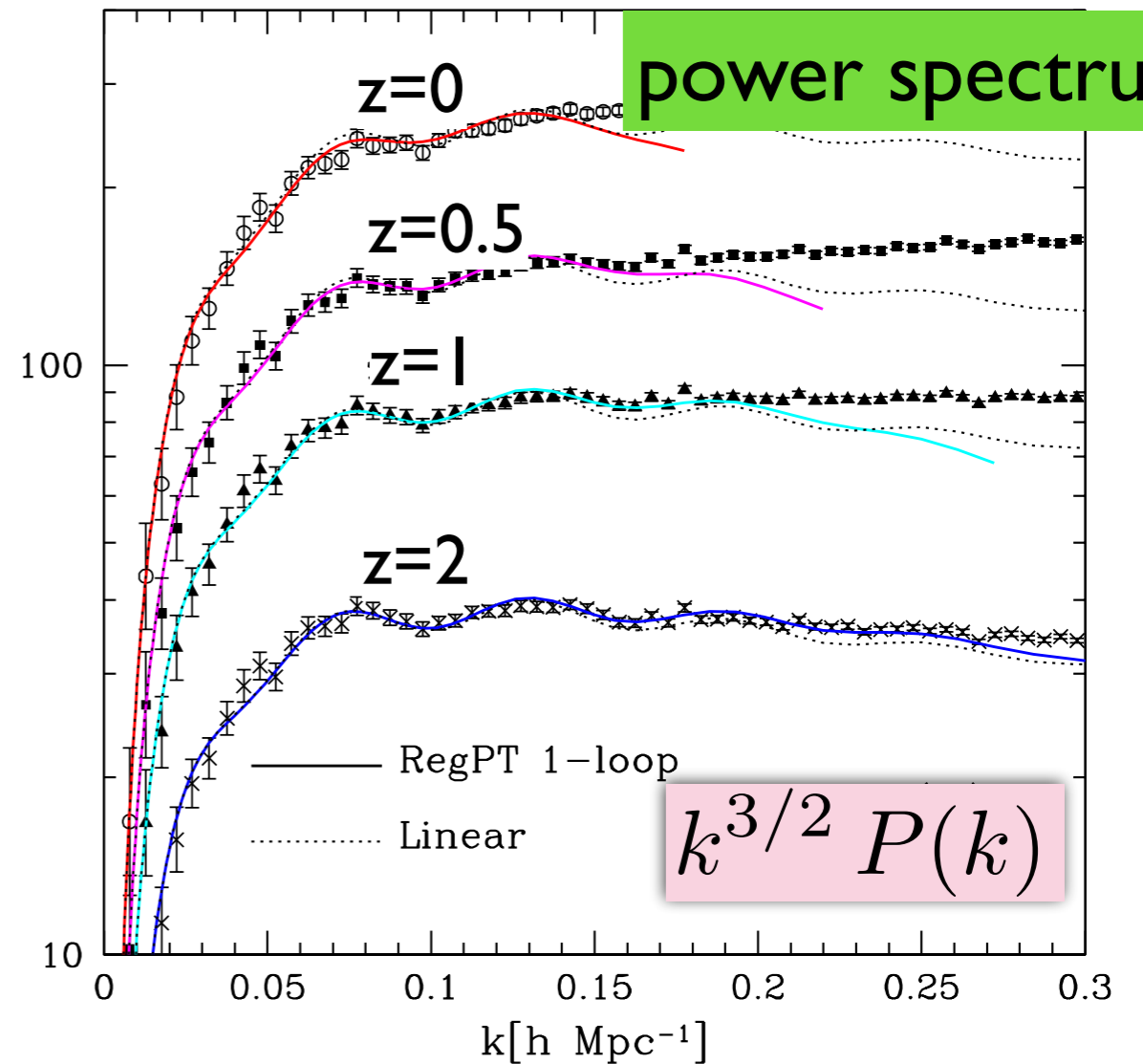
Even in modified gravity, well-controlled expansion with RegPT

propagators



N-body data: Baojiu Li

power spectrum



AT, Nishimichi, Bernardeau, et al. ('14)